UNIVERSITÄTSKLINIKUM HAMBURG-EPPENDORF

Gynäkologisches Forschungslabor
Zentrum für Operative Medizin, Klinik und Poliklinik für Gynäkologie

Klinikdirektorin: Frau Prof. Dr. med. Barbara Schmalfeldt

Expression of glycosylation-associated genes in ovarian neoplasms and prognostic relevance of MAN1A1 and ST6GAL1 in ovarian cancer.

Dissertation

zur Erlangung des Grades eines Doktors der Medizin
an der Medizinischen Fakultät der Universität Hamburg.

vorgelegt von:

Beatrice Wichert
aus Osnabrück

Hamburg 2017

Angenommen von der Medizinischen Fakultät am: 28.11.2017

Veröffentlicht mit Genehmigung der Medizinischen Fakultät der Universität Hamburg

Prüfungsausschuss, der/die Vorsitzende: Frau Dr. Karin Milde-Langosch

Prüfungsausschuss, 2. Gutachter/in: PD Dr. Christine Stürken

Table of contents

List of abbreviations

ANOVA	analysis of variance
APS	ammonium persulfate
aq. dist.	distilled water
BOT	borderline ovarian tumour
BSA	bovine serum albumin
cDNA	complementary deoxyribonucleic acid
C_q	quantification cycle in qPCR
CRC	colorectal cancer
DISC	death inducing signalling complex
eds	editors
EDTA	ethylenediaminetetraacetic acid
EMT	epithelial-mesenchymal transition
ER	endoplasmic reticulum
EtOH	ethanol
FIGO	Fédération Internationale de Gynécologie et d'Obstétrique
GalNAc	N-acetylgalactosamin
H_2O_2	hydrogen peroxide
HCC	hepatocellular cancer
HCL	hydrochloric acid
HE	haematoxylin and eosin
HNC	head and neck cancer
HRP	horseradish-peroxidase
IgG	immunoglobulin G
IHC	immunohistochemistry
LGSC	low grade serous carcinoma
M0	no metastasis
M1	distant metastasis (excluding peritoneal metastasis)
mRNA	messenger ribonucleic acid
N0	no nodal involvement
N1	nodal involvement
NaCl	sodium chloride
NICE	British National Institute for Health and Care Excellence
Nonidet P40	octylphenoxypolyethoxyethanol
OAS	overall survival
OSC	ovarian serous cystadenoma
OvCa	ovarian cancer
PFI	progression-free interval
p-value	probability value
qPCR	quantitative real-time polymerase chain reaction

REC	recurrence
RFI	recurrence-free interval
RIPA	radioimmunoprecipitation assay
RNA	ribonucleic acid
SDS	sodium dodecyl sulphate
shRNA	short hairpin ribonucleic acid
siRNA	small interfering ribonucleic acid
TBS	tris-buffered saline
TBST	tris-buffered saline with Tween20
TCGA	The Cancer Genome Atlas
TEMED	tetramethylethylenediamine
TFT	tumour-free tissue
Tris	tris(hydroxymethyl)aminomethane
Tween 20	polysorbate 20
UKE	University Clinic of Eppendorf, Hamburg
vs	versus
WB	Western Blot

Gene Symbols,
approved names from HUGO Gene Nomenclature Committee

AKT	AKT serine/threonine kinase 1
ALDH1	aldehyde dehydrogenase 1 family member A1
Apo2L/TRAIL	TNF superfamily member 10
ATP5J	ATP synthase, H+ transporting, mitochondrial Fo complex sub-unit F6
CA125	mucin 16, cell surface associated
CD133	prominin 1
CD45	protein tyrosine phosphatase, receptor type C
cFOS	Fos proto-oncogene
CLN3	CLN3, battenin
c-Myc	MYC proto-oncogene, basic helix-loop-helix transcription factor
EGFR	epidermal growth factor receptor
ERK1	mitogen-activated protein kinase 3
ERK2	mitogen-activated protein kinase 1
FAK	protein tyrosine kinase 2
FAS	Fas cell surface death receptor
GALNT12	polypeptide N-acetylgalactosaminyltransferase 12
GALNT14	polypeptide N-acetylgalactosaminyltransferase 14
GALNT-family	polypeptide N-acetylgalactosaminyltransferases
GANAB	glucosidase II alpha subunit
GAPDH	glycerinaldehyde-3-phosphate dehydrogenase
GCNT3	glucosaminyl (N-acetyl) transferase 3, mucin type

IGF-1	insulin like growth factor 1
IGFBP-3	insulin like growth factor binding protein 3
IGF-II	insulin like growth factor 2
L1CAM	L1 cell adhesion molecule
MAN1A1	mannosidase alpha class 1A member 1
MMP2	matrix metallopeptidase 2
MMP9	matrix metallopeptidase 9
mTOR	mechanistic target of rapamycin
MUC1	mucin 1, cell surface associated
MUC13	mucin 13, cell surface associated
NEU1	neuraminidase 1
P53	tumour protein p53
PI3k	phosphatidylinositol-4,5-bisphosphate 3-kinase catalytic subunit alpha
Ras	RAS type GTPase family
ST3Gal 1	ST3 beta-galactoside alpha-2,3-sialyltransferase 1
ST3GAL6	ST3 beta-galactoside alpha-2,3-sialyltransferase 6
ST6GAL1	ST6 beta-galactoside alpha-2,6-sialyltransferase 1
TNFR1	tumour necrosis factor receptor superfamily member 1A
TNF-α	tumor necrosis factor
TrkA	neurotrophic receptor tyrosine kinase 1
TβR	transforming growth factor beta receptor
UGGT	UDP-glucose glycoprotein glucosyltransferase
VEGF	vascular endothelial growth factor

List of tables

List of figures

1.   Aim of this study

There is a growing body of evidence that glycosylation changes have major effects on the malignant processes of carcinogenesis.

One of the pillars of our research group of the Gynaecology department of the University Clinic of Eppendorf, Hamburg (UKE) is the search for prognostic and predictive markers for ovarian tumours. In a preceding research project of our working group a gene expression analysis of the transcription factor cFOS led to the hypothesis that its beneficial effects in the context of ovarian cancer were at least partly transmitted via glycosylation changes. Taking into account the importance of aberrant glycosylation for carcinogenesis, the glycosylation genes affected by cFOS-induction became thus interesting as potential new markers. Consequently, seven promising candidates, representing candidates of all major glycosylation pathways, were selected for this study. GALNT12, GALNT14, GCNT3, and STG6GAL1 had been significantly down regulated upon cFOS induction while GANAB, MAN1A1, and NEU1 expression increased.

This study wished to analyse the aforementioned genes for their aptitude as prognostic markers for recurrence free interval and overall survival of patients diagnosed with ovarian cancer and to show possible associations with established prognostic factors using histopathological, clinical, and follow-up data of the Hamburg tumour database. To achieve this goal, mRNA expression levels of the selected genes were analysed with qPCR on a small patient collective, including macroscopically healthy tissue, serous cystadenomas, borderline tumours, primary serous ovarian cancer and recurrences. Based on the results of these experiments, four genes were chosen for further analysis on a more extensive patient collective on a protein level by Western Blot analysis and partly immunohistochemistry.

Furthermore, mRNA and protein expression levels between neoplasms of varying malignancy were compared.

These newly gained insights into the expression patterns of GALNT12, GALNT14, GCNT3, GANAB, MAN1A1, NEU1, and ST6GAL1 could lead to a better understanding of their role in glycosylation changes in ovarian cancer and thus increase our knowledge on the complex processes of glycosylation in carcinogenesis.

2.   Introduction

2.1   Ovarian tumours – an overview

2.1.1 Epidemiology and risk factors

Ovarian cancer (OvCa) ranks seventh in the list of most common cancer in women worldwide, with over 65.000 new cases diagnosed in 2012 in Europe alone. When it comes to deadliness OvCa ranks even higher, being responsible for over 42.000 deaths in Europe in 2012. This makes it one of the leading causes of death from cancer, especially in the economically more developed regions of the world (for pie charts see Fig. 1, taken from the EUCAN-website based on J. Ferlay et al 2013). Nevertheless, for Germany falling trends for incidence and mortality rates have been observed since 2000 (J. Ferlay et al 2013, J. Ferlay et al 2015, RKI 2015).
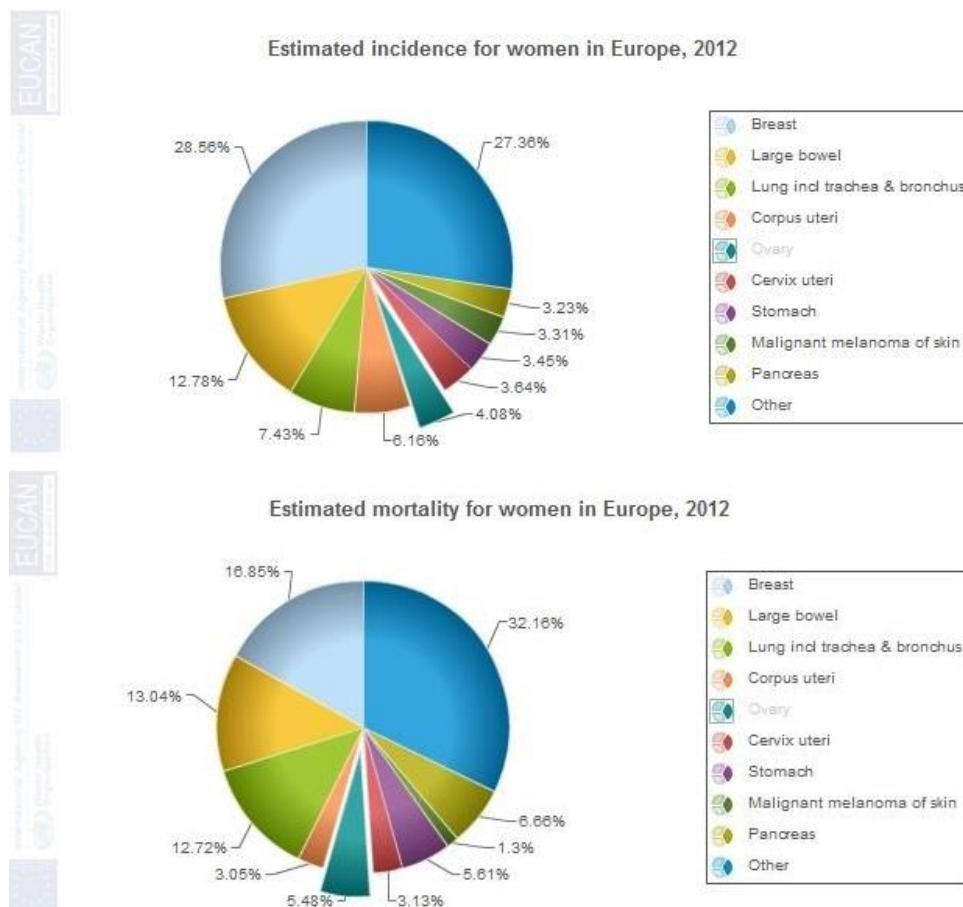
Fig. 1. Pie charts for the estimated incidence and mortality for women in Europe, 2012 (graphic taken from EUCAN – project; http://eco.iarc.fr/eucan)

Mostly postmenopausal women are affected by ovarian cancer with a median age of 69 years at diagnosis. Five year survival rates are poor, as 61% of patients will already be in an advanced stage of the disease (FIGO III or above) at presentation, meaning that the cancer has spread widely within the abdomen. The all stage five year survival in Germany is around 41% (RKI 2015).

Epidemiological risk factors

The risk of developing OvCa increases with age. Furthermore, it is associated with hormonal factors. Risk increases proportional to the number of ovulatory cycles a woman has in her lifetime. Thus, pregnancy or taking a contraceptive pill is associated with a protective effect, while nulliparity is a risk factor. Similarly, a history of ovarian or breast cancer cases in the family or a personal history of breast, corpus uteri or large bowel cancer leads to an increased risk of developing ovarian cancer (Fleming et al 2006, RKI 2015).

Genetic risk factors

Women with a genetic predisposition for OvCa are affected by this disease around 10 years earlier than median age of diagnosis. Especially BRCA1 and BRCA2 mutations are known risk factors for high grade serous OvCa, with a lifetime risk of developing OvCa by age 70 around 59% and 16.5%, respectively. Other conditions associated with a higher risk of developing ovarian cancer include the hereditary non-polyposis coli, Lynch, and Peutz-Jegher syndrome (Jayson et al 2014, Mavaddat et al 2013). Furthermore, abnormalities of TP53 are found nearly universal in high grade serous OvCa (Köbel et al 2010).

2.1.2 Histopathology and classification systems

There is a diverse set of histological types of ovarian cancers. In this study, focus will be put on the most common ovarian cancer of epithelial origin, high grade serous carcinoma, which accounts for about 70 % of the cases. Other ovarian cancers of epithelial origin include low grade serous carcinoma (LGSC) (5%), endometroid (10%),

clear cell (10%), and mucinous (3%) cancer. The rare non-epithelial types, that make up approximately 10% of malignant ovarian tumours, include germ cell tumours and stromal tumours (Kurman et al 2014).

Ovarian cancers are separated into type I and type II tumours that show different malignant potential and are characterized by certain sets of mutations.

Type I tumours are low grade, slowly growing and generally confined to the ovary at diagnosis. They are thought to develop stepwise from precursor lesions over benign ovarian serous cystadenomas (OSC) to borderline ovarian tumours (BOT) and finally LGSC. The non-serous epithelial OvCa are included in type I tumours (Kurman and Shih 2010).

Benign serous cystadenoma originate from proliferation of the ovarian surface epithelium that invaginates into the cortex and forms an inclusion cyst. They are mostly located in the cortex or surface of the ovary and are often found incidentally during ultrasound due to their mostly asymptomatic behaviour. Cysts are typically 1-10cm in diameter and lined by an epithelium of ciliated or non-ciliated secretory cells (Tavassoli and Devilee 2003).

Serous borderline tumours are a neoplasia of low malignant potential without stromal invasion. BOT is diagnosed more often in younger patients (mean 45 years) and may present with abdominal pain or infertility, though they are often asymptomatic. The tumorous epithelia form branching papillae and micropapillae with detached cell clusters. Stage I BOT has an excellent 5-year survival rate of up to 99%. However, rarely BOT can progress to an invasive tumour with a poor prognosis and 5-year survival rates of 55-75% (Tavassoli and Devilee 2003).

Type II tumours include high-grade serous carcinomas, carcinosarcomas und undifferentiated carcinomas. They grow rapidly, are genetically instable, associated with TP53 and BRCA1/2 mutations, and highly aggressive. Well defined precursor lesions have not been described yet. However, it has been found that a large percentage of serous OvCa may in fact develop from intraepithelial carcinoma in the fallopian tube (serous tubal intraepithelial carcinoma/STIC) that implants on the denuded surface of the ovary and not from the ovarian surface epithelium itself (Kurman and Shih 2010, Perets and Drapkin 2016).

This led to the revision of FIGO classification in 2013. The revised FIGO staging, that unifies staging criteria for the ovary, fallopian tube, and peritoneum, is shown in Table 1.

Table 1. Revised FIGO classification (based on Prat for the FIGO Committee on Gynecologic Oncology 2015)

Stage I: Tumour confined to ovaries or fallopian tube(s). **T1 – N0 – M0**	IA: Tumour limited to 1 ovary (capsule intact) or fallopian tube; no tumour on ovarian or fallopian tube surface; no malignant cells in the ascites or peritoneal washings
	IB: Tumour limited to both ovaries (capsules intact) or fallopian tubes; no tumour on ovarian or fallopian tube surface; no malignant cells in the ascites or peritoneal washings
	IC: Tumour limited to 1 or both ovaries or fallopian tubes, with any of the following:
	IC1: Surgical spill
	IC2: Capsule ruptured before surgery or tumour on ovarian or fallopian tube surface
	IC3: Malignant cells in the ascites or peritoneal washings
Stage II: Tumour involves 1 or both ovaries or fallopian tubes with pelvic extension (below pelvic brim) or primary peritoneal cancer. **T2 – N0 – M0**	IIA: Extension and/or implants on uterus and/or fallopian tubes and/or ovaries
	IIB: Extension to other pelvic intraperitoneal tissues
Stage III: Tumour involves 1 or both ovaries or fallopian tubes, or primary peritoneal cancer, with cytologically or histologically confirmed spread to the peritoneum outside the pelvis and/or metastasis to the retroperitoneal lymph nodes. **T1/T2-N1-M0**	IIIA1: Positive retroperitoneal lymph nodes only (cytologically or histologically proven):
	IIIA1(i) Metastasis up to 10 mm in greatest dimension
	IIIA1(ii) Metastasis more than 10 mm in greatest dimension
	IIIA2: Microscopic extrapelvic (above the pelvic brim) peritoneal involvement with or without positive retroperitoneal lymph nodes
	IIIB: Macroscopic peritoneal metastasis beyond the pelvis up to 2 cm in greatest dimension, with or without metastasis to the retroperitoneal lymph nodes
	IIIC: Macroscopic peritoneal metastasis beyond the pelvis more than 2 cm in greatest dimension, with or without metastasis to the retroperitoneal lymph nodes (includes extension of tumour to capsule of liver and spleen without parenchymal involvement of either organ)
Stage IV: Distant metastasis excluding peritoneal metastases: **Any T – any N – M1**	Stage IVA: Pleural effusion with positive cytology
	Stage IVB: Parenchymal metastases and metastases to extra-abdominal organs (including inguinal lymph nodes and lymph nodes outside of the abdominal cavity)

2.1.3 Clinical presentation and diagnostics

Symptoms of ovarian cancer are often non-specific and commonly found in a general practitioner practice. Women present, in many cases repeatedly, with symptoms like abdominal distension, increased girth, a feeling of fullness and early satiety, changed eating habits, pelvic or abdominal pain, increased frequency or urge to urinate, weight loss or changes in bowel habit. In emergency departments women often show signs of ascites, pleural effusions, bowel obstruction, and low albumin levels (Ebell et al 2015, Jayson et al 2014).

Symptom triggered testing of the glycoprotein CA125 and transvaginal ultrasonography does not lead to a stage shift but can decrease the volume of tumour burden at surgery (Gilbert et al 2012). A flow chart for diagnosis of ovarian cancer based on guidelines from the British National Institute for Health and Care Excellence (NICE), printed in the BMJ clinical review <Diagnosis of ovarian cancer> (Sundar et al 2015) is shown in Fig. 2.

Problems with the current system of diagnosis lie in the absence of specifity of CA125, which can be increased in benign conditions like endometrioses and menstruation or ovarian cysts and the lack of an established scoring systems for ultrasonography, especially in primary care settings (Sundar et al 2015). New markers that can help to differentiate between benign and malign conditions and lead to earlier diagnosis are dearly needed.
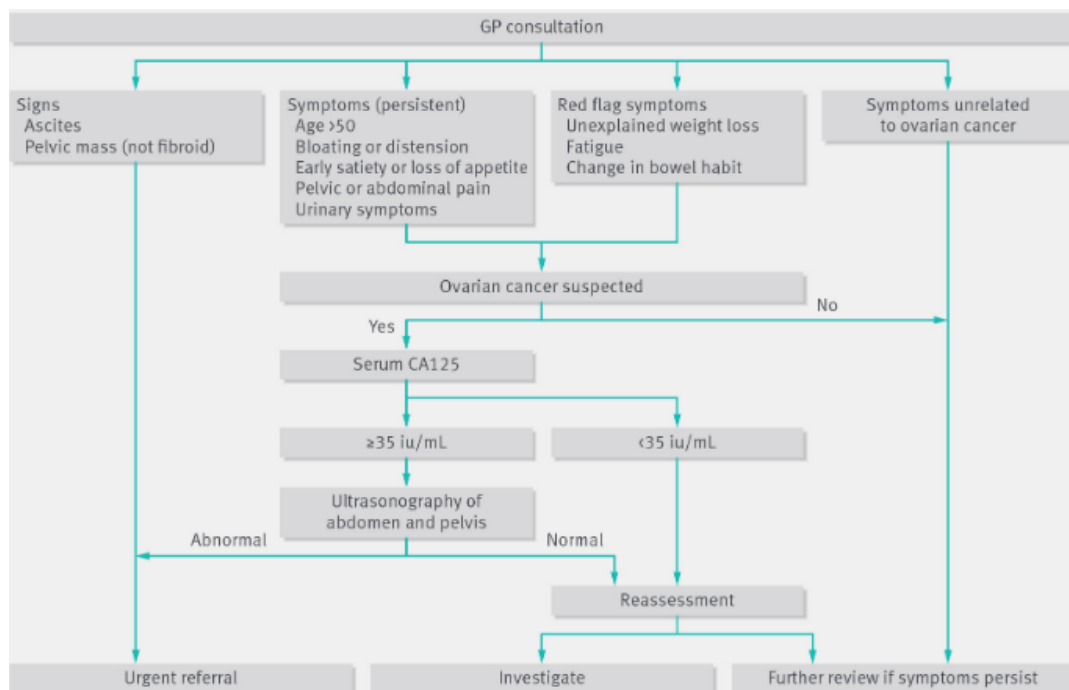
Fig. 2. Flow chart for diagnosis of OvCa, adapted from NICE (graph taken from Sundar et al 2015)

2.1.4 Standard therapy and emerging therapeutic options

Standard of care for OvCa remains maximal cytoreductive debulking surgery and 6 cycles of platinum/taxane-based cytotoxic chemotherapy. Subsequently, there is a follow-up surveillance for potential recurrences. Second-line chemotherapy is based on the duration of the progression-free interval (PFI), with platinum resistance being defined as recurrence occurring less than 6 months from the time of initial chemotherapy completion. When the cancer is deemed platinum sensitive it will be rechallenged with a platinum double chemotherapy (Leitlinienprogramm Onkologie 2013).

Unfortunately, recurrent disease tends to follow a relapse-response pattern with ever shorter disease free intervals before ultimately becoming resistant to treatment (Coleman et al 2013, Lheureux et al 2015). Widely accepted factors that impact poor prognosis for recurrence-free interval (RFI) and overall survival (OAS) include age at diagnosis, histology, size of residual disease, and FIGO staging (Winter et al 2007).

Nevertheless, the deeper understanding of OvCa and the importance of its molecular subtypes lead to new treatment-regimes and several trials are on the way, examining treatment timing and strategy and trying out new substances to improve the RFI, PFI, and OAS of patients. Maintenance therapy, that could delay tumour progression, holds promise, though effective agents and strategies remain to be validated (Lheureux et al 2015). Another emerging field is the targeting of tumour micro-environment with anti-angiogenesis and immunological approaches. Most prominently, the addition of anti VEGF monoclonal antibody bevacizumab to chemotherapy led to a prolongation of PFI and is now approved as first-line standard for patients in several countries (Eskander and Tewari 2014, Sven Mahner et al 2015). Further molecular profiling is needed to find new targets and compounds and improve the micro-environment based approaches.

2.2   Glycosylation in Neoplasia

Research on glycosylation changes in neoplasia is an emerging and promising field in cancer research.

Approximately half of all proteins are glycosylated with around 3000 different glycan structures. Glycosylation differs depending on cell type, physiology, and tissue. These changes are especially marked when the cell function is altered. During the process of malignant transformation a loss or overexpression of functional groups can be observed and even novel structures, which are specific to cancerous tissues, appear (Varki et al 2009a).

Glycan-synthesis differs from template-based approaches like protein-synthesis. Substrate availability and the presence of enzymes, that regulate the addition or removal of glycan structures, will decide the final synthesis product. Glycosylation enzymes compete for the available substrates and glycan chains. Altered protein expression in cancer cells can thus lead to altered glycosylation, as the likeliness of a glycosylation step happening can be changed by enzyme availability (Brockhausen 1999, Varki et al 2009a).

This affects the malignant transformation in a myriad of ways. When cell surface carbohydrate structures are changed, potential ligands of interaction between tumour cells and microenvironment are modified. This may notably affect adhesion properties of the cell with enhanced abilities to invade and metastasize, cell-signalling and cell surface receptors, which can influence growth and survival of the cells, and the response triggered by the immune system. Thus the properties of tumour cells are changed and the more aggressive and potent tumour cells survive (Brockhausen 2006, Potapenko et al 2010, Varki et al 2009a). Fig. 3 is an image taken from Potapenko et al 2010, which illustrates the most important changes during carcinogenesis that can be altered by aberrant glycosylation.
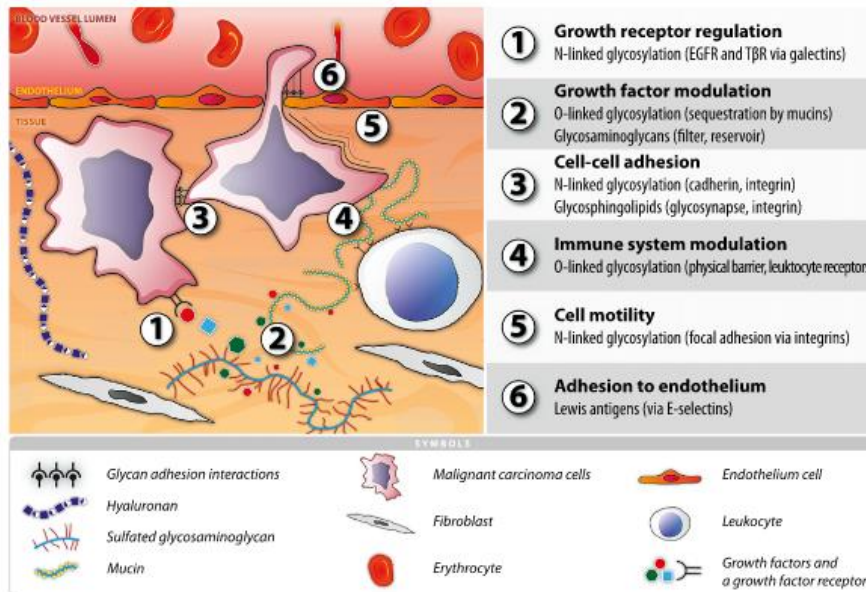
Fig. 3. Glycosylation in carcinogenesis. <<Six important processes for cancer development and progression (1-6) influenced by various glycosylation types are indicated. 1: growth receptors (especially EGFR and TβR) are influenced by N-glycosylation in concert with galectins; 2: growth factors and other signaling molecules may have elevated concentrations, filtered or sequestered by glycosaminoglycans and O-glycosylated mucins; 3: cell-cell adhesion might be mediated either directly by for example glycosynapses consisting mainly of glycosphingolipids – or, more importantly, indirectly by modulation of integrins and cadherins by N-linked glycosylation; 4: O-glycosylated mucins, both secreted and membrane-bound, may constitute a physical barrier or act on specific leukocyte receptors thereby modulating Immune system response towards the malignant cells; 5: N-linked glycosylation may enhance motility of transformed cells be regulating integrin functionality; 6: adhesion to endothelium can be mediated by a number of mechanisms, including binding of Lewis antigens by endothelial selectins>> (image and description taken from Potapenko et al 2010).

Furthermore, glycoproteins serve as cancer biomarkers, e.g. CA125 for ovarian cancer, and can help to classify subtypes of tumours and thus advance a more personalized medicine. In addition to that, knowledge of glycosylation changes in specific cancers can lead to more effective treatment regimes, as glycoproteins could serve as drug targets or chemical tags and modification of certain glycoproteins could change the malignant potential of the tumour (Alper 2003, Tian et al 2011, Vajaria et al 2015).

During glycosylation, saccharide units are covalently attached to target-structures and then sequentially elongated, branched, and trimmed. There are four main types of glycans: N-linked glycans, O-linked glycans, glycosaminoglycans, and glycosphingolipids. The most common changes of glycosylation found in cancer are an increased branching of N-glycans, truncated and incomplete O-glycans, especially in combination with an overexpression of mucins, which are heavily O-glycosylated glycoproteins,

an accumulation of precursors, high levels of sialic acids, and the formation of Lewis antigens (Varki et al 2009a).

Glycomic analysis of ovarian cancer began in the 1960s and has since then been a thriving field of research (Garcia-Bunuel and Monis 1964).

Especially as aberrant glycosylation is considered to happen early in the transformation process, hopes are high that future research may lead to the development of markers to diagnose ovarian cancer sooner and to establish more sensitive and specific screening methods, for example via auto-antibodies (Abbott 2010, Cho et al 1994, Wandall et al 2010). Furthermore, there is a need for prognostic markers that could help stratify patients and further elucidate molecular processes affecting the malignancy of ovarian cancer.

One example of a prognostic marker is the transcription factor cFOS. Being also linked to oncogenic functions in other cancers, cFOS´ role in ovarian cancer is distinctive. Here it is associated with a favourable outcome and was shown to suppress ovarian cancer progression by changing adhesion properties, possibly via changing glycosylation, as several glycosylation enzymes were deregulated by cFOS expression changes (S Mahner et al 2008, Oliveira-Ferrer et al 2014). These intriguing results led to the question of the importance of these deregulated enzymes in ovarian cancer and ultimately to the creation of this thesis.

This study concentrates on changes mediated by N- and O-linked glycans and the optional trimming of glycans. These processes will be outlined in the following and details will be given on the 7 glycosylation enzymes that entered this study and are involved in the formation of these glycans and their sialylation status. However, the methods used in this study are limited to indirect approaches to the actual state of glycosylation by measuring messenger ribonucleic acid (mRNA) and protein expression of the selected glycosylation enzymes via real-time quantitative polymerase chain reaction (qPCR), Western Blot (WB), and Immunohistochemistry (IHC). Nonetheless, due to the lack of highly sensitive and specific detection methods for glycan structures themselves, these are well established methods in search for aberrant glycosylation in cancer (e.g. Milde-Langosch et al 2014, Stern et al 2010, P Wang et al 2005).

2.2.1 O-Glycosylation and its role in malignant transformation

O-glycans are linked to proteins through a covalent bond between N-acetylgalac-tosamin (GalNAc) and either serine or threonine (Tn antigen) in the golgi apparatus. They are subdivided in 8 core structures, depending on enzyme expression and activity that control the different pathways. Exemplary synthesis of Core 1 and Core 2 structures via enzymes of the GALNT-family and GCNT3 is shown in Fig. 4.
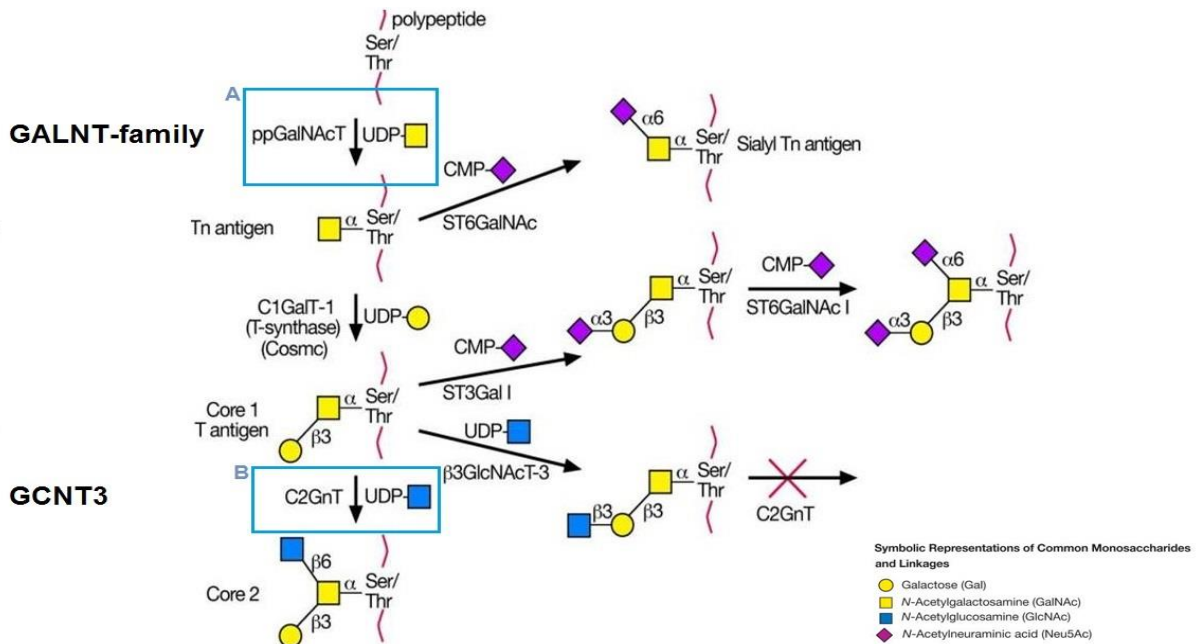
Fig. 4. Biosynthesis of O-Glycans (Core 1 and Core 2). First, N-acetylgalactosamine is transferred from UDP-GalNAc to serine or threonine, catalyzed by an enzyme of the GALNT-family (or ppGal-NAcT) (A) in the golgi apparatus creating the base for all core structures, the Tn antigen, which is of-ten found in mucin O-glycans in cancerous tissues. Then core structures are synthesized. GCNT3 (or C2GnT) and ST3Gal I compete for Core 1 T-antigen to continue their respective synthesis pathways (image adapted from Varki et al 2009b).

O-glycans are implicated in attachment and invasion of cancer cells and cell survival by influencing immunological properties, protecting proteins from degradation, epitope control, and expression and control of cell surface receptors. The enzymes involved in O-glycan biosynthesis are often deregulated in cancer cells. Especially incomplete, short, truncated or highly sialated mucin O-glycans are found abundantly in cancerous tissues (Brockhausen 1999, Varki et al 2009a).

2.2.1.1   Members of the GALNT-family: GALNT12 and GALNT14 in cancer

The first step of O-linked glycosylation forming Tn antigen is catalysed by members of a family of 20 isoenzymes, the GALNT-family (see Fig. 4), which are located throughout the golgi apparatus. They are redundantly expressed and have overlapping but distinct substrate specificities. Expression differs from tissues to cells and is affected by malignant processes. Altering of their expression has been shown to have functional and molecular effects in cancerogenesis and metastasis, and analysis with IHC or molecular approaches qualified members of the GALNT-family as prognostic markers in a variety of epithelial cancers (Beaman and Brooks 2014).

2.2.1.1.1   GALNT12 in cancer

GALNT12 is highly regulated and mainly expressed in digestive organs with a low baseline expression in the ovaries (Guo et al 2002).

In a small qPCR study GALNT12 absence was found to be a marker for metastatic gastric and colorectal cancer (CRC), being downregulated in the tumorous tissues and cell lines (Guo et al 2004).

Furthermore, GALNT12 was thought to be a major susceptibility gene for unexplained CRC but this hypothesis was refuted on a larger patient cohort. Nonetheless, it remains a candidate for a moderate to low susceptibility gene in familial CRC (Guda et al 2009, Valle et al 2014).

A 1.5 fold upregulation was found in the ovaries of rats with endometriosis versus (vs) the control group, possibly induced by the inflammation due to elevated levels of TNF-α in peritoneal fluids (Birt et al 2013).

In a micro-array analysis of changes in gene expression mediated by the transcription factor cFOS, a 2.1-3 fold downregulation of GALNT12 was found in ovarian cancer cell lines, and a 6 fold downregulation in a mouse model upon cFOS upregulation (Oliveira-Ferrer et al 2014).

Much remains to be known on GALNT12´s role in cancer, especially in ovarian tumours. This study hopes to elucidate its possible importance in ovarian neoplasms via

an analysis of mRNA levels in types of tumour of increasing malignancy and in combination with patient data.

2.2.1.1.2   GALNT14 in cancer

GALNT14 is ubiquitously expressed and expression changes have been linked to various cancers and shown to affect apoptosis pathways (Han Wang et al 2003).

In an IHC assay GALNT14 was deregulated in several kinds of breast carcinomas, positioning it as an interesting candidate for a potential breast cancer biomarker (Chen Wu et al 2010). Huanna et al found that breast cancer cell lines showed increased cell migration, cell invasion, and proliferation levels upon GALNT14 overexpression. Furthermore, mRNAs of epithelial-mesenchymal transition genes (EMT) including N-cadherin, vimentin, and VEGF, were upregulated, while E-cadherin was downregulated upon GALNT14 overexpression or vice versa upon knockdown (Huanna et al 2014).

During EMT a combined loss of cell junction proteins, e.g. E-cadherin, and the gain of mesenchymal markers, e.g. vimentin and N-cadherin, can be observed. Thus, cells that were once epithelial dedifferentiate, turn mesenchymal, and become more motile and invasive (Zhou et al 2014). Hence, it was hypothesized that GALNT14 takes part in breast cancer malignancy by altering cell invasiveness possibly via changed expression levels of EMT genes (Huanna et al 2014).

In a prospective study of patients with advanced hepatocellular carcinoma by Yeh et al, single nucleotide polymorphisms on GALNT14 were associated with response to combination chemotherapy (FMP protocol including 5-fluorouracil, mitoxantrone, and, notably, ovarian cancer first-line treatment, cisplatin), including a favourable effect on time to progression and OAS. However, GALNT14 expression levels were not regarded (Chau-Ting Yeh et al 2014).

More recently, germ-line mutations in GALNT14 were found to be associated with the paediatric tumour neuroblastoma, possibly acting as a predisposition gene. Furthermore, higher GALNT14 expression was associated with a worse OAS, thus suggesting an effect on neuroblastoma phenotype, as well (De Mariano et al 2015).

In addition to the hypotheses of GALNT14 being involved in malignant transformation and the malignant potential of tumour cells via changed expression levels of EMT genes, GALNT14 was also identified as a binding partner or regulator for growth and transcription factors and genes involved in apoptosis.

GALNT14 expression was observed to correlate with Apo2L/TRAIL sensitivity in numerous tumours, such as pancreatic carcinoma, non-small cell lung cancer, and melanoma. Apo2L/TRAIL induces apoptosis in many cancer cells, while healthy cells appear to be resistant, which makes it an interesting target for clinical investigation. GALNT14 overexpression was found to increase responsiveness of the pro-apoptotic ligand Apo2L/TRAIL, possibly via O-glycosylation of the death receptors 3 and 4 (Bouralexis et al 2005, Wagner et al 2007). In the same study a relative mRNA over-expression of GALNT14 was found in up to 30% of samples from various cancers, compared to the respective normal tissue, among them ovarian cancer. Thus, GALNT14 expression could possibly be used to characterize a patient cohort with a better response-rate to Apo2L/TRAIL-based therapy in various tumours. Furthermore, the dynamic expression of GALNT14 in cancer may prove its value as a potential predictive biomarker for continued therapy sensitivity (Wagner et al 2007).

Furthermore, in breast cancer cell lines expression of factors like MMP2 and MUC1, which have been associated with angiogenesis, proliferation, and metastasis, are influenced by GALNT14 expression. This might be mediated indirectly via IGFBP-3, an enzyme that controls the anti-apoptotic effects of IGF-1, and which was shown to be a binding partner of GALNT14. It is likely that effects on expression levels that correlate with GALNT14 are mediated via glycosylation of transcriptional factors, like IGFB-3, rather than GALNT14 itself, as it is not a transcriptional factor but a glycosyltransferase (Huanna et al 2014, Chen Wu et al 2012).

For the effect of GALNT14 specifically on ovarian cancer Yang et al published a study in 2013. Firstly, they found varying degrees of GALNT14 expression on a mRNA and protein level in different OvCa cell lines, with SKOV3 cells showing faint GALNT14 expression (Yang 2013).

Then, they showed that knockdown of endogenous expression of GALNT14 led to the detection of less O-glycosylated proteins by VVA lectin blot, hinting at the importance of GALNT14 for the glycosylation status in ovarian tissue. This knockdown also suggested changes in phenotype, as ovarian cancer cell lines with GALNT14 knockdown showed significantly suppressed cellular migration in wound healing and cell migration assays and altered cellular morphologic characteristics. The study suggested that the effects of GALNT14 on malignancy in ovarian cancer could possibly be attributed to changed glycosylation of MUC13. MUC13 is a transmembrane protein

that is significantly higher expressed in OvCa and showed aberrant glycosylation upon GALNT14 expression changes. MUC13 has previously been shown to be involved in carcinogenesis and tumour progression by changing adhesion, cell motility, and proliferation in various cancer, including ovarian cancer (Chauhan et al 2009, Yang 2013).

In the micro-array analysis of changes in gene expression mediated by cFOS, a 45.2 – 128 fold downregulation of GALNT14 was found in ovarian cancer cell lines, and a 4.6 fold downregulation in a mouse model upon cFOS upregulation, suggesting the association of GALNT14 downregulation with a less malignant phenotype of ovarian cancer (Oliveira-Ferrer et al 2014).

Findings on GALNT14´s role in cancer remain controversial with beneficial and malignant phenotypes having been linked to its expression changes and genetic mutations being prevalent in several cancers. This study hopes to further clarify GALNT14´s role in ovarian cancer via an analysis of mRNA levels in types of tumour of increasing malignancy in combination with patient data.

2.2.1.2   GCNT3 in cancer

GCNT3 is a member of the family of core 2 β-1,6-N-acetylglucosaminyl-transferases (C2Gnt), that is involved in the formation of Core 2 and Core 4 branches of O-glycans on mucins and blood group I branches. It is located in the golgi apparatus. (Jiunn-Chern Yeh et al 1999).

GCNT3 was found to be down regulated in the majority of colon cancer cell lines and primary colon tumours as opposed to normal tissues. Similarly, upregulation of GCNT3 was shown to have profound effects on the tumour cell´s phenotype leading to suppressed adhesion, motility, invasion, and colony formation ability. Furthermore, proliferation was suppressed and apoptosis induced upon GCNT3 overexpression, possibly via an integrin-signalling pathway. The tumour suppressing properties of GCNT3 upregulation were confirmed in vivo in a xenograft model that showed suppressed tumour growth (Huang et al 2006). In addition to that, GCNT3 showed potential as a prognostic biomarker, as high expression was associated significantly and independently with a longer RFI in patients with stage II colon cancer. It was also suggested as a marker of response to therapeutic treatment. Chemotherapeutic drugs (5-FU, bortezomib, and paclitaxel) dose-dependently induced GCNT3 expression in colon

and breast cancer cell lines proportional to the anti-tumorous effects of increased dosage, even showing no deregulation of GCNT3 in chemo-resistant cells (González-Vallinas et al 2015).

Contrary to the beneficial association of high GCNT3 expression in colon cancer, in hepatocellular cancer (HCC) GCNT3 upregulation was associated with metastasis. An upregulation was found in metastatic HCC cell lines, orthotopic xenograft tumours, and clinical tissue samples with metastasis as compared to non-metastatic HCC controls as part of a transcriptional profiling of glycogenes (Tianhua Liu et al 2014).

Similarly, GCNT3 was upregulated in prostate cancer cell lines upon hypoxia, a condition associated with rapidly growing tumours that is countered by tumours by hypoxia-inducible transcription factors. Furthermore, GCNT3 was shown to be essential for the synthesis of an epitope in prostate cancer cell lines that is recognised by the cytotoxic monoclonal antibody F77 (Nonaka et al 2014).

In ovarian cancer cell lines GCNT3 showed a 7.6 – 12.9 fold downregulation and a 14.6 fold downregulation in a xenograft model in the micro-array analysis of changes in gene expression mediated by the beneficial prognostic factor cFOS (Oliveira-Ferrer et al 2014).

The possible role of GCNT3 in cancer generally and ovarian cancer especially remains largely unknown. This study hopes to further elucidate the importance of GCNT3 in ovarian cancer via an analysis of mRNA levels in types of tumour of increasing malignancy in combination with patient data.

2.2.2 N-Glycosylation and its role in malignant transformation

Synthesis of N-linked glycans is a complex, cotranslational process of precursor synthesis, attachment to asparagine residues of nascent glycoproteins, followed by early processing, maturation, and decoration and capping of the N-glycans on the luminal side of the endoplasmic reticulum (ER).

There are 3 types of N-glycans depending on the elongation of their common core structures: high-mannose N-glycans, which are extended only by mannose residues, complex N-glycans, which are modified by the additional binding of other residues like sialic acids or fucose, and hybrid N-glycans, which are a combination of the two. A flowchart showing an example of N-glycan synthesis, adapted from Varki et al to highlight the steps catalysed by the enzymes covered in this thesis, is shown in Fig. 5.
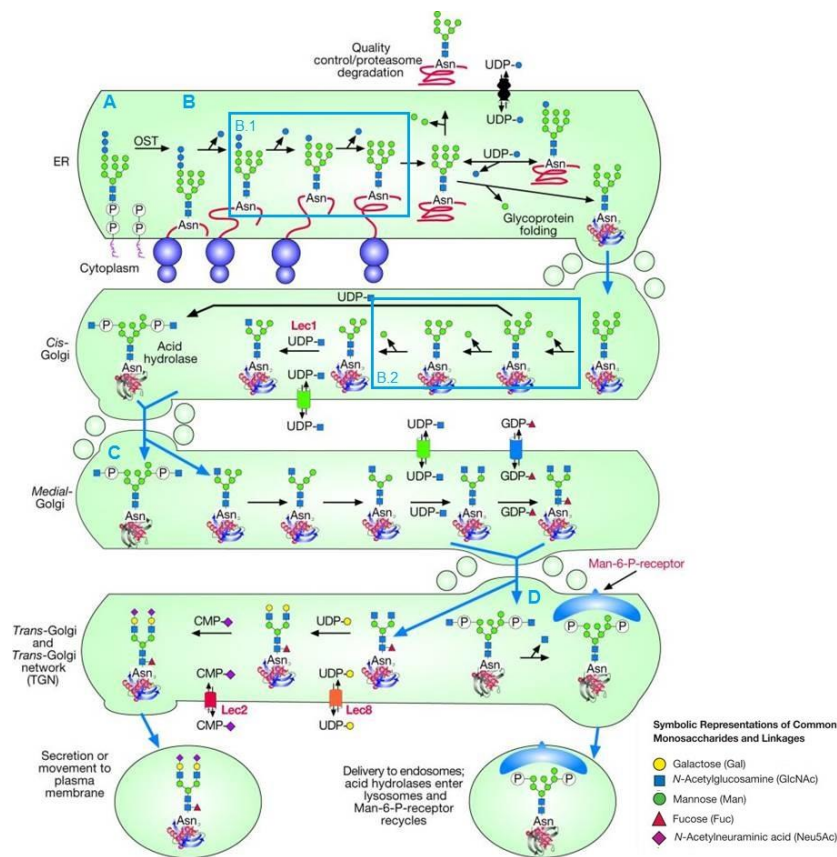
Fig. 5. Processing and maturation of N-glycans. (A) The mature precursor is transferred to an asparagine residue of a nascent glycoprotein. (B) During early processing N-glycans are trimmed by α-glucosidases, like GANAB (B.1), and mannosidases. Via the glycosylation protein folding and correct conformation is also assured. Then, they are transferred from the ER to the golgi and further trimmed and branched by mannosidases, like MAN1A1 (B.2). (C) On their passage through the golgi apparatus the N-glycans undergo late processing and become hybrid and complex N-glycans. (D) With further sugar additions they mature, are further elongated, and finally decorated and capped before the now N-glycosylated glycoprotein is trafficked on to its destination (image adapted from Varki et al 2009c).

An increased size, altered branching, and heavy sialylation of N-glycans have been observed in cancer. Furthermore, expression or activity of surface receptors involved in malignant transformation like EGFR, TβR and adhesion to integrins and cadherins, which are important for metastatic potential of tumour cells, were shown to be influenced by N-glycosylation (Potapenko et al 2010, Varki et al 2009a).

2.2.1.1   GANAB in cancer

Glucosidase II is a heterodimeric enzyme found in the ER and is crucial for the second step of N-glycan dependent folding of nascent glycoproteins. GANAB is the α-subunit of Glucosidase II, which acts as a molecular chaperone and controls the quality of correct protein folding via de- and reglycosylation cycles with a glycosyltransferase (UGGT) before properly folded enzymes are trafficked on to the golgi apparatus. As the two subunits of Glucosidase II are differently expressed and the GIIβ-subunit was found to interact with other receptors, GANABs function might surpass the glycosylation process and regulate other cell processes, too (Anji and Kumari 2006, D'Alessio et al 2010).

GANAB was downregulated in invasive head and neck cancer (HNC) cell lines as compared to their less invasive parental cell lines. Further GANAB knockdown with shRNA enhanced cell growth and led to an altered, more malignant phenotype of the cell lines. Cells showed considerably increased migration and invasion upon GANAB knockdown, which indicates that GANAB inhibits cell growth, migration, and invasion. In patients with HNC, low GANAB expression had a significant correlation with cancer aggressiveness, higher staging, and poor survival. It was thus hypothesized that the loss of the tumour suppression function of GANAB contributes to aggressive cancers. This makes it a possible candidate as a prognostic marker or target for cancer drug development (Chiu et al 2011).

Strikingly, a study by Cressey et al found glucosidase II, of which GANAB is a subunit, to be structurally similar to the tumour suppressor p53, as it was recognised by an antibody raised against p53. Additionally, it behaved similar to p53 upon UV radiation and tunicamycin-induced ER stress. The possible tumour suppressor function could explain its frequent upregulation in tissues of human lung cancer and lung adenocarcinoma cells as a protection mechanism. However, the role of glucosidase II remains ambivalent as Cressey et al hypothesized that increased levels of glucosidase

II could also make cells more resistant to ER stress. Cells could thus avoid apoptosis despite an accumulation of misfolded proteins in the ER, which may ultimately lead to a more malignant phenotype (Cressey 2013).

In ovarian cancer cell lines, GANAB showed a 1.5 – 2.0 fold upregulation in the micro-array analysis of changes in gene expression mediated by the beneficial prognostic factor cFOS, linking higher GANAB levels to a more favourable phenotype (Oliveira-Ferrer et al 2014).

Though research is still very limited, GANAB holds promise as a beneficial factor in various cancers. Therefore, this study hopes to further elucidate the role of GANAB in ovarian cancer via an analysis of mRNA and protein levels in types of tumour of increasing malignancy in combination with extensive patient data.

2.2.1.2   MAN1A1 in cancer

MAN1A1 is a part of the mannosidase family and is found mainly in the golgi, but also in smaller quantities in the ER. In the golgi apparatus it participates in the trimming of oligosaccharides and thus facilitates the formation of high-mannose glycans. MAN1A1 is heterogeneously expressed in different tissues with a strong expression level in lymphocytes and the spleen (Gebuhr et al 2011, Moremen and Nairn 2014).

MAN1A1 was found to be downregulated in metastatic human HCC cell lines and orthotopic xenograft tumours as compared to non-metastatic HCC controls as part of a small study on transcriptional profiling of glycogenes (Tianhua Liu et al 2014).

In line with the findings in HCC, in a microarray analysis of patients with primary breast cancer, high mRNA expression of MAN1A1 was shown to be of independent prognostic significance and associated with significantly longer RFS and OAS (Milde-Langosch et al 2014). These findings seem to be backed by yet unpublished data of our working group.

Furthermore, MAN1A1 was shown to be relevant for the glycosylation of prognostic markers in ovarian cancer cell lines. Upon application of the MAN1A1-inhibitor Kifunensine, processing of high-mannose to complex glycans was disturbed. Conse-

quently, adhesion molecules like L1CAM showed lower levels of N-glycosylation. How-ever, the possible effects of this on malignancy remain to be learned. Furthermore, the composition of extracellular vesicles of the ovarian cancer cell lines were changed upon inhibition of MAN1A1. This could open a path for novel biomarkers based on glycosignatures detected in the extracellular vesicles (Altevogt et al 2016, Gomes et al 2015).

In a micro-array analysis of changes in gene expression mediated by transcription factor cFOS, a 2.2 – 2.3 fold upregulation of MAN1A1 was found in ovarian cancer cell lines, and a 8.0 fold upregulation in a xenograft model upon cFOS upregulation, sug-gesting the association of MAN1A1 upregulation with a less malignant phenotype of ovarian cancer (Oliveira-Ferrer et al 2014).

MAN1A1 is an emerging candidate in the field of glycosylation cancer research. Thus, there is the necessity of further research of MAN1A1´s implications in carcino-genesis. To gain deeper insights of its role in ovarian cancer this study hopes to ex-amine its expression patterns on an mRNA and protein level and its prognostic value by using extensive patient data.

2.2.3 Sialylation of glycoproteins and glycolipids

Sialic acids are found widely at terminal positions of sugar chains on glycoconjugates. Forming the terminal epitopes, sialylation patterns have crucial effects on cell adhesion, protein targeting and conformation, and cell-cell/cell-matrix interaction. Sialylation is mediated by a family of 4 sialidases and 20 sialyltransferases.

Cancer cells often show abnormal sialylation mediated by altered activity or expression of these two enzyme families. At least in part these changes are due to transcription regulation by proto-oncogenes (e.g. Ras, c-Myc), substrate availability or tumour microenvironment, e.g. hypoxia. The resulting hypersialylation has been linked to the process of malignant transformation with effects on the invasiveness, tumour growth, apoptosis evasion, chemo- and radiation therapy resistance, and the metastatic potential of cancerous cells, resulting in a correlation with poor survival for patients (Vajaria et al 2015).

Novel approaches to target aberrant sialylation, for example with the sialyltransferase inhibitor Lith-O-Asp or the sialidase inhibitor Tamiflu and targeted drug delivery to the tumour with sialic-acid recognising antibodies, are explored in vitro and in mouse models and show some promising potential to advance cancer therapy (Büll et al 2014, Chen et al 2011, Fuster and Esko 2005, Vajaria et al 2015, Varki et al 2009a).

2.2.3.1   NEU1 in cancer

The family of sialidases differ in subcellular localization, tissue specificity and their catalytic properties. NEU1, one of the currently known 4 human sialidases, is mainly located in the lysosomes and lesser so in plasma membranes. It shows high substrate specificity, catalysing the removal of α-2,3-glycosidically bound sialic acid residues from oligosaccharides and glycopeptides. In its active form, NEU1 is associated with its so called protective protein cathepsin A and a β-galactosidase. By forming complexes with other proteins, it can also react on glycoproteins on the cell surface and thus affect cell growth, cell signalling, and immune responses (Liang et al 2006, Miyagi et al 2008, Pshezhetsky and Hinek 2011, Vajaria et al 2015).

The once largely beneficial picture painted on NEU1 expression in cancer, being linked to increasing differentiation, inhibition of metastatic potential, and sensitizing cancer cells to apoptosis, has recently been extended by studies proposing opposite

effects, with NEU1 inhibition, not upregulation, having beneficial effects on cancer cell phenotype and treatment responses.

Miyagi et al found a significant inverse correlation between NEU1 expression and the metastatic ability of cancer cells. Especially upon the transfection with oncogenes NEU1 expression levels were further reduced in transformed fibroblasts as metastatic potential increased (Miyagi et al 1994).

Induction of NEU1 and its protective protein in human colon cancer cells supressed cell migration and invasion and vice versa. Interestingly, this effect could also be re-produced in vivo. Trans-splenical injection of NEU1 overexpressing cells in mice led to fewer liver metastasis. Desialylation of β4 integrin by NEU1 was proposed as a possi-ble pathway for the reduced metastatic potential, as it was shown to be significantly desialylated and integrin hypersialylation had been linked to metastatic potential be-fore. Besides desialylation, β4 integrin also underwent decreased phosphorylation by reduction of the FAK / ERK1/2 pathway upon NEU1 upregulation. Immunofluorescence staining showed that NEU1 expressed at the cell surface was accessible to the integ-rin, thus indicating the importance of NEU1 mediated β4 integrin signalling (Uemura et al 2009). This is in line with observations by Kato et al that forced expression of NEU1 in B16 murine melanoma cells suppressed tumour progression and metastatic potential and increased sensitivity to apoptosis in vitro and in vivo in a mouse model (Kato et al 2001).

NEU1 was shown to affect activation of various cell surface receptors, like the insu-lin-like growth factor (IGF-II) receptor, toll-like receptors, Trk receptors, and EGFR by cross-talking with other proteins (Gilmour et al 2013, Pshezhetsky and Hinek 2011).

Most prominent is the regulation of EGFR by NEU1. Lillehoj et al showed that EGFR was an in vivo substrate of NEU1. In the assay, conducted on repair mechanisms in human airway epithelium, NEU1 knockdown enhanced EGFR phosphorylation and thus activation (Lillehoj et al 2012). However, investigating a MUC1-EGFR-NEU1 sig-nalling pathway in triple-negative breast carcinoma, Garbar et al could find no correla-tion between NEU1 and EGFR expression (Garbar et al 2015).

Recently, new insights were gained into NEU1 and EGFR interaction in cancer cells that opened up a new role for NEU1 in carcinogenesis. Cross-talk between NEU1 and MMP9 in association with a G-Protein were shown to be required for EGF-induced EGFR activation. NEU1 and MMP9 formed a complex with EGFR on the cell surface.

Upon activation MMP9 induced NEU1 by a yet unknown mechanism which consequently hydrolysed sialic acids of terminal β galactoside and thus removed steric hindrance of EGFR activation. Targeting this pathway with NEU1 inhibitor oseltamivir phosphate (Tamiflu) dose-dependently decreased cell viability in vitro and attenuated human pancreatic cancer growth and metastasis in vivo in mice with heterotopic implantation of tumour tissues. Notably, the Tamiflu treatment showed no apparent deteriorating side effect on the health of the rodents. Upon histological examination EGFR-phosphorylation was decreased in these tumours (Gilmour et al 2013). These findings were supported by a follow up study of the same working group where oseltamivir phosphate treatment reversed chemoresistance of human pancreatic cancer cells to cisplatin and gemcitabine and disabled apoptosis evasion of the cells. Furthermore, treatment with the NEU1 inhibitor led to a partial reversal of EMT, as demonstrated by an upregulation of E-cadherins and a downregulation of N-cadherins. However, this time in vivo Tamiflu treatment alone or in combination with gemcitabine could not prevent metastasis in the mice bearing the chemoresistant pancreatic cancer, suggesting the need to find an optimal Tamiflu dosage. Still, NEU1 inhibition shows the potential to increase chemosensitivity of resistant cells (Szewczuk, O'Shea, et al 2014).

A pathway similar to EGFR activation was identified for cell-surface and intracellular toll-like receptors and TrkA receptor, where MMP-9 –NEU1 crosstalk led to an activation of these receptors, that have been extensively linked to cancerous processes before. Possibly, NEU1 inhibition by Tamiflu attenuates all of these pathways to a certain extent thus providing a promising horizontal approach to target various cell signalling pathways that are involved in cancer progression with a drug that has already been commonly used on patients (Abdulkhalek and Szewczuk 2013, Jayanth et al 2010).

An analysis of Cancer Genome Atlas data of NEU1 expression levels by Ren et al revealed high expression of NEU1 mRNA in ovarian cancer compared to normal adjacent tissue. In the same study Ren et al found that treatment of ovarian cancer cell lines with NEU1 siRNA led to an inhibition of cancer proliferation, cell cycle arrest, and increased apoptosis rates compared to the mock group. Additionally, transwell invasion was suppressed significantly. In this study changes were attributed to regulation of lysosomal and oxidative phosphorylation pathways, for example via CLN3 or ATP5J that showed decreased expression upon NEU1 knockdown (Ren et al 2015).

These findings were not supported by a micro-array analysis of changes in gene expression mediated by transcription factor cFOS. Here a 1.3 – 2.6 fold upregulation of NEU1 was found in ovarian cancer cell lines, and a 1.3 fold upregulation in a mouse model upon cFOS upregulation, suggesting the association of NEU1 upregulation with a more beneficial phenotype of ovarian cancer (Oliveira-Ferrer et al 2014).

NEU1´s implications in carcinogenesis are complicated and contradictory but further investigation shows great promise. Thus, this study hopes to further elucidate NEU1´s role in ovarian cancer via an analysis of mRNA and protein levels in types of tumour of increasing malignancy in combination with patient data.

2.2.3.2   ST6GAL1 in cancer

ST6GAL1 is a member of the family of sialyltransferases, anabolic enzymes that catalyse the transfer of sialic acids to terminal positions of carbohydrate groups of nascent glycoproteins and glycolipids. ST6GAL1 facilitates the transfer of sialic acids to terminal galactose residues of N-glycans with an α-2,6-linkage in the golgi apparatus. ST6GAL1 can also be cleaved by cathepsin-like proteases to be released in the extracellular space (Park and Lee 2013, Vajaria et al 2015).

ST6GAL1 upregulation has been found in numerous cancers and was associated with changes in adhesion, migration, invasion, apoptosis evasion, dedifferentiation of cancer cells, and poor prognosis for patients. Even plasma levels of ST6GAL1 were found to be elevated, e.g. in metastasizing CRC and could thus function as a biomarker for tumour progression or treatment response (Geßner et al 1993).

Several studies pointed to a ST6GAL1 mediated aggressive phenotype in cancer. ST6GAL1 upregulation led to a metastatic spread with an invasive multicellular outgrowth in human CRC cells and vice versa (Park and Lee 2013, Zhu et al 2001). Interestingly, ST6GAL1 expression was shown to be transcriptionally upregulated by Ras-oncogene, with the consequence of increased sialylation of integrin β1. This sialylation of integrin β1 significantly heightened cell motility and altered adhesion to collagen I. (Seales et al 2003). Similarly, high ST6GAL1 levels in mammary carcinoma cells and human anaplastic large cell lymphoma led to increased adhesion to extracellular matrix structures and increased invasiveness (Lin et al 2002, Suzuki et al 2015).

Inhibition of Galectin 3 –signalling through ST6GAL1 mediated over-sialylation was found to lead to apoptosis evasion in colon cancer cells and α-2,6-hypersialylation of glycoconjugates of the TNFR1 and the CD45 receptor blocked several apoptosis pathways via regulating receptor retention (Amano 2003, Z. Liu et al 2011, Zhuo and Bellis 2011).

Alteration of ST6GAL1 expression levels affected the invasiveness and chemosenstivity of HCC cell lines in vitro and in vivo, with a more invasive, proliferative, and chemoresistant (5-FU) phenotype upon ST6GAL1 upregulation and vice versa upon ST6GAL1 knockdown. This was at least in part attributed to the sialylation status of the cell lines itself and a changed phosphorylation status and thus activity of PI3K/AKT pathway, that were manipulated by ST6GAL1 expression levels (Zhao et al 2014).

Similarly, the regulation of PI3K/AKT pathway by ST6GAL1 was shown to be implicated in multidrug resistance in human leukaemia cell lines in vitro and vivo and bone marrow mononuclear cells of leukaemia patients (Ma et al 2014).

Another substrate of ST6GAL1 mediated sialylation conferring chemoresistance is the EGFR. Hypersialylation was shown to decrease sensitivity to chemotherapy in CRC cell lines and vice versa, suggesting EGFR sialylation status as a possible biomarker for anti-EGFR therapy (Park and Lee 2013).

Fittingly, Swindall et al found that ST6GAL1 knockdown led to a loss of cancer stem cells, which are known for their multidrug resistance and aggressive phenotype, within cancer cell populations of a human colon carcinoma cell line. In the same way, chemoresistance provoked by continuous chemotherapy treatment led to the selection of cancer stem cells with increased levels of ST6GAL1 expression. Additionally, ST6GAL1 expression correlated with the cancer stem cell markers ALDH1 and CD133 which led Swindall et al to the hypothesis of ST6GAL1 as a possible candidate for a cancer stem cell marker (Swindall et al 2013).

The importance of ST6GAL1 expression for the differentiation of non-cancerous human pluripotent stem cells was studied by Wang et al ST6GAL1 was enzymatically active and preferentially expressed in undifferentiated stem cells. Experimental silencing of ST6GAL1 with a consequential loss of terminal sialylation led to a loss of pluripotency (Yu-Chieh Wang et al 2015).

Besides cell differentiation, metastasis, and chemoresistance, ST6GAL1 activity has also been linked to resistance to radiation treatment. ST6GAL1 expression can be induced by radiation treatment and thus increases cell survival, presumably again by

β1 integrin mediated activation of the AKT pathway. (Lee et al 2010, Park and Lee 2013).

In an analysis of differing glycan structures of normal ovarian and ovarian cancer cell lines, Anugraham et al found a strong correlation between α-2,6-sialylation of hybrid and complex N-glycans and ST6GAL1 mRNA expression levels. This provides evidence that in the case of ovarian cancer the differences observed in membrane N-glycan structures on non-cancerous and cancerous cell lines are mediated by the expression rates of ST6GAL1 (Anugraham et al 2014).

With the knowledge that in ovarian cancer α-2,6-binding of sialic acids by ST6GAL1 is preferred to α-2,3-binding by the competing sialyltransferase ST3GAL6, Kuzmanov et al searched for N-linked α-2,6-sialylated glycoproteins as potential biomarkers in ascites and fluids of ovarian cysts of ovarian cancer patients and ovarian cancer cell line medium. Using ST6GAL1 sialylation as a selection criterion, they could identify 8 glycoproteins that were exclusively found in both, the biological fluids and the cancer cell medium, but not in the control fluids of benign ovarian cysts and peritoneal effusion. Furthermore, they characterized ST6GAL1 as the only consistently upregulated sialyltransferase across multiple ovarian tumour subtypes after an microarray database analysis (Kuzmanov et al 2012, P Wang et al 2005).

ST6GAL1 upregulation was also found on an mRNA level and in IHC staining of OvCa. However, no correlation was found with clinico-pathological parameters, like stage, grade or CA125 levels (Swindall et al 2013, P Wang et al 2005).

Nonetheless, a study by Christie et al showed the effect of α-2,6-sialylation on the phenotype of OvCa cell lines. Via sialylation of membrane-associated β1 integrin, the adhesive and invasive potential of the cell lines were increased upon ST6GAL1 upregulation. Cells showed increased cell adhesion to and migration towards collagen I, a known β1 integrin ligand. These changed properties are in line with a more metastatic phenotype and thus shed light on ST6GAL1´s possible contribution to peritoneal metastasis in ovarian cancer (Christie et al 2008).

As ST6GAL1 was shown to be involved in a myriad of apoptotic pathways, Schultz et al conducted a study on ST6GAL1 expression in OvCa cell lines and chemo-resistance to cisplatin treatment. Platinum derivatives belong to the first line treatments of OvCa and induce apoptosis by crosslinking DNA that leads to the activation of

caspases, amongst others via the FAS death receptor pathway. Forced overexpression of ST6GAL1 led to lower activity levels of caspase 3 and the OvCa cells could withstand higher doses of cisplatin. Likewise, ST6GAL1 silencing sensitized tumour cells to cisplatin therapy and greater activity of caspase 3 was measured. As Swindall et al showed with their selection of ST6GAL1 overexpressing colon cancer stem cells by continuous irinotecan–chemotherapy (see above), Schultz et al were able to model cisplatin resistance mechanisms by prolonged low-dose cisplatin treatment in OvCa cells. This again led to the selection of cells with higher ST6GAL1 expression (Schultz et al 2013).

The FAS pathway is a key mediator of apoptosis induction. Thus disabling of this pathway leads to a survival advantage in cancer cells. The Fas cell surface death receptor serves as a substrate for ST6GAL1 in OvCa cells and hypersialylation was shown to disable its signalling by preventing the formation of the death inducing signalling complex (DISC) and by hindering internalization of the Fas receptor and thus interrupting a positive feedback loop of apoptotic signalling (Swindall and Bellis 2011).

Recently, another pathway of ST6GAL1 expression regulation was discovered by Man Ip et al. Silencing and upregulation of p70^{S6} kinase, a downstream effector of mTOR, that was linked to peritoneal metastasis and OvCa progression, affected ST6GAL1 expression likewise. Furthermore, P-cadherin was found to be a transcriptional modulator of ST6GAL1 expression, too. P-cadherin is a possible mediator of tumour-mesothelial cell adhesion and interacts with β1 integrin. According to ST6GAL1 expression, β1 integrin sialylation status changed and with it the adhesive properties of the OvCa spheroids on the peritoneum. This provides further evidence for the ST6GAL1 mediated effects on metastasis in OvCa cells via β1 integrin sialylation and adds p70^{s6} kinase and P-cadherin as possible regulators of this pathway. Knockdown of p70^{S6} kinase and P-cadherin both led to fewer metastasis in a mouse model opening the possibility for ST6GAL1 to be a valuable target for early treatment before metastatic spread or in patients with microscopic residue (Man Ip et al 2014).

Similarly, a micro-array analysis of changes in gene expression mediated by beneficial transcription factor cFOS found a 4.3 – 5.6 fold downregulation of ST6GAL1 in ovarian cancer cell lines, and a 4.5 fold downregulation in a mouse model upon cFOS upregulation, adding another candidate for ST6GAL1 transcription regulation and

providing a further link of ST6GAL1 downregulation being associated with a less malignant phenotype in ovarian cancer (Oliveira-Ferrer et al 2014).

To my knowledge, so far no study has been published on ST6GAL1 expression as a predictive marker for clinical outcome in patients with ovarian cancer. However, increased levels of ST6GAL1 in tumours have been correlated with poorer prognosis for patients with localized clear-cell renal cell carcinoma, with ST6GAL1 expression, measured via IHC, serving as an independent predictive factor of OAS and RFI (Hai-Ou Liu et al 2015). For patients with CRC findings were not consistent. Belluco et al found a correlation for increased α-2,6 sialylation with poorer OAS, while Vasquez et al could not find a significant correlation (Lise et al 2000, Vázquez-Martín et al 2005).

Some controversy remains on the role of ST6GAL1 in cancer development, as studies emerge that do not support the widely recognized oncogenic implications of ST6GAL1. For example, in muscle invasive bladder cancer an ST6GAL1 downregulation was observed with increasing invasiveness (Antony et al 2014). Similarly, ST6GAL1 knockdown in one CRC cell line led to a more rapidly growing phenotype (Park et al 2012).

Taken in sum, the majority of findings suggest that ST6GAL1 overexpression leads to an aggressive, often metastatic phenotype in cancer cells in vitro and in vivo. ST6GAL1 expression promotes cell migration, tumor invasiveness, and multiple pathways of apoptosis evasion. Furthermore, its implication in the differentiation and selection of (cancer) stem cells could be key mechanisms explaining ST6GAL1´s association to a more malignant phenotype. Thus, downregulation of ST6GAL1 and decreased sialylation could prove to be promising targets for future anti-cancer agents.

This study will look for the applicability of ST6GAL1 expression as a prognostic marker for patient survival on an mRNA and protein level and its correlations with clinico-pathological markers and expression levels in ovarian tumours of varying malignancy.

3.   Materials and methods

3.1   Tissue samples of patients and cell lines

The tumour samples used for this study were obtained during debulking-operations of patients in the UKE between 1996 and 2012. They contain epithelial ovarian carcinoma, borderline ovarian tumour, and serous ovarian cystadenoma. Furthermore, samples of tumour free tissue (TFT), which had been extracted during the debulking process, and recurrences (REC) are included in this study. IHC was performed on formalin fixed and paraffin embedded sections. Samples used to extract ribonucleic acid (RNA) and proteins were stored in liquid nitrogen until being used. Informed consent to access their tissue and review their medical records was obtained of all the patients, and the study was conducted according to the declaration of Helsinki (Masic et al 2014).

The Hamburg tumour database stores detailed histopathological characterisations and follow-up data for most cases. Clinical outcome was followed from the date-of-surgery to the date-of-death or until December of 2014. In total, samples of 71 women were used for the qPCR, and of 213 women for the WB-analysis. Due to different assessments of quality, as described in the respective methods, the final subset actually entering statistical analysis was reduced to 52 cases for qPCR-analysis and 204 cases for the WB-analysis (Table 2). Detailed characteristics of the patient cohort of the Hamburg study collective that entered the final analysis can be found in Table 3.

Additionally, tissue samples of 24 patients were stained for an exemplary IHC. 10 of those samples (5 BOT and 5 OSC) were kindly offered by Prof. Dr. Thomas Löning from the Institute for Pathology of the Albertinen-Hospital, Hamburg.

The control for this study, the human OvCa cell line SKOV3, was obtained from the American Type Culture Collection, Manassas, VA, USA.

Table 2. Cohorts for WB and qPCR analysis and IHC including different types of ovarian tumour

	qPCR	Western Blot	IHC[d]
n	52	204[a]	24
Type of tumour			
Benign tissue	3	0	0
Ovarian serous cystadenoma	4	4[b]	5
Borderline ovarian tumour	15	12	5
Ovarian Cancer	26	176[c]	14
Recurrence	4	12	0

a – for ST6GAL1: n=202; b – for ST6GAL1: n=3; c – for ST6GAL1: n=175; d – performed with GANAB and MAN1A1

Table 3. Cohort characteristics of OvCa patients analysed in qPCR and WB

	qPCR	Western Blot
N	26	176
Age at diagnosis (Years) mean (median)	57.8 (62)	59.2 (61)
Histology of epithelial ovarian cancer		
serous-papillary	24 (92.3)	148 (84)
endometroid	1 (3.8)	10 (5.7)
mucinous	0	4 (2.3)
others/unknown	1 (3.8)	13 (7.3)
FIGO staging of ovarian cancer		
FIGO IA-IC	0	8 (4.6)
FIGO IIA-IIB	0	6 (3.4)
FIGO IIIA-IIIC	21 (80.7)	125 (71)
FIGO IV	4 (15.4)	37 (21)
Grading		
G1	2 (7.7)	9 (5.1)
G2	7 (26.9)	46 (26.1)
G3	15 (57.7)	117 (66.5)
Serum CA 125 (kU/l) at diagnosis/ before operation mean (median)	2596.9 (723)	1546.6 (542)
min- max (kU/l)	20 - 22617	18 - 22617

	qPCR	Western Blot
N	26	176
Nodal involvement		
Negative (N0)	4 (15.4)	44 (25)
Positive (N1)	16 (61.5)	101 (57.4)
Metastasis		
no metastasis (M0)	21 (80.8)	138 (78.4)
distant metastasis (excluding peritoneal metastasis) (M1)	4 (15.4)	37 (21)
Organ infiltrated by distant metastasis		
pleural effusion	1	2
pleural carcinosis	0	8
liver	2	15
others	1	9
Tumour residuum after surgery		
not macroscopically visible	21 (80.8)	122 (69.3)
<1cm^3	3 (11.5)	33 (18.8)
>1cm^3	1 (3.8)	19 (10.8)
Recurrence		
No	3 (11.5)	57 (32.4)
Yes	22 (84.6)	114 (64.8)
Recurrence-free interval (months) mean (median)	24.4 (16)	27.4 (16)
min-max (months)	11 - 83	0 - 176
Survival at the point of last follow-up		
Alive	15 (57.7)	83 (47.2)
Dead	10 (38.5)	93 (52.8)
Overall survival [a] (months) mean (median)	40.1 (31)	38.4 (30.5)
min-max (months)	15 - 103	0 - 176
Chemotherapy administered		
Carboplatin/Paclitaxel (Taxol)	19 (73.1)	127 (72.2)
other regimes based on Carboplatin	6 (22.9)	35 (19.9)
Others	0	14 (7.8)

a – including patients still alive at the last point of follow up; % in brackets, missing cases to 100% unknown

3.2   Reverse transcription and real-time qPCR

3.2.1   RNA-isolation and cDNA-synthesis

The starter cohort contained 71 RNA-samples. However, these were reduced to 52 samples that entered final analysis (see Table 2). Where there was insufficient material or signs of degradation, new RNA was isolated.

Firstly, cryo-cut sections were stained with haematoxylin and eosin (HE) after a standard protocol to assess the quality of the tumour sample. Tissue samples were used for RNA extraction, if there were more than 50% tumour-cells. Following histological assessment, three samples of tissue, which had formerly been classified as healthy, had to be excluded from further analysis as signs of tumorous infiltration were found. One sample had to be excluded as it was found to be a Mixed Mullerian Tumour and not an epithelial ovarian cancer. The selection criterion, based on the percentage of tumorous cells of the tissue, had to be softened for the samples of OSC due to the histology of this tumour, which contains often little tumorous cells (see Fig. 14).

Next, RNA was yielded by homogenising the tissue with the QIAshredder and isolating the RNA with the RNeasy Mini kit from QIAgen (for protocol see QIAGEN 2012). RNA-concentration off all samples was measured with the Thermo Scientific NanoDrop 1000 Spectrophotometer according to protocol (Thermo Fisher Scientific Inc. 2008). Thus, eight samples had to be excluded from further experiments due to signs of degradation or RNA-levels that were too low, despite the attempt of renewed RNA-isolation. A typical NanoDrop graph of a good quality probe with sufficient RNA-concentration can be seen in Fig. 6.
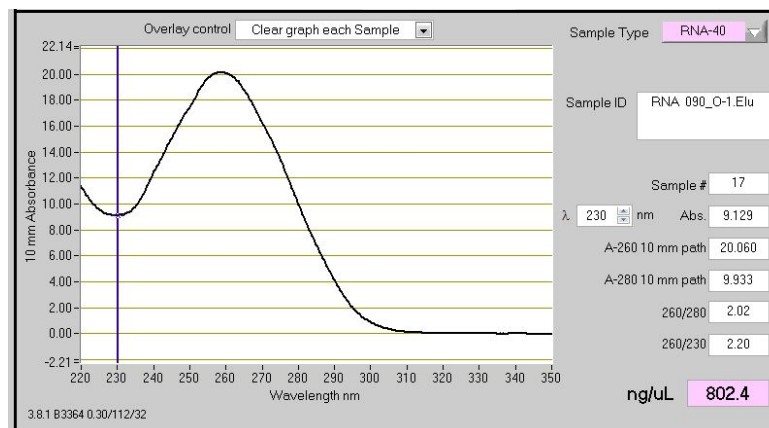
Fig. 6. Graph example for RNA concentration measurement with NanoDrop

Then cDNA (complementary deoxyribonucleic acid) was synthesized with the Thermo Scientific Maxima First Strand cDNA Synthesis Kit for qPCR according to protocol (Thermo Fisher Scientific Inc. 2012). For each probe 5µg of RNA was used as a template. For incubation the DNA Engine – PTC-200 Peltier Thermal Cycler (MJ Research) was used.

3.2.2 qPCR

Real-time qPCR was performed on 59 samples using the SYBR Premix Ex Taq II (Takara) with the multiwell-based Light Cycler 480 (Roche) according to the manufacturer's instructions (Takara Bio Inc. 2014). 1 µg of RNA-template was used per sample well. Sequence information for primers used (all of Eurofins MWG-Operon) can be found in Table 4.

All primers were diluted to a final concentration of 10 pmol/µl with RNAse-free aq. dist. prior to use. Different thermal profiles were used for GAPDH-qPCR and the other primers. Details can be found in Table 5.

Samples were analysed in duplicates and averaged using the LightCycler 96 Software. To minimise errors in measurement, the difference in C_q-value between duplicates had to stay below 0.5. The expression of target genes was normalized to the endogenous reference-gene GAPDH and put in relation to the SKOV3-control based on the $2^{-\Delta\Delta C_t}$ method (Livak and Schmittgen 2001). A GAPDH cut-off for positivity was established at $C_q < 16.1$. This led to the exclusion of seven samples from further analysis and a final cohort of 52 probes for analysis (see Table 2).

Table 4.   Sequence information of primers used for qPCR

Primer	Sequence information
GALNT12 -f	5'-CCT GGT CAA CTC TCC TTC GG -3'
GALNT12-r	5'-CCA GGC CCT CTC TCT TGT TG-3'
GALNT14-f	5'-TGC TGC TGT TCT TCT GGG TAA-3'
GALNT14-r	5'-CAG CAA GGT GTC CTC CTG TAG-3'
GCNT3-f	5'-TGA GAA GAC CAA GCT GAC GC-3'
GCNT3-r	5'-CCG TGG CAG CAA ATG TGA AC-3'
GANAB-f	5'-CCC AAT GGC CCT GTA TGG GT-3'
GANAB-r	5'-AGC GAACAT CTG TCT GTG GG-3'
MAN1A1-f	5'-GAA GGC ATG GCC CAA CAC T-3'
MAN1A1-r	5'-GTA GCG ATG GCT TCA ACA CC-3'
NEU1-f	5'-GCG ATG GAG CTT CAG CAA TG-3'
NEU1-r	5'-TGT AGT GGT TCC GGC CTT TC-3'
ST6GAL1-f	5'-AGC ACC CAG GAC CCC CAC AG-3'
ST6GAL1-r	5'-ACA TGG TCC CGG AGG TGG CA-3'
hGAPDH-f	5'-GTC AGT GGT GGA CCT GAC CT-3'
hGAPDH-r	5'-TGC TGT AGC CAA ATT CGT TG-3'

f – forward primer; r – reverse primer

Table 5.   LightCycler qPCR - thermal profile

	GAPDH		GALNT12, GALNT14, GCNT3, GANAB, MAN1A1, ST6GAL1, NEU1	
	Cycles	**Description**	**Cycles**	**Description**
Preincubation	1	95°C for 6 s	None	None
3 Step Amplification	40	95°C for 15 s 60°C for 10 s 72°C for 26 s	40	95°C for 5 s 60°C for 20 s
Melting	1	57°C for 15 s 95°C for 1 s	1	65°C for 15 s 95°C for 1 s
Cooling	1	37°C for 30 s	1	40°C for 30 s

3.3 Western Blotting

3.3.1 Measuring protein concentration

Proteins used for the Western Blots had already been isolated and stored at -80°C. 196 samples had been lysed in ice-cold b1-buffer (50 mM Tris, pH 6.8, 1% sodium dodecyl sulphate [SDS], and 10% sucrose), and 17 samples in RIPA-buffer (65 mM Tris, pH 7.4, 1% Nonidet P40, 1% Na-deoxycholate, 1 mM EDTA). Concentrations for the whole sample set were calculated via colorimetric detection using bovine serum albumin (BSA) as standard. For this the Pierce BCA Protein Assay (Thermo Scientific) was used according to the manufacturer´s instructions (Thermo Fisher Scientific Inc. 2015). The dilution scheme for the standard can be found in Table 6. Protein extracts were diluted 1:5 with 50 mM Tris/HCL-buffer and absorbance was measured on the plate reader Sunrise Remote (Tecan) at 540 nm. RIPA- or b1-buffer were used for standard dilutions depending on the buffer base in which the proteins had been lysed.

Table 6. Preparation of diluted albumin (BSA) standards

Vial	Volume of diluent (µl) B1-buffer/ RIPA-buffer	Volume of diluent (µl) 50mM Tris/HCL	Volume and source of BSA[a] (µl)	Final BSA concentration (µg/ml)
A	100	400	500 of stock	1000
B	100	525	375 of stock	750
C	50	450	500 of A	500
D	50	450	500 of C	250
E	50	450	500 of D	125
F	50	450	500 of E	62,5
G	100	400	500 of E	31,25
H	100	400	None	0 = blank

a – 2mg/ml stock concentration; dilution scheme for microplate procedure (working range = 31.25-1000µg/ml)

3.3.2 Western Blot

Samples were diluted with a 1:1 mixture of sample buffer b1/RIPA and b2 (containing 50 mM Tris, pH6.8, 3% SDS, 10% sucrose, 10% β-mercapto-ethanol, and 0.01% bromophenol-blue) to a final volume of 60µl and a final protein concentration of

333,33µg/ml. Equal amounts of protein (20µg) of each sample were loaded per well and equal loading was verified by immunoblotting with GAPDH antibodies (Santa Cruz Biotechnology, Inc.). Control samples, proteins of the cell line SKOV3, and one specific ovarian cancer sample, were loaded on each gel. The Spectra Multicolor Broad Range Protein Ladder (Thermo Scientific) was loaded as a marker on each gel. Then electrophoresis was performed using the SE600 Standard Dual Cooled Vertical Unit by Hoefer with a 10% polyacryl-amide separating gel and a 5% stacking gel. Proteins were transferred to a polyvinylidene-difluoride (PVDF) membrane (Immobilon P Transfer Membrane; Millipore). Composition of the gels and cathode-, anode and transfer buffers used are found in Tables 7 and 8. Incubation and blocking varied depending on the antibodies used (see Table 9).

Table 7. Composition of gels used for WB

WB-gels	AA/BAA-solution (ml)	Gel buffer 3x (3M Tris (pH 8.45); 0.3% SDS) (ml)	Glycerine 87% (g)	Aq. dist. (ml)	APS 10% (µl)	TEMED (µl)
10% seperating gel	7.5	10	4	8.5	150	15
5% stacking gel	1.15	2.35	0	5.95	112.5	12.5

Table 8. Composition of buffers used for electrophoresis and blotting in WB

Anode buffer	200 mM Tris (pH 8.9)
Cathode buffer	100 mM Tris (pH 8.25) 100 mM Tricine 0.1% SDS
Transfer buffer	100 mM Tris 193 mM Glycin

Western Blots were performed for GANAB, MAN1A1, NEU1, and ST6GAL1. However, a stable protein detection of NEU1 could not be established. Following antibodies failed to perform consistently: NEU1 polyclonal antibody [H00004758-A01] by abnova®, NEU1 monoclonal antibody (F-8) [sc-166824], and (H-300) [sc-32936], both by Santa Cruz Biotechnology, Inc.

After incubation with the primary antibodies (details in Table 9), blots were washed 3 times for 10 min in TBST (20 mM Tris.HCl, pH 7.6, 0.137 M NaCl, 0.05% Tween 20)

and incubated with the peroxidase-conjugated secondary antibodies for 1 hour at room temperature. For GANAB, MAN1A1, and GAPDH an anti-rabbit mouse IgG [sc-2054], for ST6GAL1 an anti-goat donkey IgG [sc-2056] (all by Santa Cruz Biotechnolgy, Inc.) were used in a 1:8000 dilution in 1.5% milkpowder.

Blots were visualized by chemiluminescence reagent (Supersignal West Pico Chemiluminescent Substrate, Thermo Scientific) using Fuji Medical X-Ray Film (Fujifilm Corporation). Band intensities were quantified by densitometry (GS-700 Imaging Densitometer, Bio-Rad) and calculated as percent-intensity of the SKOV3 control sample after correction for equal GAPDH loading.

For MAN1A1 a 2nd band around 60 kDa could be detected in most tumour samples. Hence, bands were quantified three times: (1) 72 kDa, (2) 72 kDa + 60 kDa, and (3) 60 kDa.

Nine samples appeared to be degenerated on visualisation and were excluded from further analysis (final n=204). Two samples appeared to be degenerated only in the detection of ST6GAL1, while they seemed normal in the other blots. These samples were only excluded from further analysis of ST6GAL1.

Reblots were performed according to the manual with Re-blot Plus Mild Antibody Stripping Solution (Millipore) (Millipore 2008).

Table 9. Primary antibodies used for WB analysis

Antibodies	Species	Dilution	Blocking	Time for incubation	Predicted band size (kDa)
GANAB [EPR12376] (abcam) Lot: GR162882-1	Rabbit IgG, mc	1:3000 in 1.5% milkpowder	5% milkpowder	1 hr at rt	107
MAN1A1 [EPR9957(B)] (abcam) Lot: GR103953-2	Rabbit IgG, mc	1:1000 in 1.5% milkpowder	5% milkpow-der	1 hr at rt	72
ST6GAL1 [AF5924] (R&D Systems) Lot: CDSF0113081	Goat IgG, pc	1:1000 in 1% Blocking reagent (Roche), diluted in 0,1M Maleic acid buffer	1% Blocking reagent (Roche), diluted in 0,1M Maleic acid buffer	Overnight, 4°C	50
GAPDH (FL335) [sc-25778] (Santa Cruz) Lot: D1613	Rabbit IgG, pc	1:5000 in 1.5% milkpowder	5% milkpow-der	1 hr at rt	37

mc – monoclonal; pc – polyclonal; rt – room temperature

3.4   Immunohistochemistry

Exemplary IHC was performed on formalin-fixed and paraffin-embedded tissue sections for GANAB and MAN1A1. The 14 sections of OvCa were selected based on differing expression rates in the Western Blots. No further data was available for the 5 BOT and 5 OSC. Thus, they were chosen on tissue availability.

Based on standard horseradish-peroxidase (HRP)-protocol (e.g. abcam 2014), sections were deparaffinised in xylene and rehydrated through descending alcohol to water (100% EtOH, 96% EtOH, 80% EtOH, water). 10 mM Sodium Citrate buffer was used for heat-induced antigen-retrieval with a vegetable steamer at 100°C for 20 minutes. Activity of the endogenous peroxidase was quenched, using 0.5% H_2O_2 for 30 minutes to reduce background-staining, and sections were washed with TBS pH7.6. Then, they were incubated overnight at 4°C in a humidified chamber with the respective primary antibody. GANAB rabbit IgG (ab 76349, abcam) was used in a 1:100 dilution with antibody diluent (DAKO), MAN1A1 rabbit IgG (NB600-077, Novusbio; Lot: 04K4799) in a 1:4000 dilution. As an isotype control Rabbit IgG (X0903, DAKO) was used in identical IgG end concentrations.

Sections were rinsed the next day with TBS pH 7.6 and incubated for 30 min with the secondary antibody (BA-1000 Biotinylated Anti-Rabbit IgG, Vector), then washed again and incubated for 30 min with Vectastain ABC Elite Reagent (Vector), washed again, and finally stained with DAB Peroxidase substrate Solution (Linearis) until the desired stain intensity developed (GANAB ~ 40sec; MAN1A1 ~ 3min). All sections were then counterstained in HE, dehydrated cleared, and mounted.

Stained sections were digitalized using a Mirax Midi slide scanner (Zeiss).

3.5   Statistical Analysis

Statistical analysis was conducted by using SPSS software Version 21 (IBM SPSS Statistics). Differences in expression/intensity between the five groups of tumour (TFT, OSC, BOT, OvCa, and REC) in the qPCR and WBs were evaluated by one-way ANOVA. Scheffé tests were used for post-hoc analysis as sample size varied between the groups.

Analysis of clinical data from the Hamburg Tumour database was only conducted for patients with ovarian cancer, due to the small sample size of the other types of tumour. RFI and OAS, starting from the time after operation, were analysed by Kaplan-Meier analysis and log-rank tests. Cases were divided into four equal groups depending on their expression of the respective genes. If quartiles showed similar characteristics, they were merged to two groups, e.g. lower 75% vs upper 25%. Mann-Whitney U tests were used to analyse qPCR expressions or WB intensities with clinicopathological factors (groups as shown in Table 10). When there were less than 5 observations in one group the exact significance (2-sided test) p-value (probability value) was regarded, otherwise the asymptomatic significance (2-sided test) was stated. Cox regression models were calculated for uni- and multivariate analysis.

For measurement of associations across assays, Pearson correlation was used.

Probability values (p-values) less than 0.05 were regarded as statistically significant and p-values less than 0.1 as statistical trends

Table 10. Groups used for analysis of prognostic parameters

Vs	
Grading	
G1 + G2	G3
FIGO stage of Ovarian Cancer	
FIGO I + FIGO II	FIGO III + FIGO IV
Nodal involvement	
Negative (N0)	Positive (N1)
Metastasis	
no signs of distant metastasis (M0)	distant metastasis (excluding peritoneal metastasis) (M1)
Tumour residuum after surgery	
not macroscopically visible	macroscopically visible

4. Results

4.1 Analysis of the Hamburg study cohort

4.1.1 qPCR

A total of 52 patients were included in this study for qPCR analysis, with 26 of them being diagnosed with ovarian cancer (detailed characteristics of the study cohort are listed in Table 2 and 3). All patients with ovarian cancer underwent a state-of-the-art treatment and in the vast majority optimal debulking could be achieved (only one patient [3.8%] with more than 1 cm^3 residual tumour). 25 patients (96%) received a first-line chemotherapy based on platinum, predominantly in combination with a taxane.

Mean age at diagnosis was 57.8 years and the RFI ranged between 11 and 83 month with a mean of 24.4 months; OAS ranged from 15 to 103 months with a mean of 40.1 months, this includes the 57.7% of patients that were still alive at the last point of follow up for this study in December 2014.

The majority of patients had a G3 (57.7%) serous papillary ovarian cancer (92.3%) and were classified as stage FIGO III or above (96.3%).

4.1.2 Western Blot

204 patients entered this study for WB analysis, of which 176 were diagnosed with ovarian cancer (detailed characteristics can be found in Table 2 and 3). In the majority of ovarian cancer patients optimal debulking could be achieved. However, 19 patients (10.8%) stayed with a residual tumour greater than 1cm^3 after surgery. First-line chemotherapy based on platinum was administered to 162 patients (92.1%), again predominantly in combination with a taxane (72.2%).

The mean age at diagnosis of the study cohort was 59.2 years with a mean RFI of 27.4 months that ranged from 0 – 176 months; OAS ranged from 0 – 176 months with a mean of 38.4 months after diagnosis, including the 47.2% of patients still alive at the last point of follow up.

Most patients had a serous papillary tumour (84%) with a G3 grading (66.5%) and were staged FIGO III or above (92%).

4.2   Enzymes of the O-Glycosylation pathway

4.2.1 GALNT12 and GALNT14 mRNA expression and correlation with clinicopathological characteristics and patient survival

Results of prior RNA analysis via microarray analysis and a xenograft model indicated a possible involvement of GALNT12 and GALNT14 in ovarian cancer progression. For GALNT12 and GALNT14, as for all the glycosylation enzymes covered in this study, a deregulation by cFOS had been found. Thus, GALNT12 and GALNT14 were included in the set of genes chosen for this study that underwent qPCR analysis by comparing expression rates depending on types of ovarian tumour with varying malignancy and correlation with histopathological data

.

Expression rates can be seen in Fig. 7. They were obtained after normalization to GAPDH and in comparison to the control SKOV3 using the $2^{-\Delta\Delta C_t}$ method. Thus, SKOV3 expression was set as 100% and gene expression is in comparison to SKOV3 expression. For GALNT12, expression varied extensively with a range between 34.6 – 1738.8% (mean 503.2%); GALNT14 had an even broader range from 4.2 – 2053.5% (mean 310.4%). Via ANOVA no significant difference in the expression rates of the types of tumour could be found (GALNT12 p=0.891; GALNT14 p=0.179). Neither were there significant correlations in the Mann-Whitney U tests with the histopathological data or with the RFI and OAS in Kaplan-Meier analysis. Solely a trend can be described that linked GALNT14 up- and downregulation to a longer RFI while medium expression was found in the patient group with the shortest RFI (p=0.052). Table 11 shows the respective p-values.
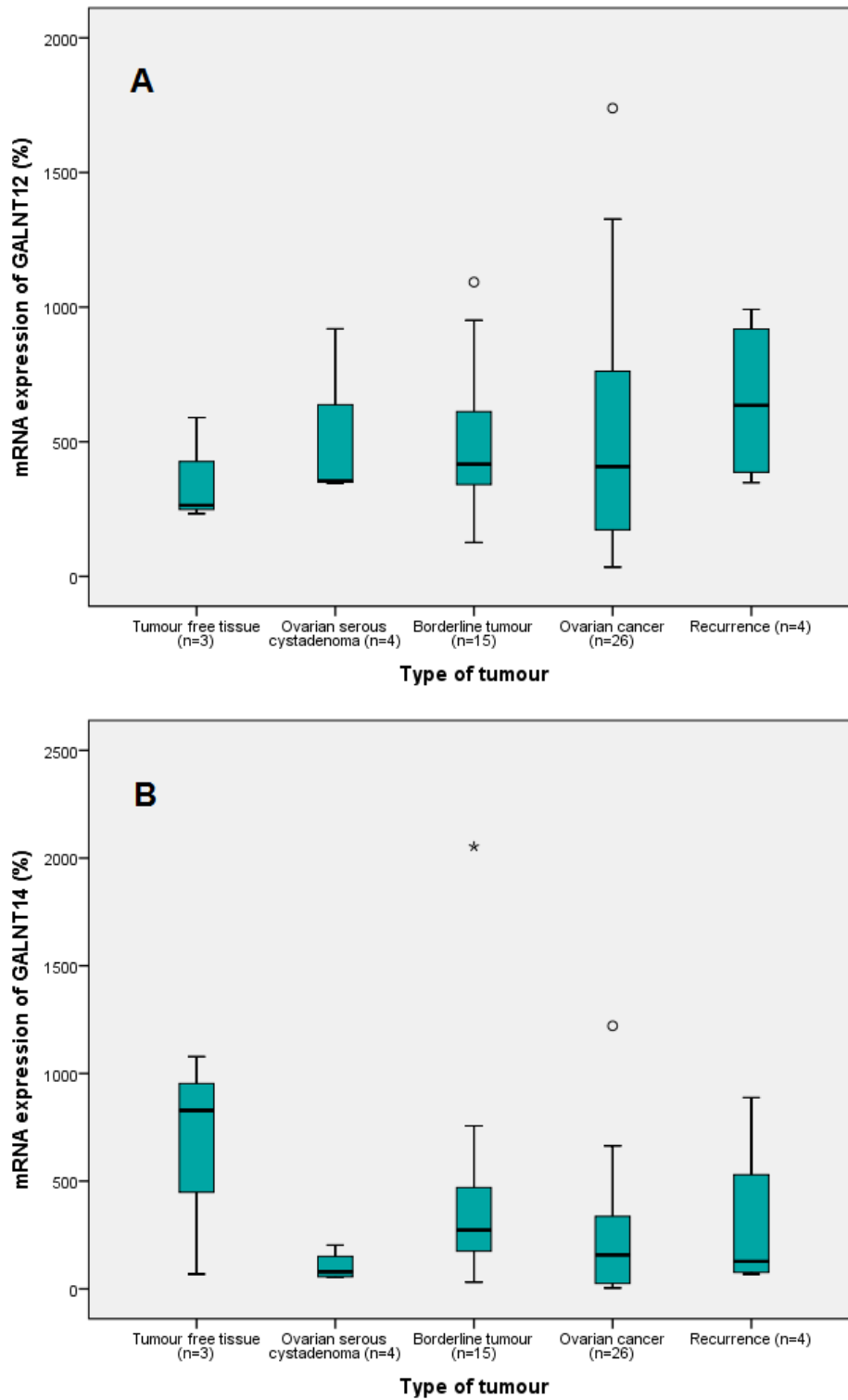
Fig. 7. GALNT12 (A) and GALNT14 (B) expression by type of tumour (qPCR). Boxplot

Table 11. Correlation (p-values) of GALNT12 and GALNT14 with clinicopathological factors (qPCR)

qPCR	Grading	Nodal involvement	Distant metastasis	Tumour residuum after surgery	Kaplan-Meier analysis RFI[b]	Kaplan-Meier analysis OAS[b]
GALNT12	0.096[a]	0.892[a]	0.858[a]	1[a]	0.759	0.659
GALNT14	0.290[a]	0.682[a]	0.496[a]	0.971[a]	0.052	0.817

a - exact significance used; b - GALNT12 and GALNT14 were divided in quartiles based on expression rates

4.2.2 GCNT3 mRNA expression and correlation with clinicopathological characteristics and patient survival

GCNT3 was chosen as a third representative of enzymes of the O-glycosylation pathway, after analysis via microarrays and a xenograft model indicated a possible involvement in ovarian cancer progression (Oliveira-Ferrer et al 2014).

Figure 8 shows a boxplot of GCNT3 expression in qPCR analysis. Overall, expression ranged from 0 – 76.3% (mean 6.6%), with BOT having the largest range of expression (0.5 – 76.3%, mean 20.4%). One-way ANOVA showed significant differences between the different types of tumour (p=0.001), which was confirmed by Scheffé post-hoc testing between BOT and OvCa (p=0.001).

Lower GCNT3 expression correlated significantly with M0 (no distant metastasis) staging in the ovarian cancer patient cohort (Mann-Whitney U=700; p=0.003, exact significance used), with 2 of 4 M1 cases, but only 1 of 21 M0 tumours showing elevated GCNT3 expression, as shown in Fig. 9.

No other significant result was found for GCNT3 expression in correlation with clinicopathological factors or in Kaplan-Meier analysis (see Table 12).
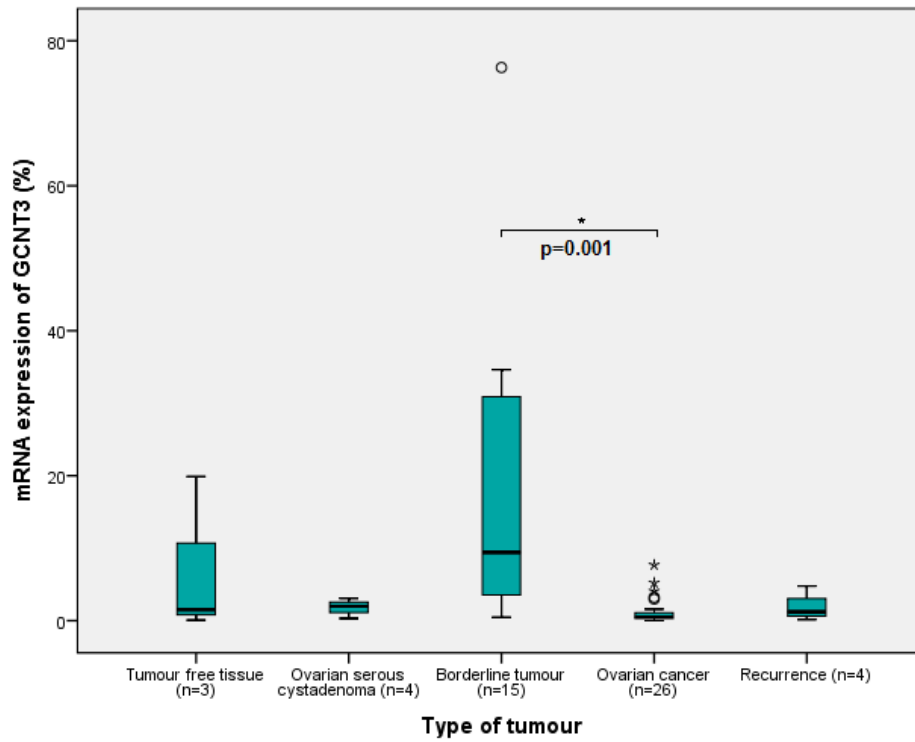
Fig. 8. GCNT3 expression by type of tumour (qPCR). BOT differed significantly from OvCa (p=0.001). Boxplot
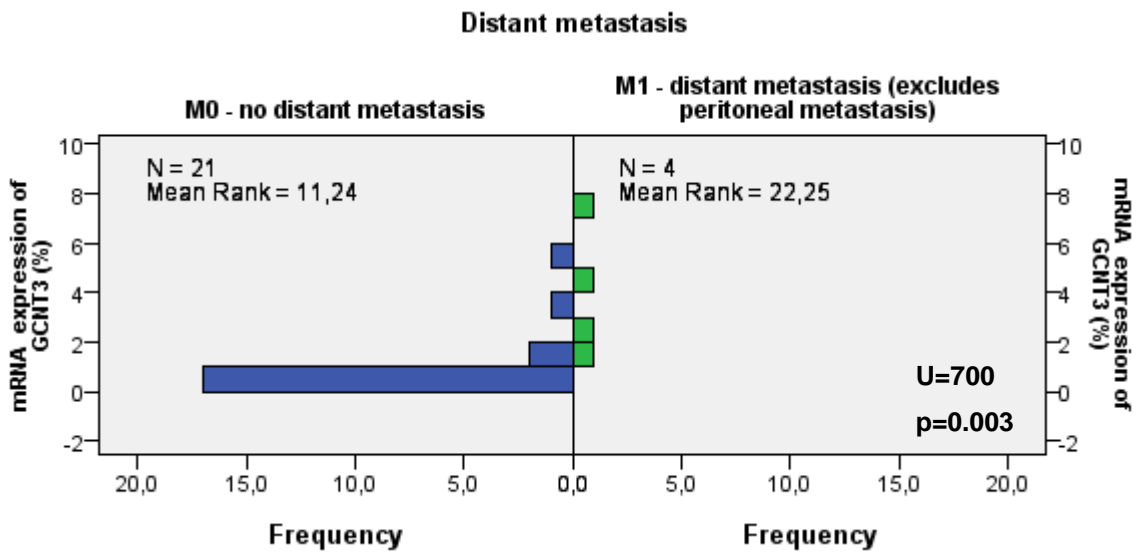

Fig. 9. Gain of GCNT3 expression correlates with distant metastasis (qPCR). Mann-Whitney U test

Table 12. Correlation (p-values) of GCNT3 with clinicopathological factors (qPCR)

qPCR	Grading	Nodal involvement	Distant metastasis	Tumour residuum after surgery	Kaplan-Meier analysis RFI[b]	Kaplan-Meier analysis OAS[b]
GCNT3	0.640[a]	0.249[a]	**0.003[a]**	0.496[a]	0.367	0.825

a - exact significance used; b – GCNT3 was divided in quartiles based on expression rates

4.3   Enzymes of the N-Glycosylation pathway

4.3.1 GANAB

4.3.1.1   GANAB mRNA expression and correlation with clinicopathological factors and patient survival

This study aimed to include not only examples of the O-glycosylation but also of the N-glycosylation pathway that is known to affect adhesion properties and expression and control of cell surface receptors in cancerous tissues (Varki et al 2009a). Previously, GANAB, which is involved in the early processing of N-glycans, had been found to be upregulated in SKOV3 by the transcription factor cFOS (Levy-Ontman et al 2014, Oliveira-Ferrer et al 2014). Therefore, it was a promising gene for further analysis.

A boxplot of GANAB qPCR expression in the different types of tumour can be seen in Fig. 10. Expression ranged from 38.4 – 557.8%% (mean 221%). One-way ANOVA showed significant differences between the different types of tumour (p=0.001). Mean expression levels of GANAB in BOT were significantly lower than those found in TFT (Scheffé post-hoc p=0.02) and OSC (Scheffé post-hoc p=0.019).

Q-PCR expression for GANAB in the case of M0 and M1 staging differed significantly, with lower expression rates in the M0 patient cohort (Mann-Whitney U=69; p=0.047, exact significance used; see Fig. 11).

No further significant clinicopathological correlations were found for GANAB in the analysis of qPCR expression-data. Kaplan-Meier analysis for RFI and OAS was insignificant. For a summary of all p-values see Table 13.
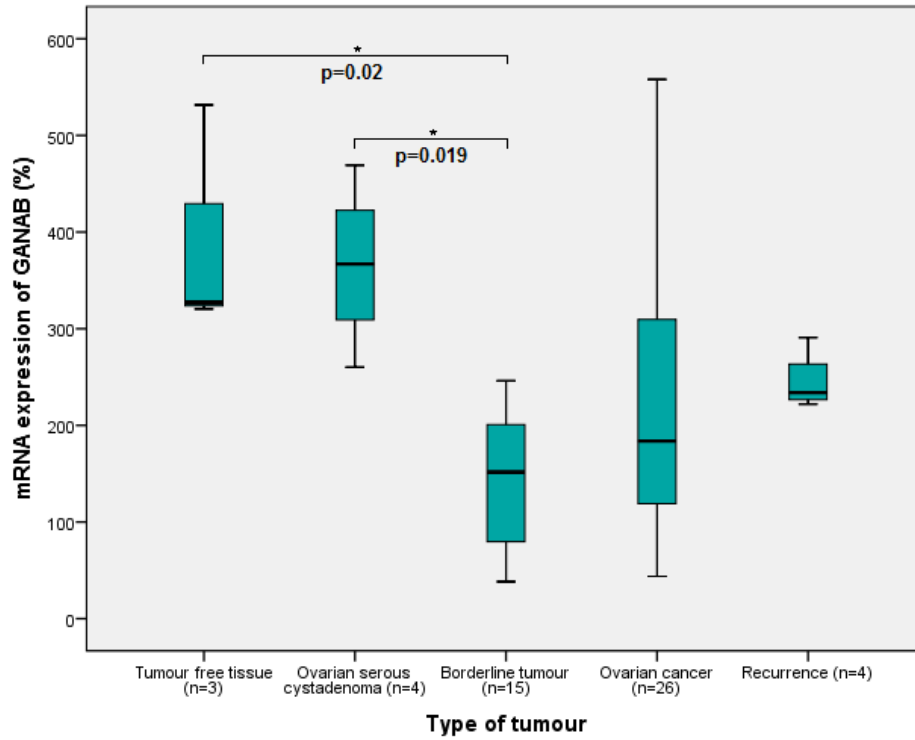
Fig. 10. GANAB expression by type of tumour (qPCR). BOT differed significantly from TFT (p=0.02) and OSC (p=0.019). Boxplot

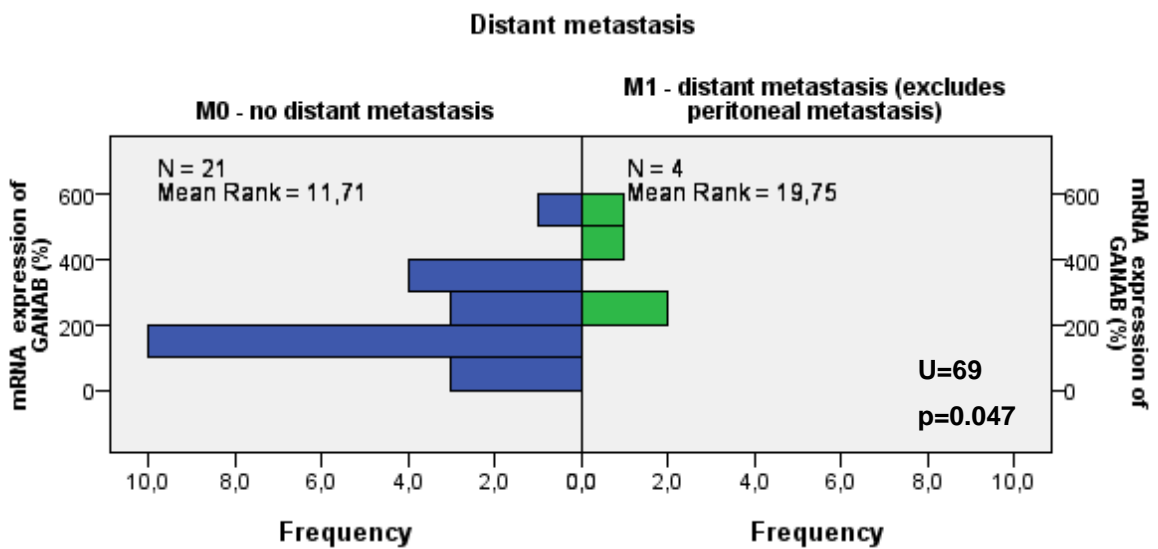Fig. 11. Gain of GANAB expression correlates with distant metastasis (qPCR). Mann-Whitney U test

Table 13. Correlation (p-values) of GANAB with clinicopathological factors (qPCR)

qPCR	Grading	Nodal involvement	Distant metastasis	Tumour residuum after surgery	Kaplan-Meier analysis RFI[b]	Kaplan-Meier analysis OAS[b]
GANAB	0.772[a]	0.750[a]	**0.047[a]**	0.154[a]	0.564	0.794

a - exact significance used; b – GANAB was divided in quartiles based on expression rates

4.3.1.2   GANAB protein expression and correlation with clinicopathological factors and patient survival

GANAB is a key regulator of the N-glycosylation pathway (Levy-Ontman et al 2014). A significant difference in mRNA expression rates for BOT had been found in qPCR analysis (see above). Thus, there was a high interest to gain more information on GANAB expression in different tumours and as a prognostic factor in ovarian cancer by examining protein expression rates via WB analysis in a larger cohort.

A representative WB of GANAB and its control for equal loading, GAPDH, are shown in Fig. 12. As control, proteins from the ovarian cancer cell line SKOV3 and a tumour from the cohort (T-control) were included in each gel. For densitometry and statistical analysis SKOV3 expression was defined at 100%.
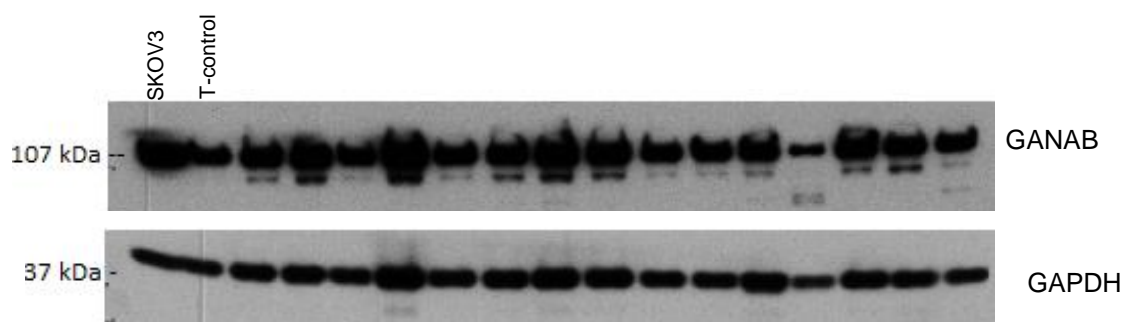

Fig. 12. Exemplary western blot of GANAB (107 kDa) and its loading control GAPDH (37 kDa) of 15 ovarian neoplasms. SKOV3 and T-control served as control between blots.

There was high expression of GANAB in SKOV3 cells at around 107 kDA and range varied from 5.4-300.3% (mean 204.4%) in tumour cells. One-way ANOVA yielded no significant differences in GANAB protein expression between the types of tumour (p=0.585). Thus, the expression difference on an RNA level between OSC and BOT could not be reproduced on the protein level for GANAB. Intensity rates after densitometry analysis can be seen in Fig. 13.

On further analysis, no statistically significant results were found for the GANAB protein expression in correlation with clinicopathological factors or in Kaplan-Meier Analysis of the RFI or OAS. For a display of p-values of all correlations tested see Table 14.
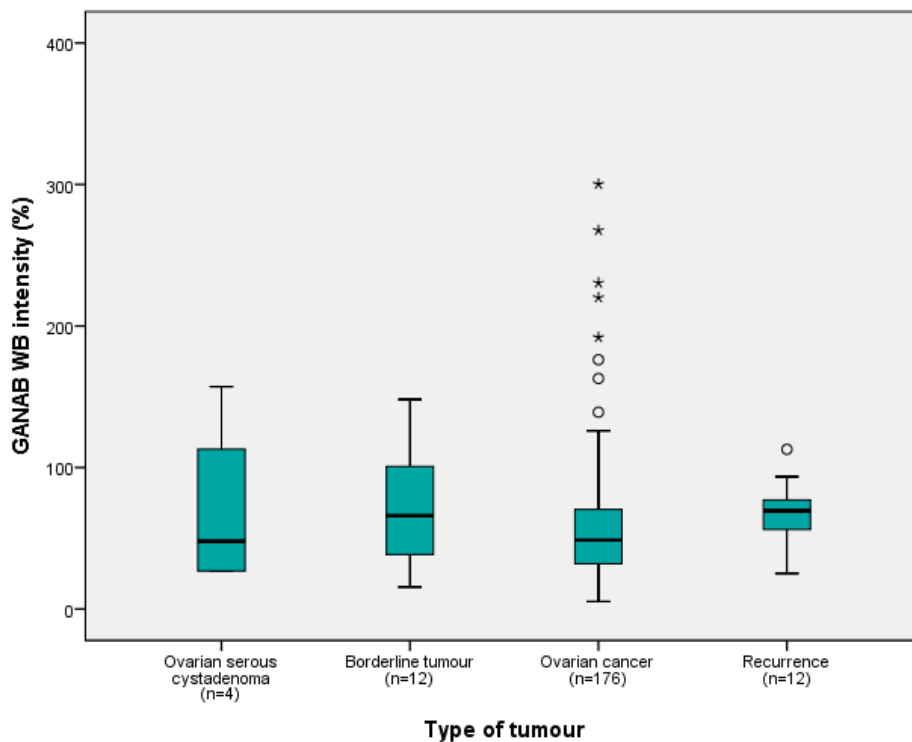
Fig. 13. GANAB intensity by type of tumour (WB). Boxplot

Table 14. Correlation (p-value) of GANAB with clinicopathological factors (WB)

WB	Grading	FIGO stage	Nodal involvement	Distant metastasis	Tumour residuum after surgery	Kaplan-Meier analysis RFI[a]	Kaplan-Meier analysis OAS[a]
GANAB	0.504	0.100	0.843	0.293	0.488	0.762	0.198

 a - GANAB was divided in quartiles based on expression rates

4.3.1.4   GANAB immunohistochemistry

To assess GANAB expression in the tumour tissue and different types of tumour, that contained varying portions of stromal fibroblasts, IHC was performed on exemplary paraffin sections of 5 OSC, 5 BOT, and 14 OvCa. Representative results, showing examples of the different types of tumours and the isotype control, are shown in Fig. 14.

Cellular GANAB immunostaining of varying, mostly strong, intensity was present in tumour cells (Fig. 14). In all sections tumour cells were stained stronger by GANAB than the weak to moderate GANAB reactivity of stromal fibroblasts. The isotype control was negative (E in Fig. 14).

Of all the types of tumours, GANAB reactivity of stromal fibroblasts was strongest in OSC, with a partly cytoplasmic and membranous staining pattern, while tumour cells showed a cytoplasmic staining with stronger intensity towards the lumen (see A in Fig. 14). A similar staining pattern could be observed for the tumour cells of BOT, while stromal fibroblasts showed weak or absent cytoplasmic or membranous staining (see B in Fig. 14). Most OvCa showed strong GANAB reactivity in the tumorous areas. Staining was mostly homogenous (e.g. C in Fig. 14), but there were also sections with a more granular cytoplasmic immunoreactivity (see D in Fig. 14). In addition, stromal fibroblasts displayed weak to no GANAB reactivity in OvCa.
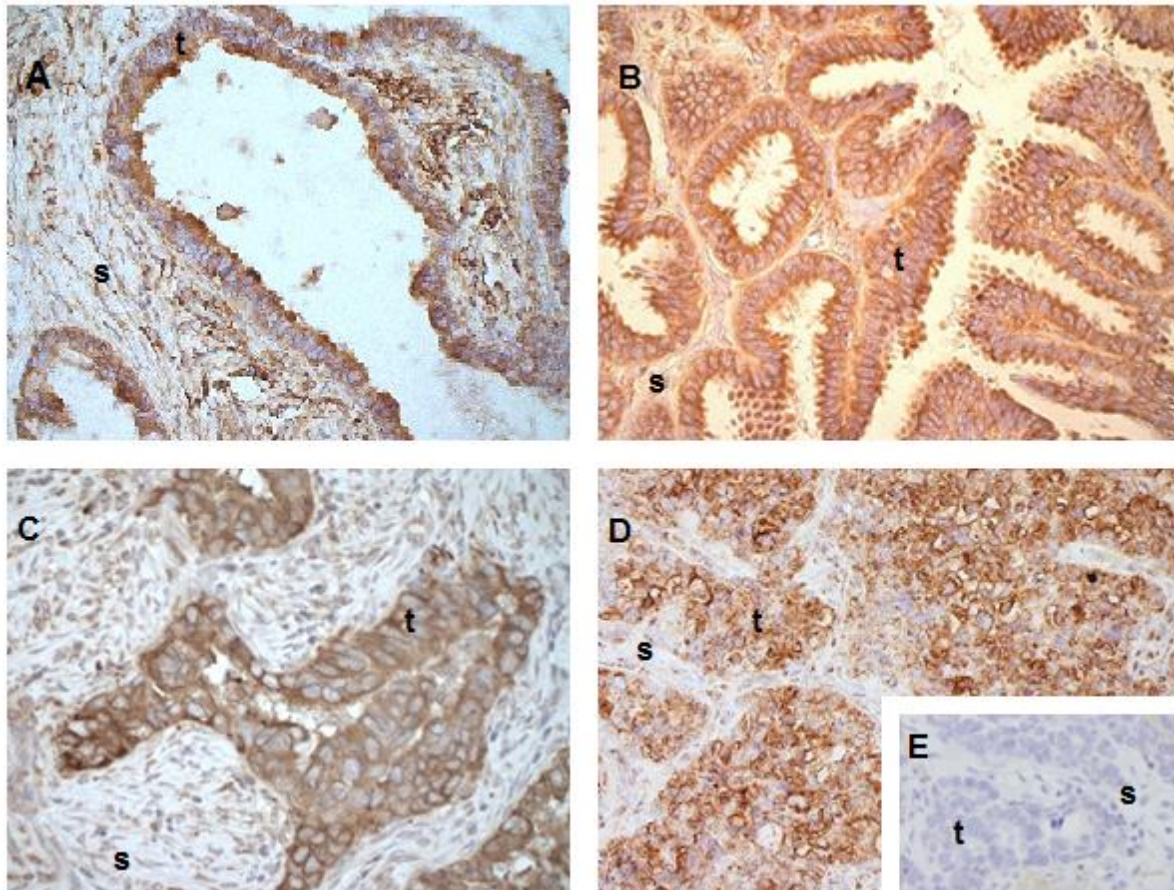
Fig. 14. GANAB immunohistochemistry on ovarian neoplasms (representative sections). (A) OSC with strong cytoplasmic immunoreactivitiy in tumour cells (t) and moderate to strong immunostaining of stromal fibroblasts (s), 200x. (B) BOT with strong cytoplasmic immunoreactivity in tumour cells (t) and weak immunostaining of stromal fibroblasts (s), 400x. (C) Moderately differentiated OvCa with homogenous strong cytoplasmic immunostaining in tumour cells (t) and weak immunoreactivity of stromal fibroblasts (s), 400x. (D) Poorly differentiated OvCa with granular cytoplasmic immunoreactivity in tumour cells (t) and weak immunostaining of stromal fibroblasts (s), 200x. (E) Negative isotype control on poorly differentiated OvCa with no staining of tumour cells (t) and stromal fibroblasts (s), 200x.

4.3.1.5   Cross-assay analysis

Protein expression is not solely regulated by gene expression as post-transcriptional, translational, and protein-degradation regulation can all affect the measured expression rate, too (Vogel and Marcotte 2012). Therefore, Pearson correlation was calculated between GANAB expression rates in qPCR and WB. Samples of 37 patients had been included in both assays. On comparison of the whole lot, a significant correlation was found between the expression rates on an mRNA and protein level (Pearson correlation 0.344; p=0.037). On the other hand, a closer comparison of only ovarian cancers showed no significant correlation (see Table 15).

Table 15. Cross-assay analysis of GANAB (qPCR and WB)

GANAB	Pearson Correlation between qPCR- and WB expression	p-value
Whole study cohort (n=37)[a]	0.344	**0.037**
OvCa (n=23)	0.313	0.146

4.3.2 MAN1A1

4.3.2.1   MAN1A1 mRNA expression and correlation with clinicopathological factors and patient survival

MAN1A1, which is involved in the optional trimming of N-glycans, was selected for further analysis as it was found to be upregulated by the transcription factor cFOS in microarrays and a xenograft model (Oliveira-Ferrer et al 2014).

Fig. 15 shows a boxplot of MAN1A1 expression in qPCR analysis. There was a wide range of expression from 77.9 – 16427.9% (mean 2055.1%). One-way ANOVA showed significant differences between the different types of tumour (p=0.000), which was confirmed by Scheffé post-hoc testing between benign tissue and all the other groups of tumour (all p=0.000) and for OSC with BOT (p=0.01) and OvCa (p=0.017).

Higher MAN1A1 expression correlated significantly with M1 staging in the patient cohort (Mann-Whitney U=74; p=0.015, exact significance used), as shown in Fig. 16.

No further significant correlations were found for MAN1A1 in the analysis of qPCR expression-data. Additionally, Kaplan-Meier analysis for RFI and OAS was insignificant (see Table 16 for a full list of p-values).
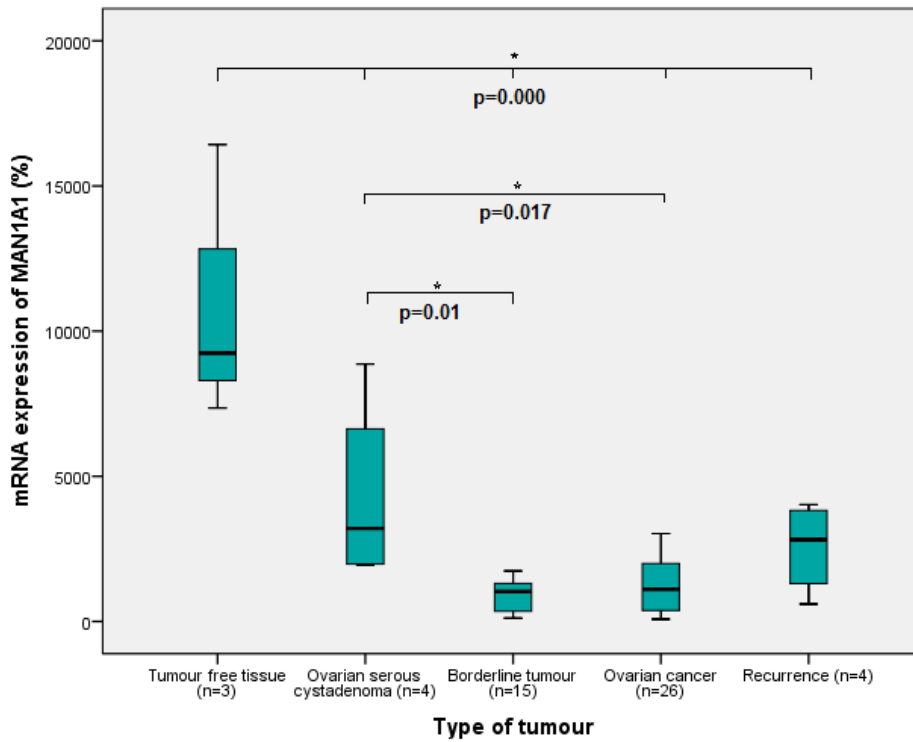
Fig. 15. MAN1A1 expression by type of tumour (qPCR). TFT differed significantly from all other types of tumours (p=0.000) and OSC differed significantly from BOT (p=0.01) and OvCa (p=0.017). Boxplot
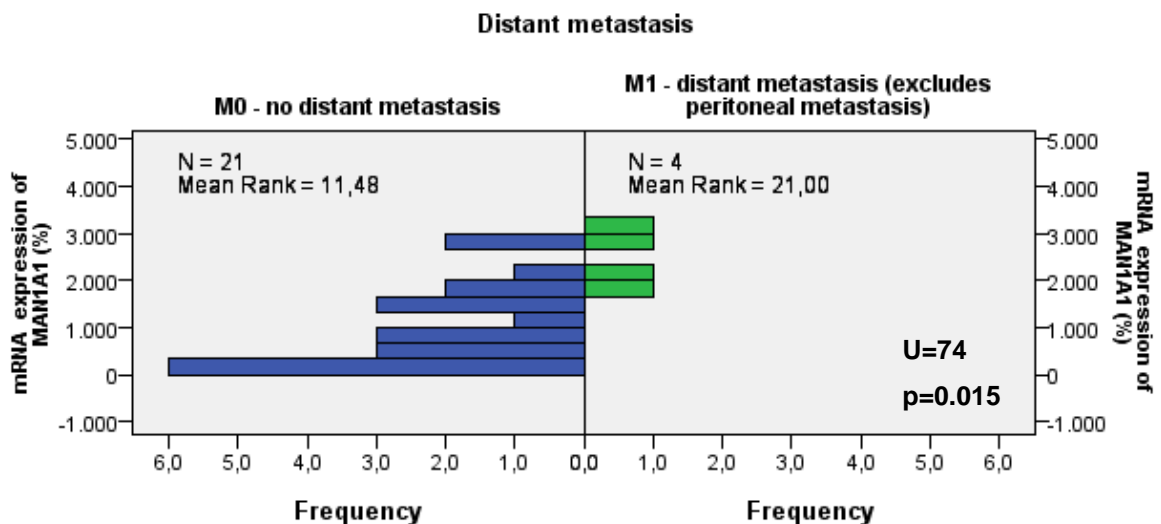

Fig. 16. Gain of MAN1A1 expression correlates with distant metastasis (qPCR). Mann-Whitney U test

Table 16. Correlation (p-value) of MAN1A1 with clinicopathological factors (qPCR)

qPCR	Grading	Nodal involvement	Distant metastasis	Tumour residuum after surgery	Kaplan-Meier analysis RFI[b]	Kaplan-Meier analysis OAS[b]
MAN1A1	0.953[a]	0.148[a]	**0.015[a]**	0.452[a]	0.689	0.607

a - exact significance used; b – MAN1A1 was divided in quartiles based on expression rates

4.3.2.2   MAN1A1 protein expression and correlation with clinicopathological factors

In order to further characterise the role of MAN1A1 in ovarian tumours, WB analysis in a cohort of 204 patients was performed.

A representative WB of MAN1A1 and its control for equal loading, GAPDH, can be seen in Fig. 17. Proteins from the OvCa cell line SKOV3 and one tumour (T-control) were included in each gel as controls. MAN1A1 expression in SKOV3 was defined at 100% for statistical analysis.

MAN1A1 was strongly expressed and consistently detected around 72 kDa in the SKOV3 control and the ovarian tumours. A second band appeared around 60 kDa in most tumour samples, whereas it could not be detected in the tumour cell line SKOV3. All densitometric analysis was conducted with expression levels of the expected band at 72 kDa. Additionally, tests were run with the cumulated expression values of the 72 kDa and 60 kDA band, and 60 kDa alone. In the following, results of these two will be stated in brackets after the main analysis, unless they are singular results, in which case they are stated in the main text.
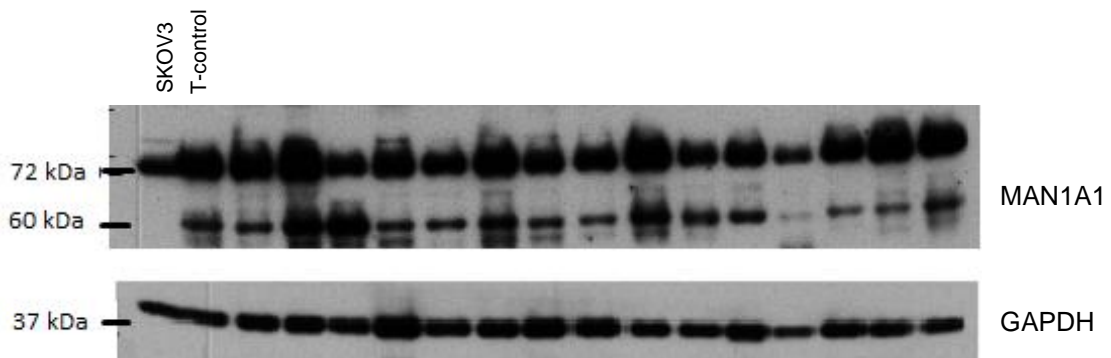
Fig. 17. Exemplary western blot of MAN1A1 (72 kDa) and its loading control GAPDH (37 kDa) of 15 ovarian neoplasms. SKOV3 and T-control served as control between blots. A second band for MAN1A1 was detected for most tumours but not the tumour cell line SKOV3 around 60 kDa.

Results of densitometry ranged between 1.1 – 2898.4% (mean: 375.6%) [72 kDa + 60 kDa: 2.7 - 4556.1%, mean: 562.1%; 60 kDa: 0.4 - 716.8%, mean: 103%]. A difference in expression via ANOVA (p=0.000) could only be detected for the 60 kDa band, with significantly higher intensity rates in OSC and BOT than in OvCa and REC (OSC vs OvCa: p=0.001; OSC vs REC: p= 0.006; BOT vs OvCa: p=0.001; BOT vs REC: p=0.035) [ANOVA 72 kDa p=0.227; ANOVA 72 kDa + 60 kDa p=0.765]. MAN1A1 intensity rates after densitometry analysis can be seen in Fig. 18.

Fig. 18. MAN1A1 intensities by type of tumour for the bands at (A) 72 kDa, (B) 60 kDa, and (C) 72 kDa + 60 kDa. In 60 kDa, OSC and BOT differed significantly from OvCa (p=0.001) and REC (p=0.006 and p=0.035 respectively) (WB). Boxplots
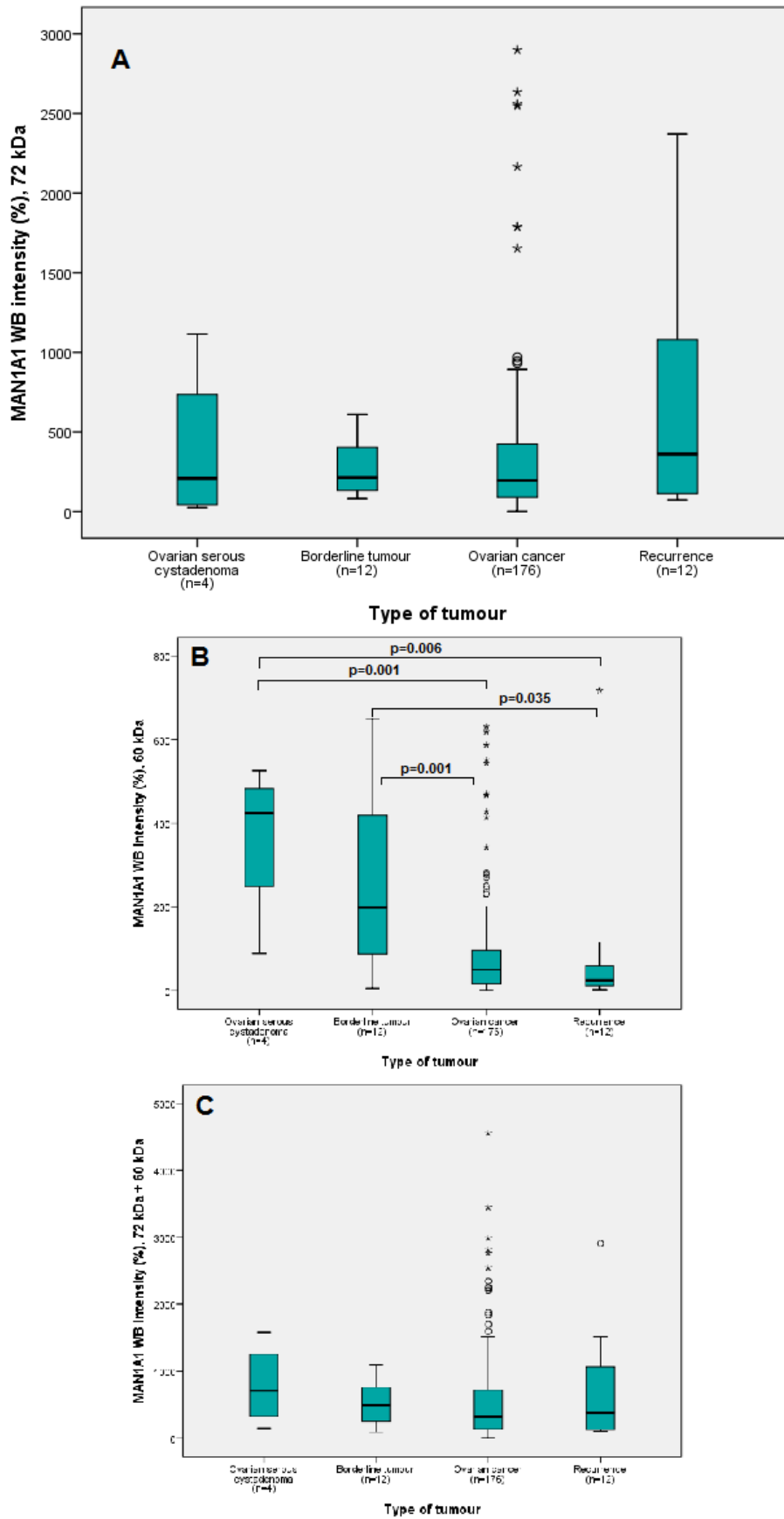
Gain of MAN1A1 expression was significantly more frequent in higher FIGO staging (FIGO I/FIGO II vs FIGO III/FIGO IV: Mann-Whitney U=1689; p=0.002; see Fig. 19) [72 kDa + 60 kDa: Mann-Whitney U=1679; p=0,003] and patients with distant metastasis (Mann-Whitney U=3199; p=0,018; see Fig. 21) [72 kDa + 60 kDa: Mann-Whitney U=3160; p=0,027]. Interestingly, a significant correlation of higher MAN1A1 expression with regional lymph node metastasis was only found in the cumulated expression values of the 72 kDa and 60 kDa bands (Mann-Whitney U=7889; p=0.026; see Fig. 20). MAN1A1 levels were also significantly elevated for patients with macroscopically visible tumour residuum after surgery in comparison to patients with optimal debulking (Mann-Whitney U=4019; p=0,005; see Fig. 22) [60 kDa: Mann-Whitney U=3931; p=0,013]. For a detailed list of all p-values obtained see Table 17.
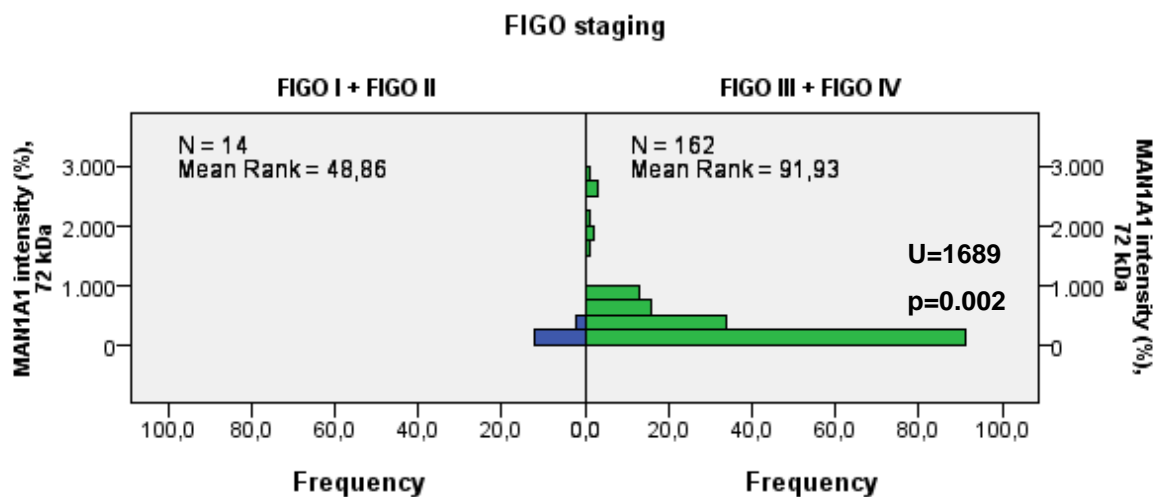

Fig. 19. Gain of MAN1A1 expression correlates with higher FIGO staging (WB). Mann-Whitney U test
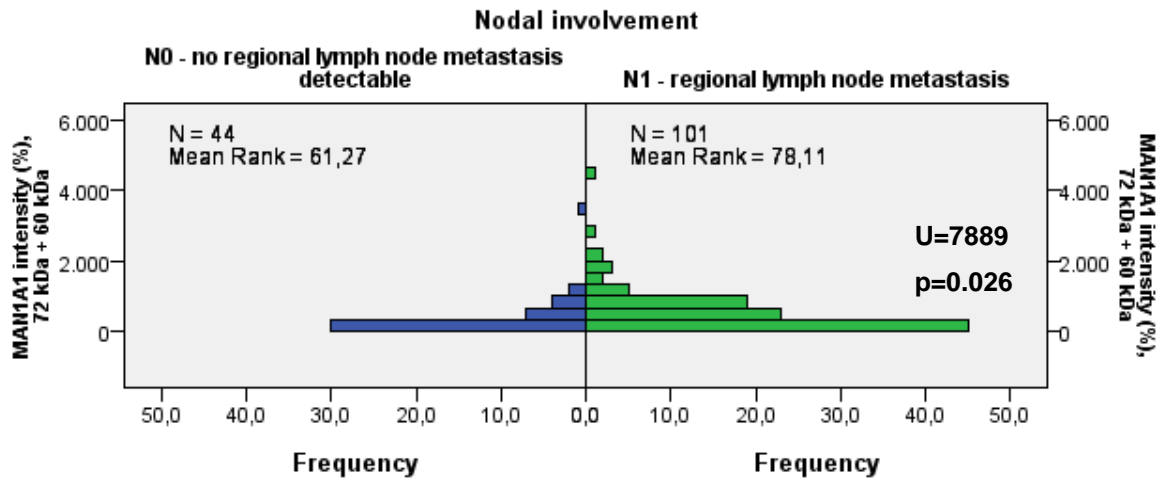
Fig. 20. Gain of MAN1A1 expression correlates with N1 staging (WB). Mann-Whitney U test
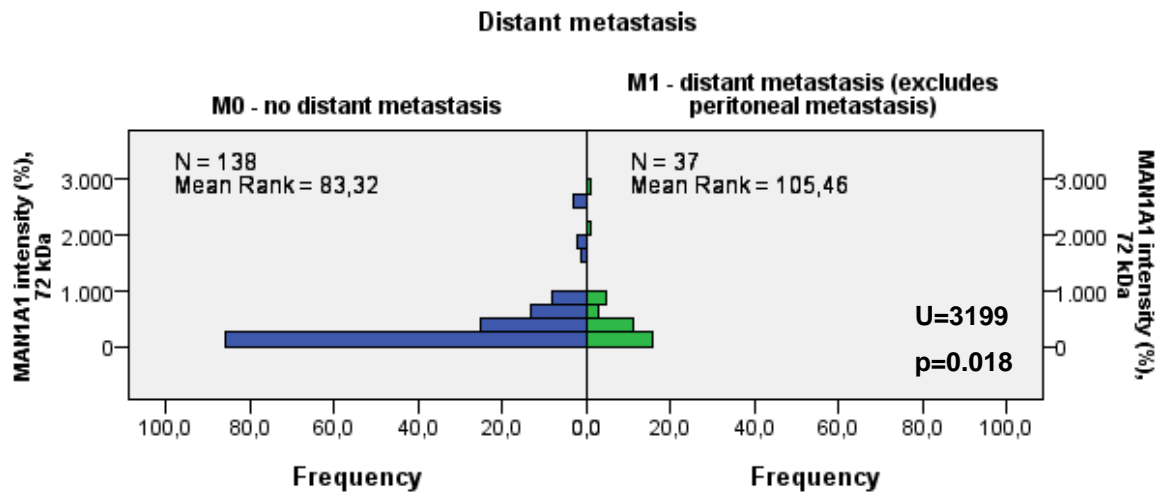
Fig. 21. Gain of MAN1A1 expression correlates with distant metastasis (WB). Mann-Whitney U test
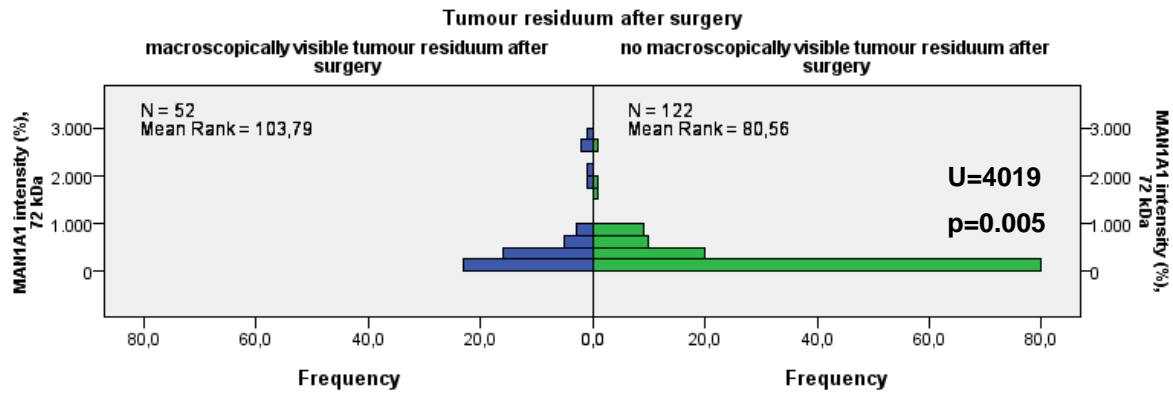
Fig. 22. Low MAN1A1 expression correlates with optimal debulking (WB). Mann-Whitney U test

Table 17. Correlation (p-value) of MAN1A1 with clinicopathological factors (WB).

WB	Grading	FIGO stage	Nodal involvement	Distant metastasis	Tumour residuum after surgery	Kaplan-Meier analysis RFI[a]	Kaplan-Meier analysis OAS[a]
MAN1A1, 72 kDa	0.405	**0.002**	0.140	**0.018**	**0.005**	**0.032**	**0.022**
MAN1A1, 72 kDa + 60 kDa	0.729	**0.003**	**0.026**	**0.027**	0.118	**0.038**	0.085
MAN1A, 60 kDa	0.585	0.883	0.921	**0.069**	**0.013**	0.399	**0.023**

a - MAN1A1 was divided by expression in the lower 75% vs upper 25%

4.3.2.3   MAN1A1 protein expression and analysis of survival

In order to study the prognostic impact of differing MAN1A1 expression levels, Kaplan-Meier analysis was performed using the long-term follow-up information for the patient cohort. To enhance the prognostic significance, survival rates of the upper quartile of MAN1A1 expression were compared to the lower 75% of expression levels. Higher MAN1A1 expression was associated with a significantly shorter RFI (mean: 24.2 and 53.8 months for patients with the upper 25% and lowest 75% MAN1A1 expression; p=0.032; median: 20 and 16 months; see Fig. 23) [72 kDa + 60 kDa:

p=0.038]. The same could be observed for OAS (mean: 40.9 and 73.2 months for patients with the upper 25% vs lowest 75% MAN1A1 expression; p=0.022; median: 41 and 54 months; see Fig. 24) [72 kDa + 60 kDa: p=0.085; 60 kDa: p=0.023].

MAN1A1 expression as a prognostic factor retained its significance for OAS in multivariate Cox regression analysis, with an increased risk of death for patients with high MAN1A1 expression (Hazard ratio 1.74; 95% CI 1.01-3.00; p=0.045), despite the correlation with the prognostic factors of high FIGO staging, less than optimal debulking, and metastases (see above). However, MAN1A1 expression did not remain a significant independent prognostic factor for RFI upon multivariate Cox regression (see Table 18 for full analysis).
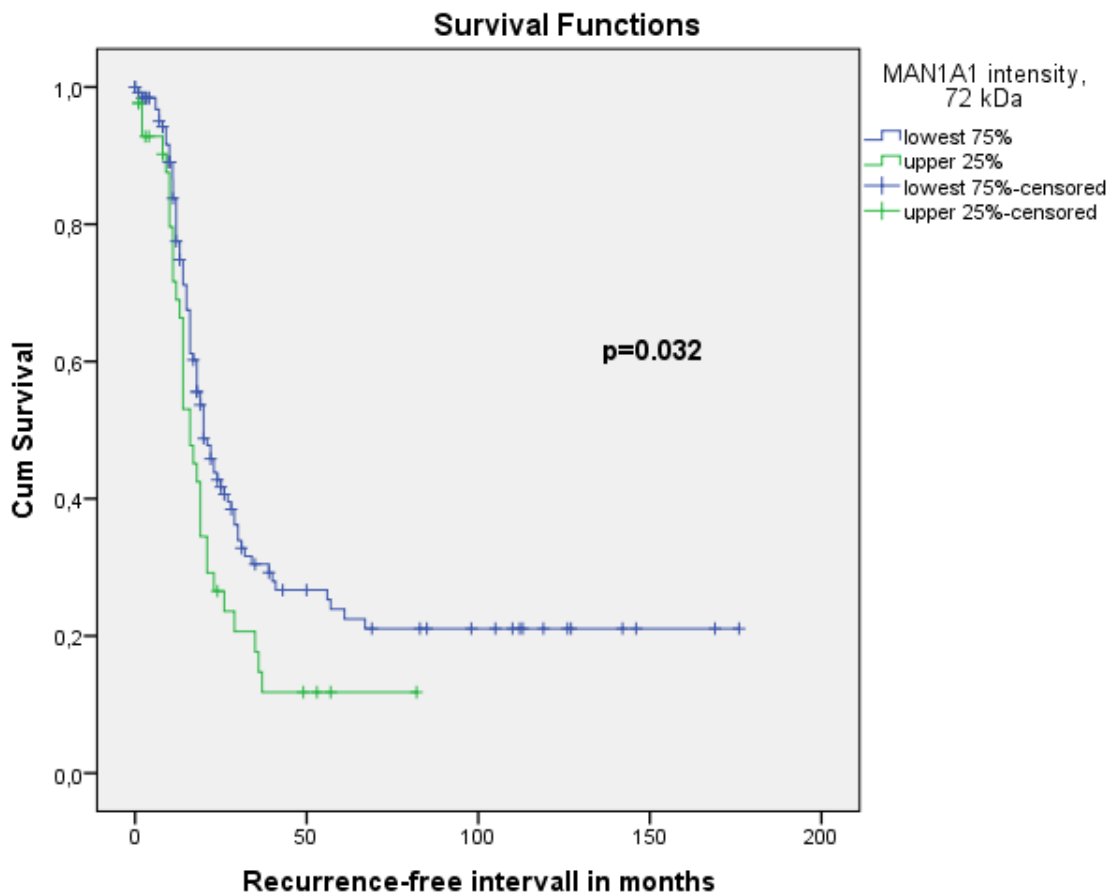
Fig. 20. Kaplan-Meier analysis of recurrence-free interval based on MAN1A1 expression. High MAN1A1 levels are associated significantly with a shorter RFI (mean: 24.2 vs 53.8 months; p=0.032). Kaplan-Meier curves were generated from 176 patients with a mean RFI of 24.4 months. Patients were stratified based on the highest quartile of MAN1A1 expression vs the lower 75%. Censored cases are indicated by vertical bars and p-value after log-rank test is shown.
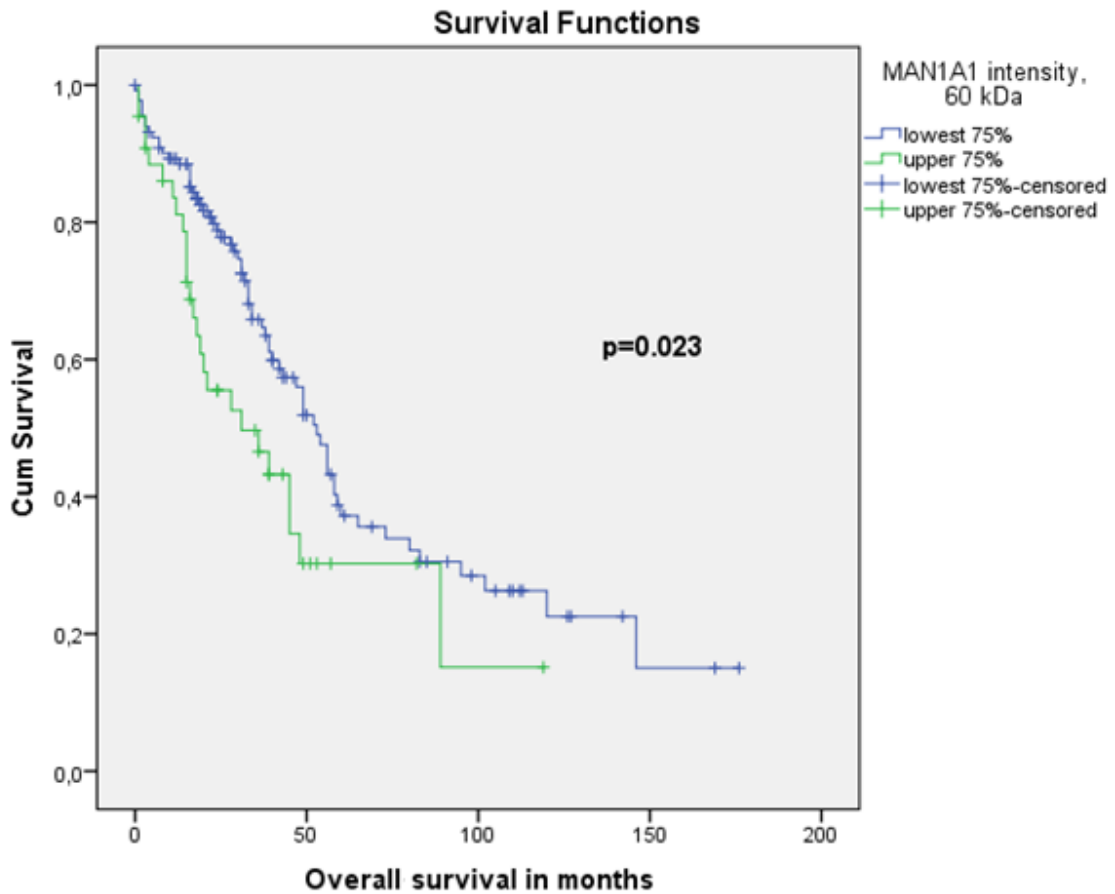
Fig. 21. Kaplan-Meier analysis of overall survival based on MAN1A1 expression. High MAN1A1 levels are correlated with a shorter OAS (mean: 40.9 vs 73.2 months; p=0.023). Kaplan-Meier curves were generated from 176 patients with a mean OAS of 40.1 months. Patients were stratified based on the highest quartile of MAN1A1 expression vs the lower 75%. Censored cases are indicated by vertical bars and p-value after log-rank test is shown.

Table 18. Multivariate Cox regression analysis including grading, FIGO stage, nodal involvement, distant metastasis, tumour residuum after surgery, and MAN1A1 expression (WB data, 72 kDa band)

| Characteristics		Hazard ratio	95% confidence interval	p-value
Recurrence-free interval (n=136)				
MAN1A1 expression	MAN1A1 lower 75% vs upper quartile	1.26	0.77-2.08	0.359
Grading	G1/G2 vs G3	0.75	0.47-1.19	0.224
FIGO stage	FIGOI/FIGOII vs FIGOIII/FIGOIV	2.87	0.82-10.03	0.099
Nodal status	N0 vs N1	2.46	1.38-4.36	**0.002**
Distant metastasis	M0 vs M1	1.76	1.04-3.00	**0.036**
Tumour residuum after surgery	not macroscopically visible vs macroscopically visible	1.70	1.02-2.83	**0.043**
Overall survival (n=141)				
MAN1A1 expression	MAN1A1 lower 75% vs upper quartile	1.74	1.01-3.00	**0.045**
Grading	G1/G2 vs G3	0.99	0.59-1.68	0.975
FIGO stage	FIGOI/FIGOII vs FIGOIII/FIGOIV	3.22	0.70-14.80	0.131
Nodal status	N0 vs N1	1.55	0.83-2.92	0.169
Distant metastasis	M0 vs M1	2.67	1.59-4.50	**0.000**
Tumour residuum after surgery	not macroscopically visible vs macroscopically visible	2.36	1.36-4.08	**0.002**

4.3.2.4   MAN1A1 immunohistochemistry

To gain further insights into MAN1A1 expression in the tumorous tissues, IHC was performed on exemplary paraffin sections of 5 OSC, 5 BOT, and 14 OvCa sections. Representative results with examples of the staining pattern of different types of tumours and the isotype control are shown in Fig. 25.

MAN1A1 immunostaining was detected in varying, mostly medium, intensity in tumour cells (Fig. 25). Generally, these were stained stronger than the stromal fibroblasts which showed only weak to no MAN1A1 reactivity. The isotype control was negative (E in Fig. 25).

OSC showed a strong cytoplasmic MAN1A1 reactivity, with a partly granular staining pattern especially towards the lumen (see A in Fig. 25). BOT showed a similarly distributed but weaker cytoplasmic MAN1A1 reactivity (see B in Fig. 25). Staining intensity of OvCa in the tumorous areas varied widely in intensity from weak to strong staining but repeated the mostly granular cytoplasmic immunoreactivity, while stromal fibroblasts showed weak to no MAN1A1 reactivity in OvCa (see C and D in Fig. 25).
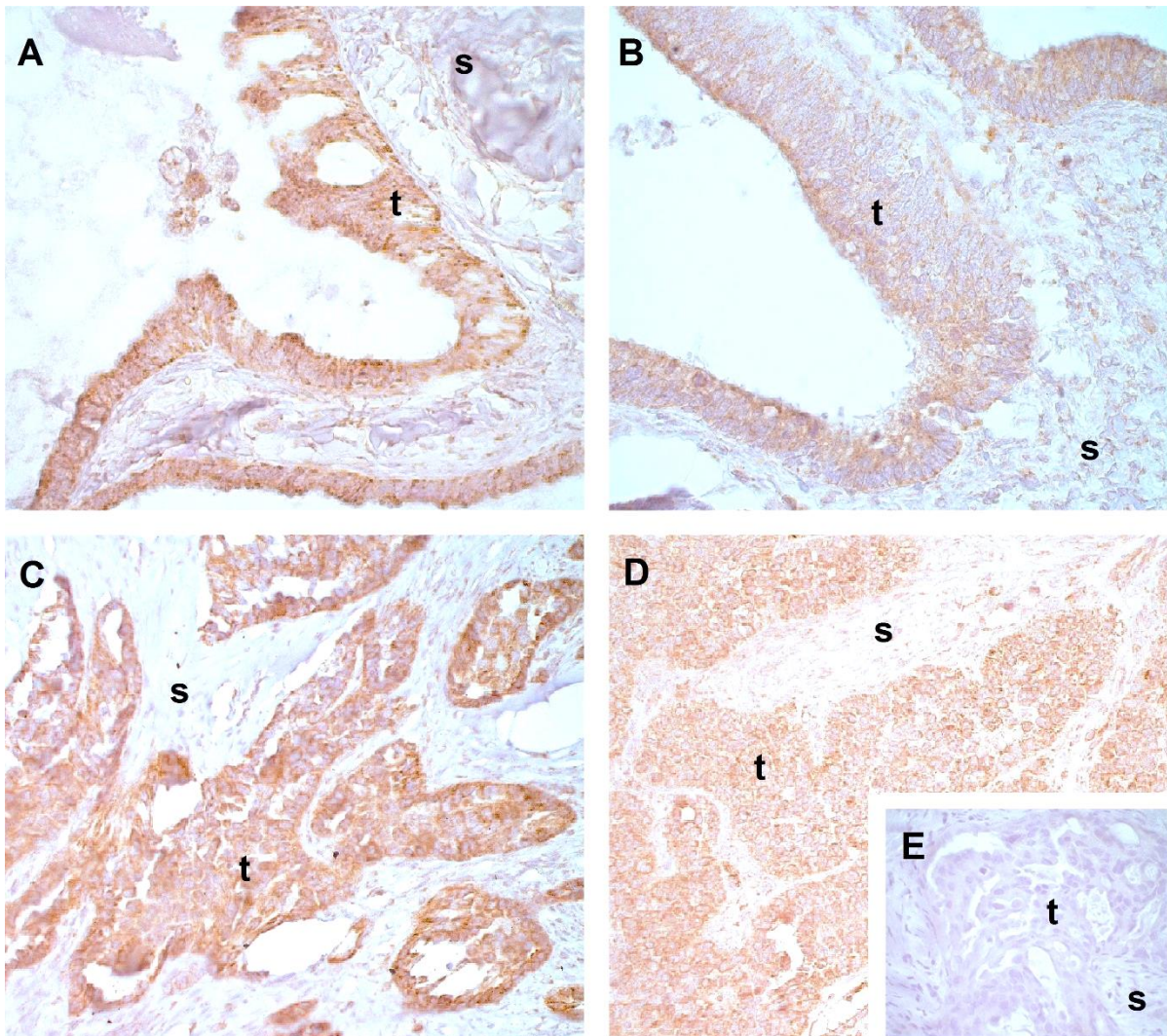
Fig. 22. MAN1A1 immunohistochemistry on ovarian neoplasms (representative sections). (A) OSC with strong cytoplasmic immunoreactivity in tumour cells (t) and weak immunostaining of some stromal fibroblasts (s), 400x. (B) BOT with medium cytoplasmic immunoreactivity in tumour cells (t) and weak immunostaining of some stromal fibroblasts (s), 400x. (C) Moderately differentiated OvCa with medium to strong granular cytoplasmic immunostaining in tumour cells (t) and weak immunoreactivity of some stromal fibroblasts (s), 200x. (D) Moderately differentiated OvCa with medium granular cytoplasmic staining in tumour cells and weak immunostaining of stromal fibroblasts (s), 200x. (E) Negative isotype control on moderately differentiated OvCa with no staining of tumour cells (t) and stromal fibroblasts (s), 400x.

4.3.2.5   Cross-assay analysis

Expression levels of MAN1A1 were obtained on an mRNA and protein level. Thus, Pearson correlation was calculated between the two assays to test for possible regulation processes between the two steps in protein synthesis.

Protein and mRNA expression levels for the 37 corresponding probes correlated significantly (Pearson correlation 0.586; p=0.000) [72 kDa + 60 kDa: Pearson correlation 0.493; p=0.002; 60 kDa: Pearson correlation 0.379; p=0.021]. However, only the correlation for OvCa remained statistically significant on a closer comparison by each type of tumour (Pearson correlation 0.583; p=0.003; n=23) [60 kDa: Pearson correlation 0.556; p=0.003].

Table 19. Cross-assay analysis of MAN1A1 (qPCR and WB)

MAN1A1	72 kDa		72 kDa + 60 kDa		60 kDa	
	Pearson Correlation between qPCR- and WB expression	p-value	Pearson Correlation between qPCR- and WB expression	p-value	Pearson Correlation between qPCR- and WB expression	p-value
Whole study cohort (n=37)[a]	**0.586**	**0.000**	**0.493**	**0.002**	**0.379**	**0.021**
OvCa (n=23)	**0.583**	**0.003**	0.336	0.117	**0.556**	**0.006**

4.4   Enzymes participating in optional trimming of sugar residues

4.4.1 NEU1

4.4.1.1   NEU1 mRNA expression and correlation with clinicopathological factors and patient survival

The sialidase NEU1 is implicated in optional trimming of sugar residues and thus participates in the last steps of glycosylation. Results of prior RNA analysis via microarrays and xenograft model indicated a possible involvement of NEU1 in ovarian cancer progression (Oliveira-Ferrer et al 2014).

A boxplot of NEU1 qPCR expression in the different types of tumour can be seen in Fig. 26. Expression ranged from 151.6 – 3701.4% (mean 1133.6%). One-way ANOVA showed significant differences between the different types of tumour (p=0.026). However, this could not be confirmed on Scheffé post-hoc testing.
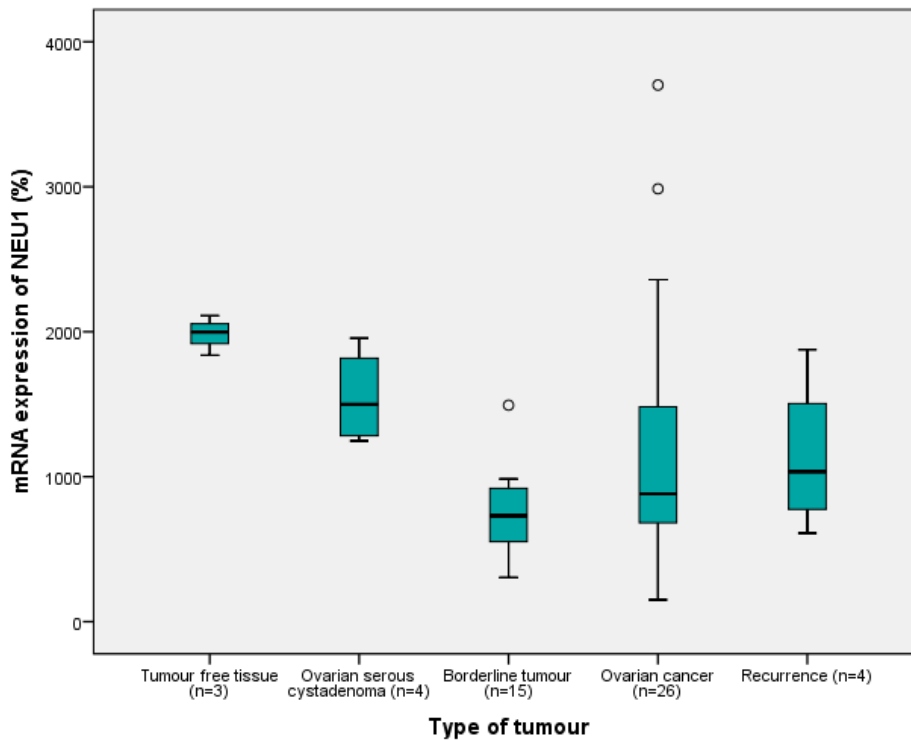
Fig. 23. NEU1 intensities by type of tumour (qPCR). Boxplot

Low NEU1 expression in ovarian cancers was associated significantly with N0 staging (Mann-Whitney U=53.5, p=0.039, exact significance used; see Fig. 27) and M0 staging (Mann-Whitney U=80; p=0.002, exact significance used, see Fig. 28). Low NEU1 expression was also found significantly more often in patients where optimal debulking had been achieved (Mann-Whitney U=72, p=0.025, exact significance used; see Fig. 29). For a detailed list of p-values of all clinicopathological factors analysed with qPCR expression data, see Table 20. Kaplan-Meier analysis of RFI and OAS was not significant for NEU1.
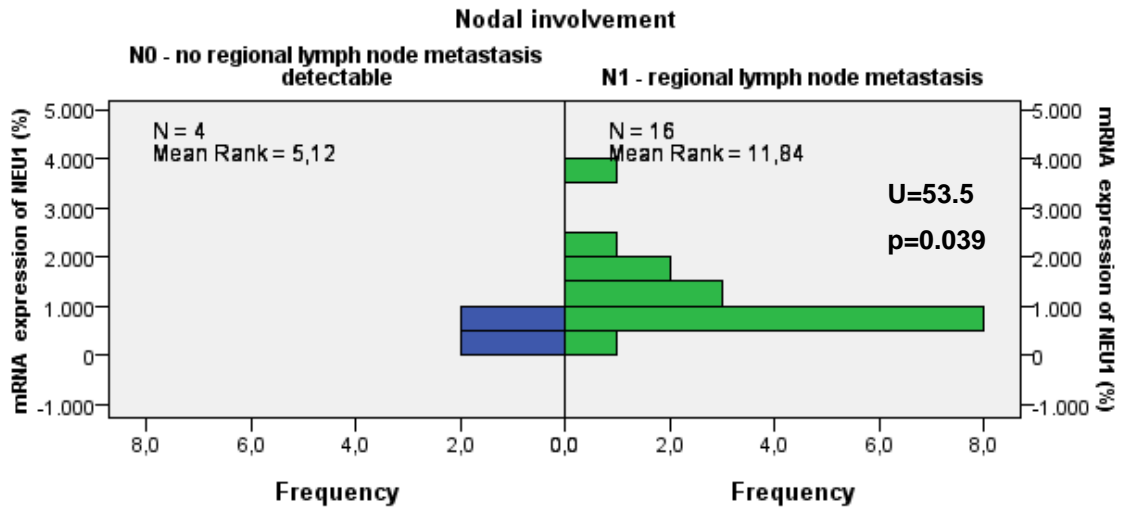
Fig. 27. Gain of NEU1 expression correlates with N1 staging (qPCR). Mann-Whitney U test
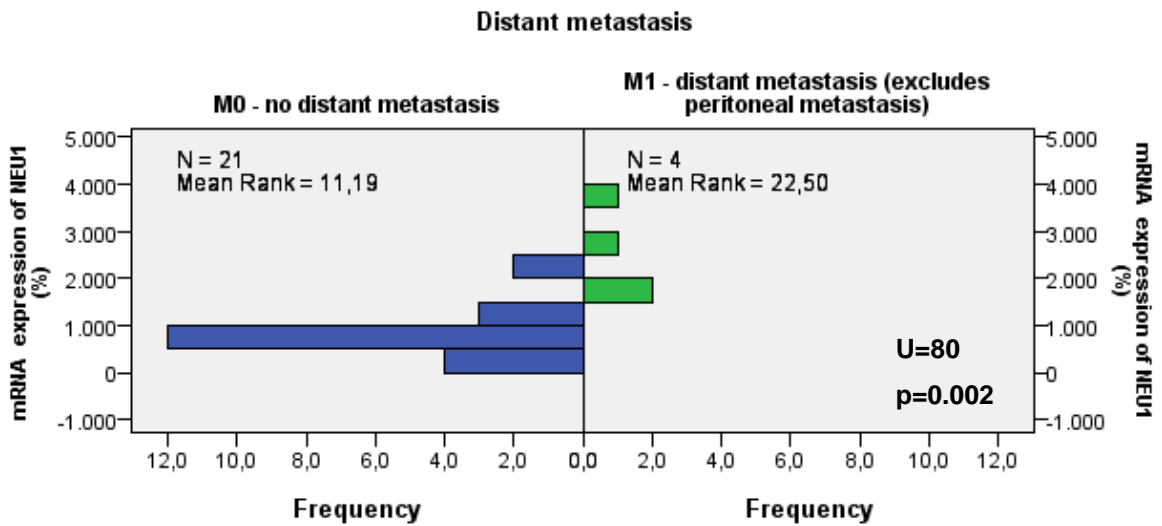
Fig. 248. Gain of NEU1 expression correlates with distant metastasis (qPCR). Mann-Whitney U test
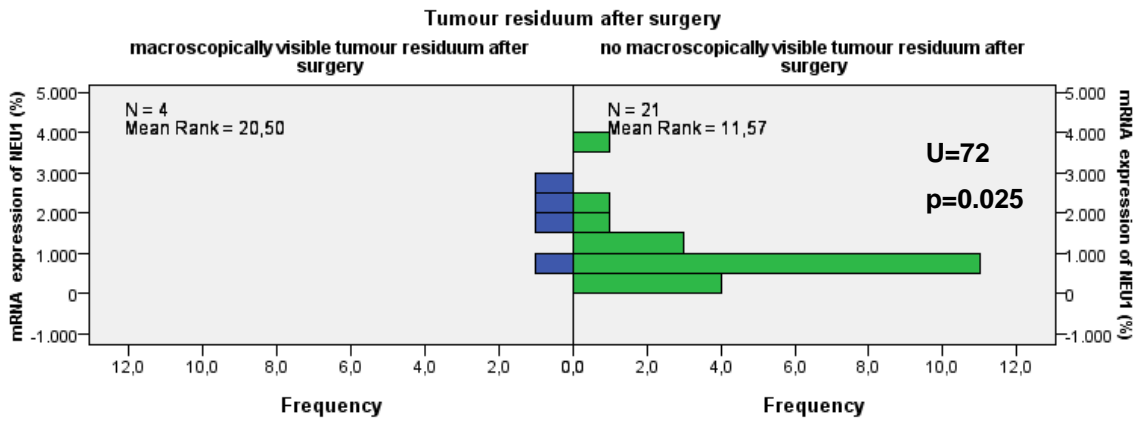
Fig. 259. Low NEU1 expression correlates with optimal debulking (qPCR). Mann-Whitney U test

Table 20. Correlation (p-value) of NEU1 with clinicopathological factors (qPCR)

qPCR	Grading	Nodal involvement	Distant metastasis	Tumour residuum after surgery	Kaplan-Meier analysis RFI[b]	Kaplan-Meier analysis OAS[b]
NEU1	0.482[a]	**0.039[a]**	**0.002[a]**	**0.025[a]**	0.764	0.810

a - exact significance used; b – NEU1 was divided in quartiles based on expression rates

4.4.2 ST6GAL1

4.4.2.1   ST6GAL1 mRNA expression and correlation with clinicopathological factors and patient survival

Since proteins involved in trimming of O- or N-glycans are deemed to be crucial for the malignant potential of ovarian cancer and ST6GAL1 was also one of the genes significantly deregulated by cFOS, it was chosen to be further investigated on an mRNA level in this study (Oliveira-Ferrer et al 2014).

Figure 30 shows a boxplot of ST6GAL1 expression in qPCR analysis. Overall, expression ranged extensively from 278.9 – 10469.1% (mean 3068.5%). One-way ANOVA showed no significant differences between the different types of tumour (p=0.196).
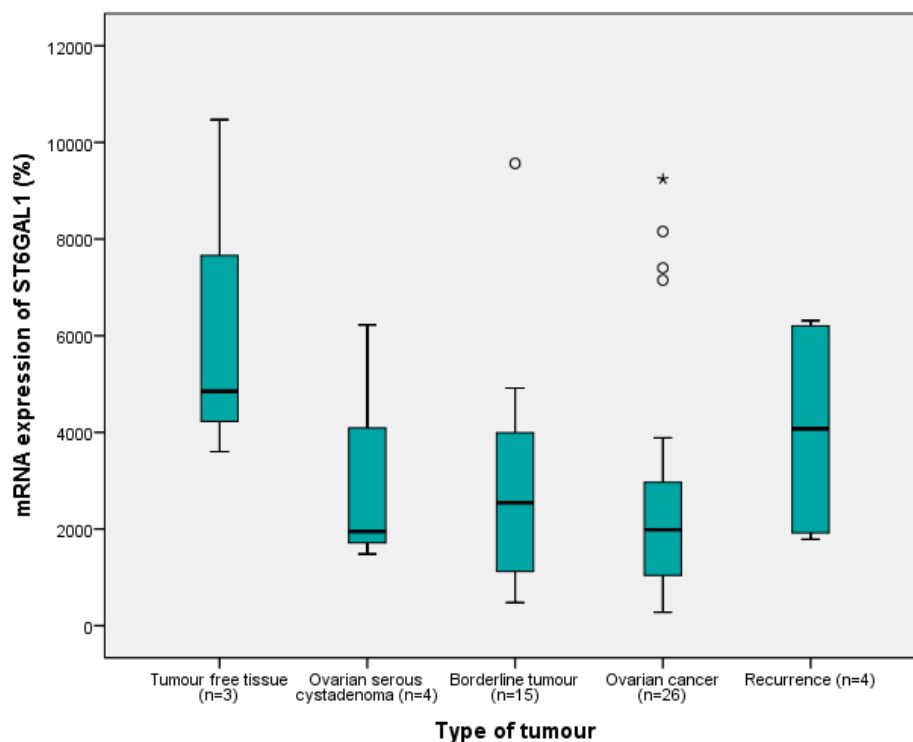
Fig. 26. ST6GAL1 expression by type of tumour (qPCR). Boxplot

Higher ST6GAL1 expression in OvCa was significantly associated with M1 staging (Mann-Whitney U=77; p=0.006, exact significance used, see Fig. 31), while no further significant clinicopathological correlations were found for ST6GAL1 in the analysis of qPCR expression-data. Kaplan-Meier analysis for RFI and OAS was not significant either (see Table 21 for a detailed list of p-values obtained).
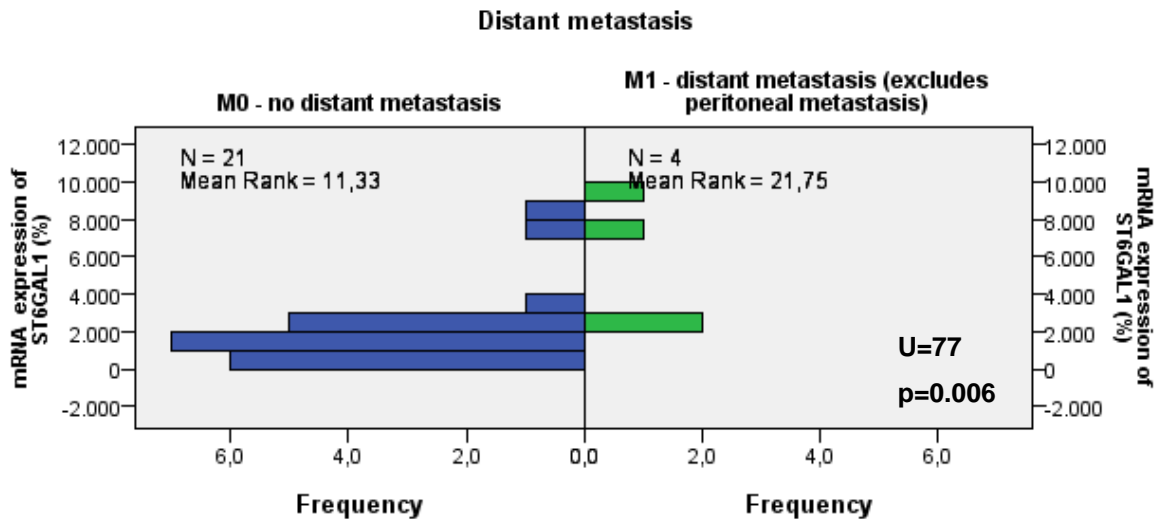
Fig. 27. Gain of ST6GAL1 expression correlates with distant metastasis (qPCR). Mann-Whitney U test

Table 21 Correlation (p-value) of ST6GAL1 with clinicopathological factors and patient survival (qPCR)

qPCR	Grading	Nodal involvement	Distant metastasis	Tumour residuum after surgery	Kaplan-Meier analysis RFI[b]	Kaplan-Meier analysis OAS[b]
ST6GAL1	0.907[a]	0.249[a]	0.006[a]	0.858[a]	0.334	0.192

a - exact significance used; b – ST6GAL1 was divided in quartiles based on expression rates

4.4.2.2   ST6GAL1 protein expression and correlation with clinicopathology

ST6GAL1 had been linked to progression and malignancy of ovarian cancer on various occasions (see above). Thus, there was a special interest to analyse the prognostic relevance of ST6GAL1 via WB with a larger cohort. 202 patients were included in the final analysis.

A representative WB of ST6GAL1 and its control for equal loading, GAPDH, are shown in Fig. 23. As control, proteins from the ovarian cancer cell line SKOV3 and the same tumour (T-control) were included in each gel. For densitometry analysis SKOV3 expression was defined at 100%.
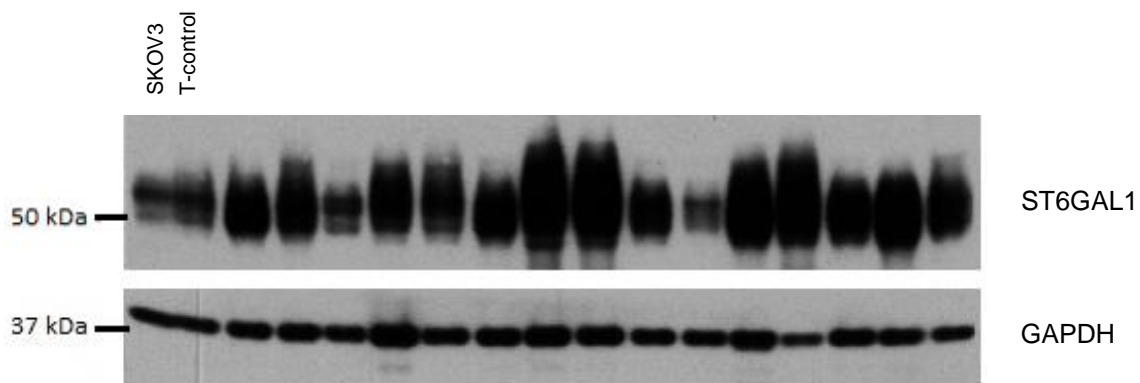
Fig. 28. Exemplary Western Blot of ST6GAL1 (50 kDa) and its loading control GAPDH (37 kDa) of 15 ovarian neoplasms. SKOV3 and T-control served as control between blots.

There was a consistent medium-strong signal around 50 kDa in the SKOV3 control and varying intensity in the ovarian tumours. The mean expression level after densitometry was 412.7% (range 1.6 – 1438.5%; see Fig. 33 for Boxplot of ST6GAL1 expression). One-way ANOVA yielded no significant intensity differences between the types of tumour (p=0.225).
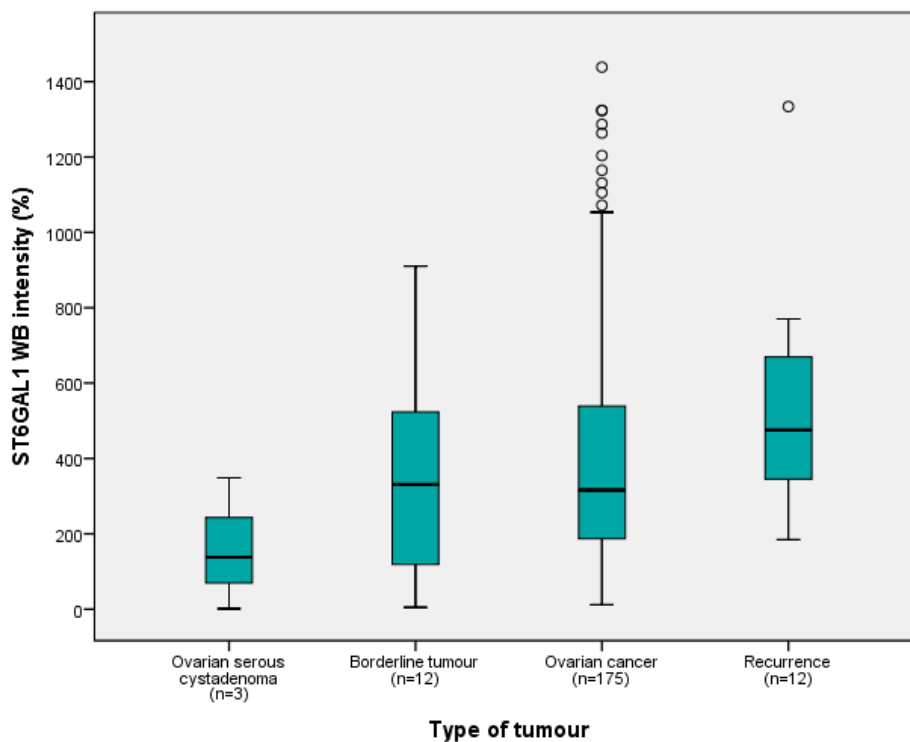
Fig. 29. Boxplot: ST6GAL1 intensities by type of tumour (WB).

As before on an mRNA level, high ST6GAL1 protein expression was found signifi-
cantly more often in patients with distant metastasis (Mann-Whitney U=3109; p=0,020;
see Fig. 34). For a full table of p-values obtained on ST6GAL1-analysis, see Table 22.
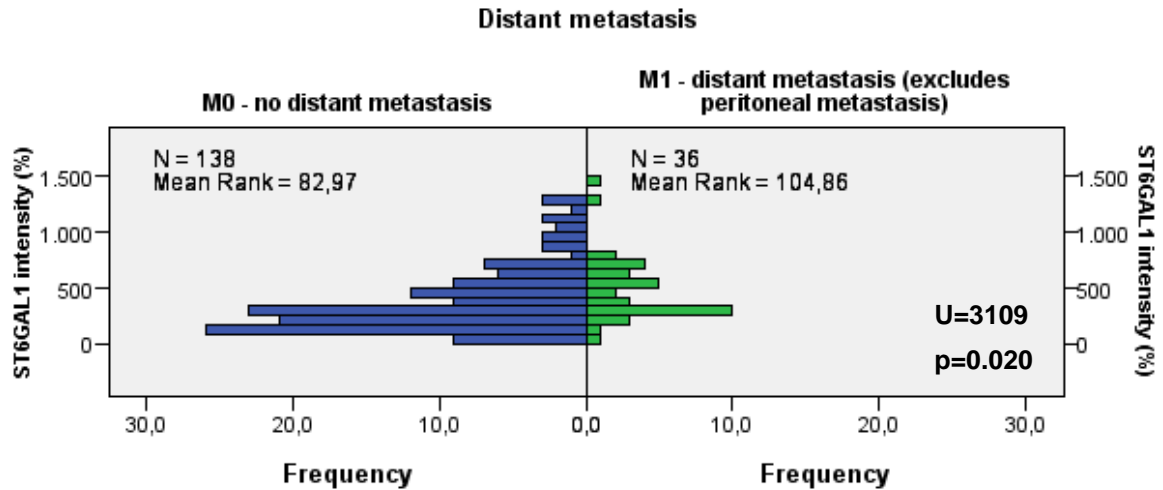
Fig. 30. Gain of ST6GAL1 expression correlates with distant metastasis (WB). Mann-Whitney U test

Table 22. Correlation (p-value) of ST6GAL1 with clinicopathological factors (WB)

WB	Grading	FIGO stage	Nodal involvement	Distant metastasis	Tumour residuum after surgery	Kaplan-Meier analysis RFI[a]	Kaplan-Meier analysis OAS[a]
ST6GAL1	0.572	0.058	0.633	0.020	0.120	0.047	0.862

a - ST6GAL was divided in a lower quartile vs the upper 75% based on expression rates

4.4.2.3   ST6GAL1 protein expression and analysis of survival

Kaplan-Meier analysis was performed using the long-term follow-up information for
the patient cohort to study the prognostic impact of ST6GAL1 expression. Survival
rates of the lower quartile of ST6GAL1 expression were compared to the upper 75%
of expression levels. Lower ST6GAL expression was associated with a significantly
longer RFI (mean: 70 and 42.2 months for patients with the lower 25% and upper 75%
ST6GAL1 expression; p=0.047; median: 22 and 18 months; see Fig. 35). However,
this did not seem to affect OAS on Kaplan-Meier analysis (p=0.862).

On multivariate Cox regression analysis, lower ST6GAL1 expression did not remain a beneficial significant factor for the length of RFI after correction for known prognostic factors like metastasis-status and tumour residuum after surgery (Hazard ratio 1.294; 95% CI 0.75-2.21; p=0.375, see Table 23 for full analysis).
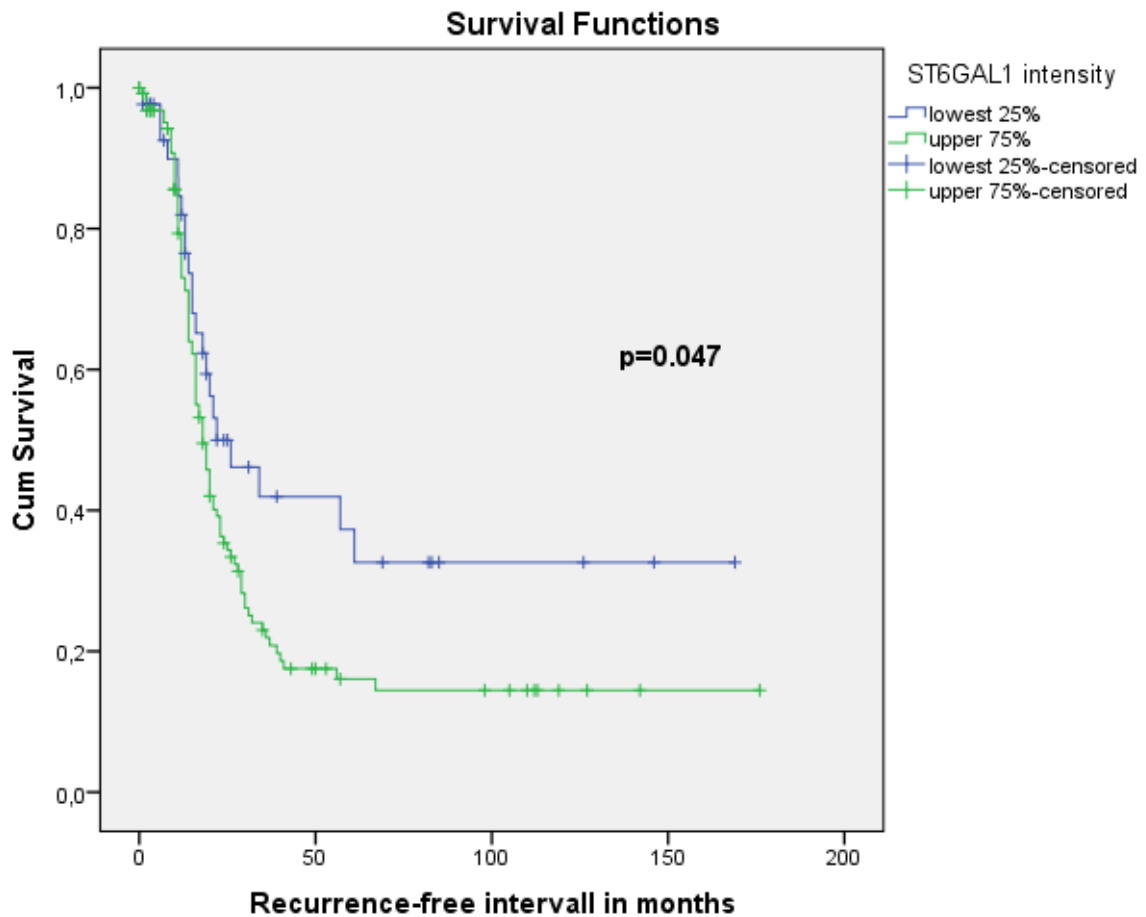
Fig. 31.   Kaplan-Meier analysis of recurrence-free interval based on ST6GAL1 expression. Low ST6GAL1 levels are associated with a longer RFI (mean: 70 vs 42.2 months; p=0.047). Kaplan-Meier curves were generated from 170 patients with a mean RFI of 24.4 months. Patients were stratified based on the lowest quartile of ST6GAL1 expression vs the upper 75%. Censored cases are indicated by vertical bars and p-value after log-rank test is shown.

Table 23. Multivariate Cox regression analysis including grading, FIGO stage, nodal involvement, distant metastasis, tumour residuum after surgery, and ST6GAL1 expression (WB)

Characteristics		Hazard ratio	95% confidence interval	p-value
Recurrence-free intervall (n=135)				
ST6GAL1 expression	ST6GAL1 lower quartile vs upper 75%	1.294	0.75-2.21	0.375
Grading	G1/G2 vs G3	0.69	0.42-1.11	0.128
FIGO stage	FIGOI/FIGOII vs FIGOIII/FIGOIV	3.08	0.89-10.75	0.077
Nodal status	N0 vs N1	2.39	1.34-4.26	**0.003**
Distant metastasis	M0 vs M1	1.72	0.99-2.98	0.052
Tumour residuum after surgery	not macroscopically visible vs macroscopically visible	1.64	0.99-2.74	0.057

4.4.2.4   Cross-assay analysis

Pearson correlation was calculated for 37 probes on comparison of their mRNA and protein expression levels of ST6GAL1 to examine possible regulation processes and was found to be significant (Pearson correlation 0.446; p=0.006). However, on a closer comparison by each type of tumour, only the correlation for ovarian cancers remained statistically significant (Pearson correlation 0.502; p=0.015; n=23, see Table 24 for a list of all p-values obtained).

Table 24. Cross-assay analysis of ST6GAL1 (qPCR and WB)

ST6GAL1	Pearson Correlation between qPCR- and WB expression	p-value
Whole study cohort (n=37)[a]	**0.446**	**0.006**
OvCa (n=23)	**0.502**	**0.015**

5.   Discussion

This discussion will first outline the general approach and limitations and strong points of the methods used, before discussing the findings of this study in the context of the research field and giving an outlook for each enzyme, respectively.

5.1   Limitations and strong points of the methods used

Continuous research provides more and more evidence that aberrant glycosylation plays a major role in the malignant processes of carcinogenesis. Research focusses on glycosylation-mediated phenotype changes e.g. tumour growth, adhesion changes and metastases formation, on altered chemosensitivity and apoptosis pathways by receptor regulation, and the search of specific and sensitive prognostic and predictive biomarkers (Alper 2003). Technical advances, like mass spectrometry- or liquid chromatography-based detection, allow a molecular analysis of sugar residues. However, these methods are still very costly and complex (Sethi and Fanayan 2015). While they are valuable in finding novel glycoconjugates that are solely expressed in cancerous tissues, they do not exclusively answer our search for meaningful new markers (Kuzmanov et al 2012). In this study, a more indirect approach was chosen, using qPCR and Western Blots to measure relative expression levels of the glycosylation enzymes GALNT12, GALNT14, GCNT3, MAN1A1, GANAB, NEU1, and ST6GAL1. These genes are involved in all major pathways of glycosylation changes in cancer - O-glycosylation (GALNT12, GALNT14, and GCNT3), N-glycosylation (GANAB, MAN1A1) , and changed sialylation status (NEU1, ST6GAL1). These genes had been selected primarily based on prior observations in our working group that the beneficial transcription factor cFOS mediated expression changes in these glycoproteins in OvCa cells (Oliveira-Ferrer et al 2014).

The chosen methods of qPCR and Western Blot analysis are established and vastly used to study gene and protein expression in the search of prognostic markers in cancer (e.g. Milde-Langosch et al 2015). Expression rates provide the possibility to reflect broader effects of glycosylation changes by searching a correlation between the expression rate and the clinical-pathological data of the patients provided. The chosen

approach is advantageous in finding these correlations, as some enzymes involved in glycosylation affect highly regulated pathways and are integral to complex processes far beyond the addition or removal of sugar residues detectable in mass spectrometry. While this study can thus provide clinical evidence of in vitro findings, e.g. on metastatic ability of cancer cells upon changed enzyme expression, and their aptitude as a prognostic marker, no mechanistic explanations can be derived from the results of this study.

In the first part of this study, the 7 genes were examined on an mRNA level to gain first insights into their expression patterns in ovarian tumours of ascending malignancy and possible correlations with the clinico-pathological presentation of the patients. This first step was primarily conducted with the intention of finding interesting candidates that should enter further analysis on a larger patient collective in the search of suitable prognostic markers for ovarian cancer. The screening-like approach allowed only limited resources. Thus, a relatively small sample set of 52 patients entered the final analysis of mRNA expression levels. 26 of these patients had been diagnosed with ovarian cancer, the rest were cases of ovarian cystadenoma (n=4), borderline ovarian tumour (n=15), recurrences (n=4), and samples of healthy tissue (n=3) obtained during debulking operations. This small case number has to be seen as a clear limitation of this part of the study. Consequently, statistical analysis of clinical correlations included comparisons of groups, e.g. with and without distant metastasis upon diagnosis, as small as 4 to 21 patients. Despite the attempt of statistical correction by using exact significances, conclusions based on a sample size that small have to be regarded with caution and demand a confirmation on a bigger scale. Interestingly, it was the correlation with metastasis that was significant in 5 out of the 7 genes analyzed in this study. This hints at the possibility of an overstated effect due to the small sample size for this clinical parameter. To omit repetition, this critique should be kept in mind for all the stated results as it will not be discussed extensively further on. Similarly, the expression ranges of the mRNA levels should be regarded with caution, as sample sizes of the different types of tumours that entered final analysis could partially be too small to lead to valid conclusions. Still, they can be considered as an initial indicator and were analyzed as such in the context of the existing literature, before further research may support the findings.

As a second step, 4 (GANAB, MAN1A1, NEU1, and ST6GAL1) of the 7 genes were selected for expression analysis on a protein level on a larger study cohort of 204 patients, including 176 patients with primary OvCa and 12 REC, 4 with OSC, and 12 patients diagnosed with BOT. Unfortunately, no consistent protein detection could be established for NEU1, thus results are limited to mRNA analysis for this gene. Generally, Western Blot analysis is an established method of semi-quantitative measuring of protein expression. However, it is an inherent shortcoming of this method that with very high protein expressions the proportionality of the extinction, measured to quantify protein levels, can be lost due to saturation of the x-ray film (Taylor et al 2013).

While the extensive clinical data on the patients is a strong advantage of this study, it was not possible to differentiate between the exact origins of all the tumorous tissues examined in this study. Samples could stem from the site of origin but also from metastasis. This could have an effect on the gene expression measured, as could have the stroma cells included in the tissue lysates (Brodsky et al 2014, Martins et al 2014). While sequential HE-staining controls of freeze-cut sections prior to lysis ensured at least 50% of tumorous cells in the lysates used, no distinction was made between more intratumoral slices or areas closer to the invasion front. Besides differences in metastasis and primaries, even intratumoral variance of gene expression has thus to be taken into account as a possible confounder of the qPCR and Western Blot results (Brodsky et al 2014, Christofori 2006). An example of intratumoral variance is showcased in the differing IHC–staining intensity for MAN1A1 in one tissue section of a patient with OvCa (see Fig. 25, C).

5.2   Enzymes of the O-Glycosylation pathway

5.2.1 GALNT12, GALNT14, and GCNT3

GALNT12, GALNT14, and GCNT3 are enzymes of the O-glycosylation pathway and had all previously been linked to carcinogenic processes (Beaman and Brooks 2014, Brockhausen 1999). They showed downregulation upon transfection of ovarian cancer cells with cFOS (Oliveira-Ferrer et al 2014).

Their functional contribution to a malignant phenotype has not been fully elucidated yet and results vary for the respective genes. They have been linked to metastasis and

shown aptitude as prognostic markers for some epithelial cancers (Beaman and Brooks 2014, González-Vallinas et al 2015). To my knowledge, they have not been tested for their prognostic value in the diagnosis of ovarian cancer prior to this study.

No significant differences in mRNA expression levels of GALNT12 and GALNT14 between the types of tumour could be detected in this study.

Previously, GALNT14 overexpression had been found in various cancers, but it had not been consistently linked to a beneficial or malign cancerous phenotype (Bouralexis et al 2005, Huanna et al 2014, Wagner et al 2007). Mechanistic explanations for GALNT14´s involvement in carcinogenesis exist and beneficial effects upon GALNT14 downregulation have already been shown for ovarian cancer cell lines in vitro (Oliveira-Ferrer et al 2014, Yang 2013). Silencing of GALNT14 in ovarian cancer cell lines suppressed cellular migration, possibly via glycosylation changes of MUC13, and low levels of GALNT14 were associated with a more beneficial phenotype upon cFOS upregulation (Oliveira-Ferrer et al 2014, Yang 2013). Interestingly, this present study noted a trend where up- and downregulation of GALNT14 were linked to a longer recurrence free period for the patients while medium expression appeared to be unfavourable ($p=0.052$). Nonetheless, analysis of a bigger patient group is needed to produce a valid statement on the prognostic value of GALNT14 expression, as the sample size was very limited, with only 25 patients entering Kaplan-Meier analysis. However, the great expression variance found in this study (4.2 – 2053.5%, Fig. 7B) might impede on the employability of GALNT14 as a prognostic marker. Notably, Wagner et al had previously described GALNT14´s expression variance as a dynamic process and future research might still strengthen evidence of GALNT14´s value as a surrogate marker of treatment response, e.g. for TRAIL-based cancer therapy (Wagner et al 2007).

For GCNT3, mRNA expression was significantly higher in BOT than in OvCa and the widest range of expression was found in BOT as compared to the relatively small and lower ranges in OvCa and OSC ($p=0.001$, see Fig. 8, range BOT=0.5 – 76.3%, mean 20.4%). This suggests a possible deregulation of GCNT3 in borderline tumours that, to my knowledge, has not been previously described. The patient cohort in this study is too small to derive immediate conclusions, but follow up research on GCNT3's involvement in borderline tumours on a larger patient cohort could yield interesting results, e.g. whether it shows potential as a prognostic marker for this entity.

No significant association of expression levels with prognostic markers like metastasis or FIGO staging were detected for GALNT12 or GALNT14 in this study. Meanwhile, higher GCNT3 levels correlated significantly with patients that had already shown seeds of distant metastasis upon diagnosis, linking higher GCNT3 levels to a possibly more aggressively expanding ovarian cancer (p=0.003). GCNT3 upregulation had previously been shown for patients with metastatic HCC by Tianhua Liu et al (Tianhua Liu et al 2014). Albeit, they cautioned that while no mechanistic explanations are known this might also be due to a form of protective upregulation of GCNT3. For ovarian cancer, Oliveira-Ferrer et al found that the induction of transcription factor cFOS was associated with a less metastatic phenotype and downregulation of GCNT3 could be measured in these cell lines (Oliveira-Ferrer et al 2014). The newly described upregulation of GCNT3 in patients with already metastasized ovarian cancer would be in line with these findings.

GALNT12, GALNT14, and GCNT3 did not enter further analysis on the protein level of a larger patient cohort. Especially GALNT14 and GCNT3 show some promise as prognostic markers in ovarian cancer and borderline tumours, respectively, and further studies that would shed more light on their likely complex role in ovarian tumours could be rewarded with interesting results.

5.3   Enzymes of the N-Glycosylation pathway

5.3.1 GANAB

Higher mRNA levels of GANAB have been associated with a more beneficial phenotype after cFOS transfection in ovarian cancer cell lines (Oliveira-Ferrer et al 2014). This led to the analysis of mRNA levels of GANAB for this study.

Looking at the boxplot (Fig.10), lower GANAB values seemed to be more prevalent in the more malign conditions. In particular, expression in BOT was significantly lower than those found in tumour free tissue (p=0.02) and ovarian serous cystadenoma (p=0.019). This association of lower GANAB levels with more malignant tumours is in line with the observations by Cressey et al and Chiu et al (Chiu et al 2011, Cressey 2013). They found that Glucosidase II, of which GANAB is the α – subunit, was shown to have striking molecular similarities and comparable expression patterns to the tumor

suppressor gene p53 and that GANAB knockdown in HNC was associated with higher staging and poor survival of patients (Chiu et al 2011, Cressey 2013). However, GANAB showed a wide expression range on the mRNA level in this study and the analysis of the clinico-pathological data of the patient-subset with ovarian cancer showed that those with higher GANAB expressions were significantly more often diagnosed with M1 staging (p=0.047). This correlation was unexpected as GANAB downregulation has so far been associated with more invasive phenotypes and it might be attributed to the limitation of the small sample size mentioned above.

Especially GANABs proposed tumour suppressor function and the partly significant downregulation in malign tumours as compared to OSC and healthy tissues sparked the interest to study GANAB on a larger scale with the Western Blot method. Here, the significant differences in expression levels were lost, as OSC showed a similar mean expression to the more malign entities.

However, the IHC staining of exemplary tissues, conducted to show GANAB expression patterns, raised doubts about the general employability of the results for OSC expression levels of GANAB. While it is known that tumours interact with and can even change their surrounding stroma, including gene-expressions in stromal cells, the staining revealed that in OSC not only tumorous but also stromal and non-tumorous cells showed a moderate to strong reaction with the GANAB antibody (see Fig. 14) (Mueller and Fusenig 2004). Especially, as these sections had a higher percentage of stromal cells than the other tumour types, due to the histological nature of OSC, the measured GANAB levels are possibly skewed. For the other tumour types IHC validated that GANAB was mainly expressed in tumorous cells while stromal cells only showed weak expression. This suggests that the GANAB protein expression in the OvCa cohort, with the same antibody being used in IHC and WB, is representative of expression levels in the tumour. As no correlation could be confirmed between the mRNA and protein expression levels after Pearson correlation of the OvCa groups, a post-transcriptional, translational, and/or protein-degradation regulation of GANAB protein levels is suggested (Vogel and Marcotte 2012).

GANAB's association with cancer aggressiveness, staging, and survival in HNC could not be extended to ovarian cancer in this study (Chiu et al 2011). No significant correlation was measured regarding grading, FIGO staging, metastasis, nodule involvement or tumour rest after operation. Furthermore, GANAB downregulation did not

seem to affect survival in this collective as Kaplan Meier analysis yielded no significant results.

Thus, regardless of a promising start in mRNA analysis results could not be hardened in a larger scale approach via WB-analysis. Higher GANAB expression was neither associated with the more beneficial types of tumour, nor linked to a beneficial outcome for the patients entering this study. No results that manifested itself in a clinically measured altered aggressiveness of the cancer were found in this study. Still, its overexpression in cancerous cells as compared to the stroma, as shown by the IHC, and the structural similarity of glucosidase II to tumour suppressor p53 as found by Cressey et al in patients with lung cancer, leave GANAB as an interesting candidate for possible cancer drug development. Mutations in p53 are thought to be an early event in the development of high grade serous ovarian cancer and knowledge on structurally and possibly functionally similar genes could reveal new insights into carcinogenesis and open up new therapeutic pathways (Corney et al 2008).

While this study could not confirm GANAB expression levels as a prognostic marker in ovarian cancer, further research on GANAB´s function in ovarian cancer, e.g. with ovarian cancer cell lines, could be worthwhile to gain insights on its aptitude as a therapeutic target.

5.3.2 MAN1A1

Only recently mannosidases entered the focus of research of glycosylation genes and their effects on carcinogenesis. This study adds new information to the growing body of evidence that MAN1A1 deregulation is linked to the clinical presentation of the cancer and turned out to serve as a prognostic marker in this study cohort.

On the one hand, MAN1A1 expression in the qPCR analysis was significantly higher expressed in the non-affected benign tissue (p=0.000) than in all other types of tumours, and expression in the generally benign OSC was also significantly higher than in the more malign BOT and OvCa tissue samples (p=0.01; p=0.017). On the other hand, higher MAN1A1 mRNA expression levels also showed a significant correlation to the diagnosis of distant metastasis (p=0.015). These intriguing results lead to the selection of MAN1A1 to be chosen for further analysis on a protein level to gain further insights into its clinicopatholigcal correlations and expression patterns.

Interestingly, WB-analysis with MAN1A1 antibody yielded two bands for the patient lysates but not for the cell line control. One band was detected at the expected weight of 72 kDa while in most tumour lysates a second band was found at 60 kDa. Wu et al had shown that endoplasmic Mannosidase (MAN1B1) is subjected to controlled proteolysis (Y. Wu et al 2007). So far, a similar mechanism has not been reported for golgi Mannosidase MAN1A1 but its existence is thinkable, especially as the 2nd band seems to be reproducible, as it has also been detected in the tumours of breast cancer patients (unpublished data of our working group). It is mentionable that a significantly stronger expression of the 60kDa band was detected in OSC and BOT than in the OvCa and REC (e.g. OSC vs OvCa p=0.001; BOT vs OvCa p=0.001). A possible explanation would be diminished proteolytic activity with increasing malignancy. However, as neither the function nor activity of the 60 kDA band is known up to date, this study focussed on analysis of the expected band at 72 kDa. Nonetheless, clinical correlations were also calculated for the expression of the 60 kDa band alone and the cumulated expression values of the two.

The strong upregulation of MAN1A1 in benign tumour types on the mRNA level could not be replicated on the protein level. Fittingly, Pearson correlation only showed a significant correlation between mRNA and protein levels for OvCa (p=0.003) and not for the other types of tumour. IHC validated the quality of the antibody used and showed that MAN1A1 was stained mainly in tumorous cells and only marginally in stromal cells.

Clinicopathological analysis yielded significantly higher protein levels of MAN1A1 in patients with higher FIGO staging (p=0.002), patients with regional lymph node metastasis (only for 72 kDa + 60 kDa; p=0.026), and distant metastasis (p=0.018) linking higher MAN1A1 level to a generally worse clinical presentation of the patients at diagnosis. Additionally, suboptimal debulking was achieved significantly more often in patients with high levels of MAN1A1 (p=0.005), suggesting more infiltrative or expansive growth at diagnosis. This is in contrast to the scarce existing literature on MAN1A1´s role in carcinogenesis, e.g. the findings by Tianhua Liu et al who measured MAN1A1 downregulation in HCC cell lines and xenograft tumours in the more aggressive and metastatic groups (Tianhua Liu et al 2014).

Upon analysis of MAN1A1 as a prognostic factor in ovarian cancer, Kaplan Meier analysis showed significantly shorter RFI and OAS in the patients belonging to highest quarter of MAN1A1 expression. Patients relapsed after 24.3 months on an average

and died of ovarian cancer after 40.9 months, while the patients belonging to the group of the lower MAN1A1 expression had a mean RFI of 53.8 month and survived for 73.2 months (RFI: p=0.032; OAS: p=0.022). Multivariate Cox regression indicated that high MAN1A1 expression remained an independent adverse prognostic factor for OAS, despite correction for the correlation with established prognostic factors like high FIGO grading, less than optimal debulking, and distant metastases (Hazard ratio 1.74; p=0.045).

MAN1A1 entered this analysis as it was found to be upregulated by transcription factor cFOS, suggesting higher levels of MAN1A1 expression to be linked to a positive phenotype in ovarian cancer cell lines (Oliveira-Ferrer et al 2014). Unexpectedly, the opposite was found in this study, showing that high MAN1A1 expression correlated with a clinically more advanced and malign cancer, earlier recurrences, and earlier death due to their cancer even serving as an independent prognostic factor for shorter OAS in ovarian cancer.

It is striking, that while this study found correlations of negative effects and high MAN1A1 levels for ovarian cancer, the opposite can be said for breast cancer. High mRNA expression was also an independent prognostic factor, however, in breast cancer higher levels correlated with longer RFI and OAS (Milde-Langosch et al 2015). Thus, possible yanus effects of MAN1A1 deregulation have to be kept in mind in future research projects.

Altevogt et al have shown that MAN1A1 inhibition with Kifunensine disturbed the processing of high-mannose glycans and led to glycosylation changes and reduced expression of adhesion molecules like L1CAM. However, they observed these changes without relating them to clinical effects. Previously, L1CAM levels had been shown to increase from benign to advanced ovarian tumours (Altevogt et al 2016, Gomes et al 2015). The results of this study now suggest important clinical effects of the of MAN1A1 deregulation. Taken in account the findings by Altevogt et al, this could possibly be due to the changed properties and expression levels of adhesion molecules like L1CAM, which could explain the more invasive and less operable cancer. These hypotheses require further research and verification, e.g. via co-expression studies.

To sum up, this study adds a new complexity to MAN1A1 expression in cancer, linking higher levels for the first time to a negative clinic-pathological presentation of

the patients with ovarian cancer and shorter overall survival. These are intriguing results, showing that further studies on MAN1A1 in cancer, ovarian and others, is highly warranted to understand its little researched role in tumorigenesis.

5.4   Enzymes participating in optional trimming of sugar residues

5.4.1   NEU1

Studies on NEU1´s implication on cancer have shown conflicting results. Expression changes were shown to affect the phenotype of various cancer cells, however to varying results.

Its once discussed role as a tumour suppressor in cancers like melanoma and colon cancer has been put into question by more recent publications on the positive effects upon NEU1 inhibition with oseltamivir phosphate in prostate cancer (Kato et al 2001, Szewczuk, O'Shea, et al 2014, Uemura et al 2009). Ren et al found high levels of NEU1 mRNA in ovarian cancer tissue sections compared to matched, normal tissue in an analysis of data of the Cancer Genome Atlas (TCGA) (Ren et al 2015). The higher levels of NEU1 expression in OvCa could not be replicated in this study as there were no significant differences between the different types of tissue detectable. However, this study did not include specifically matched pairs of ovarian cancer samples and their respective normal tissue but rather looked for general expression differences in grouped samples of normal tissues versus cancerous tissues. The different approach might explain the altered finding.

This study could reveal a number of significant associations of low NEU1 expression levels with clinically advantageous parameters. Lower levels were found significantly more often in patients where optimal debulking had been achieved (p=0.025) and they were significantly associated with N0 and M0 staging upon diagnosis (p=0.039; p=0.002). Thus, the starting hypothesis that higher levels of NEU1 are linked to a more beneficial phenotype in ovarian cancer, triggered by the observation that cFOS transfection led to an upregulation of NEU1, cannot be hold after this study (Oliveira-Ferrer et al 2014). On the contrary, these clinical findings provide the clinical correspondence to in vitro results of Ren et al, who discovered that siRNA treatment of ovarian cancer cell lines led to an inhibition of cancer proliferation, increased apoptosis rates, cell cycle

arrest, and suppressed invasion (Ren et al 2015). This study thus proposes that these effects are also at work in vivo. Patients with low Neu1 levels developed less invasive cancers, that were growing organized enough to allow for significantly more optimal debulking, and that showed significantly less lymph node metastasis or distant metastasis (see Table 20). Unfortunately, these exciting conclusions could not be verified on a bigger patient cohort as a reliable protein detection on the Western Blot membranes could not be achieved in our laboratory.

The findings of this study are further supported by the work of Gilmour et al that showed an attenuation of pancreatic cancer growth and metastasis upon inhibition of NEU1 with oseltamivir phosphate (Tamiflu®) (Gilmour et al 2013). Additionally, this working group found an attenuation of EGFR pathways and other integral receptor pathways upon NEU1 inhibition (Abdulkhalek and Szewczuk 2013, Szewczuk, Haxho, et al 2014). Currently, the search for efficient treatment based on EGFR inhibition in ovarian cancer is ongoing (Glaysher et al 2013). Oseltamivir phosphate is a commonly used drug that appears to be well tolerated. When combining the newly found correlations with these studies, the search for a possible attenuation of multiple pathways, including the EGFR pathways, via NEU1 inhibition also in ovarian cancers presents itself as a promising project that could lead to a new therapeutic approach.

This appears to be an even more promising approach, as oseltamivir phosphate treatment reversed chemoresistance of human pancreatic cancer cells to cisplatin and gemcitabine and disabled apoptosis evasion of the cells (Szewczuk, O'Shea, et al 2014). Cisplatin is a first line treatment for ovarian cancer and chemoresistance to cisplatin is linked to early relapse (Jayson et al 2014). Additionally, the application of oseltamivir phosphate has been shown to decrease chemoresistance in triple negative breast cancer cells, showing synergistic effects with several chemotherapeutic agents also used against ovarian cancer, including paclitaxel and gemcitabine (Szewczuk, Haxho, et al 2014).

Therefore, this study, in underlining the association of a beneficial clinical presentation of the patients with low levels of NEU1, provides a strong rationale to continue the research on effects of NEU1 inhibition in ovarian cancer, to further elucidate the mechanisms and pathways involved, and to validate its aptitude as a prognostic marker for ovarian cancer on a bigger scale. If these experiments turn out to be successful, for example a screening of patients for high levels of NEU1 might lead to the selection of

a patient cohort that would especially benefit from an additional oseltamivir phosphate treatment to anticipate chemoresistance.

5.4.2 ST6GAL1

There is ongoing research on ST6GAL1's role in various cancers linking it repeatedly to malign changes of phenotype.

High levels of ST6GAL1 have been associated with a more invasive and metastatic phenotype, for example in colorectal and mammary cancer cells lines and in human anaplastic large cell lymphoma (Lin et al 2002, Park and Lee 2013, Suzuki et al 2015, Zhu et al 2001). Christie et al could extend these findings to ovarian cancer cell lines, showing increased matrigel invasion upon forced ST6GAL1 expression (Christie et al 2008).

Christie et al attributed their findings to the increased alpha 2-6 sialylation of integrin ß1 which consequently led to increased invasive potential, possibly through augmented adhesion to collagen 1, a ligand for ß1 integrin. They hypothesized this in vitro found mechanism as ST6GAL1's possible contribution to peritoneal metastasis in ovarian cancer (Christie et al 2008). This present study extends the knowledge of in vitro effects of ST6GAL1 upregulation and provides evidence that these pro-metastatic mechanisms are also at work in vivo. It was shown that patients diagnosed with distant metastasis presented with significantly higher levels of ST6GAL1 on an mRNA and protein level (p=0.006; p=0.02).

While previous IHC and mRNA studies showed higher levels of ST6GAL1 in ovarian cancer tissues compared to matched normal, this study could not replicate these findings in a comparison of expression levels of groups with different malignant potential on a mRNA or protein level (Swindall et al 2013, P Wang et al 2005). With the exception of metastatic presentation, further correlations between clinico-pathological parameters like stage or grading and the ST6Gal1 level did not prove to be significant in this study, nor were they in the study conducted by Wang et al (P Wang et al 2005).

For patients with localized clear-cell renal-cell carcinoma, increased levels of ST6GAL1 in tumours have been correlated with poorer prognosis and could be employed as an independent predictive factor of OAS and RFI (Hai-Ou Liu et al 2015). Kaplan-Meier analysis of the Western Blot data in this study could now show that

ST6GAL1 upregulation was significantly associated with a shorter RFI in ovarian cancer, too (p=0.047). However, upon multivariate Cox regression analysis for prognostic factors, like metastasis–status and nodal involvement, ST6GAL1 expression did not remain an independent prognostic marker for the length of the RFI. This might be due to the significant association of the ST6GAL1 expression level and metastasis status at diagnosis.

These results have to be linked to a study by Schultz et al conducted in 2013 that showed the association of high ST6GAL1 expression levels with apoptosis evasion and chemoresistance to cisplatin–treatment in ovarian cancer cells (Schultz et al 2013). Thus, the significant association of high ST6GAL1 levels with earlier relapses offer new in vivo evidence of the link of ST6GAL1 expression and chemoresistance.

While this study cannot confirm ST6GAL1 as an independent prognostic marker, ST6GAL1 expression levels might help stratify patients with a higher risk of metastatic relapse that require an adapted therapeutic regime. It is also thinkable to use the ST6GAL1 specific N-glycans decribed by Kuzmanov et al for a screening of patients with high ST6GAL1 levels (Kuzmanov et al 2012).

Overall, this study adds new, further in vivo evidence via correlation with patient data to the idea that ST6GAL1 is presenting itself as a target of high interest in metastatic ovarian cancer. To develop therapeutics against it includes the promising possibility to reduce metastasis formation and possibly decrease chemoresistance and thus prolong the RFI and OAS of the patients. The mechanistic explanations of ST6GAL1 function so far are encouraging the idea that ST6GAL1 silencing could lead to beneficial horizontal effects affecting different pillars of the carcinogenic phenotype like adhesion, metastasis formation, and chemoresistance (Christie et al 2008, Schultz et al 2013, Suzuki et al 2015).

5.5   Conclusion and outlook

In this study the limitations of an indirect approach of analyzing expression changes of glycosylation enzymes had to be accepted due to the lack of availability of highly sensitive and specific detection methods for glycan structures themselves (Kuzmanov et al 2012, Sethi and Fanayan 2015). This can only be a surrogate for the intricate

process of analysing changes to the actual glycans and the consequently altered expression on the cell surface, effects on e.g. cell adhesion and metastases or conformation changes of cell receptors due to the glycan changes, just to name a few (Oliveira-Ferrer et al 2017, Potapenko et al 2010). This is complicated further by the dependence of glycan structure formation on substrate availability and the presence of multiple, partly competitive, enzymes of the relevant pathway. Altered protein expression, as found in cancer, can thus lead to altered glycosylation (Brockhausen 1999, Varki et al 2009a).

Despite the complexity of the matter and shortcomings of the method, the significant results of this study underline the possible clinical relevance of glycosylation enzymes as biomarkers. Unpublished data of our working group has even shown that by combining multiple enzymes of the MAN1A1 pathway prognostic significance can be further increased.

A strong argument can thus be made for continued research on glycosylation changes in neoplasia. To find out more about the function, regulation, and effects of specific glycosylation enzymes, combining analysis of multiple enzymes with co expression- studies could provide a promising path on the search for new biomarkers for ovarian cancer.

6.   Summary/Zusammenfassung

6.1   Summary

Ovarian cancer remains one of the leading causes of death from cancer in woman, especially in the economically more developed regions of the world, despite falling trends for incidence and mortality rates. Thus, the search for diagnostic, prognostic, and predictive markers is highly warranted to advance patientcare via earlier diagnosis, risk stratification, more personalized therapies or in finding suitable targets for new therapeutic agents. Glycosylation changes in neoplasia are an emerging candidate in the expanding field of tumour molecular profiling as a possible pathway to achieve the aforementioned goals.

The primal aim of this study was to analyse the prognostic relevance for ovarian cancer of 7 glycosylation enzymes (GALNT12, GALNT14, GCNT3, GANAB, MAN1A1, NEU1, and ST6GAL1), selected on the basis of earlier results of our working group using qPCR, Western Blot analysis (WB), and immunohistochemistry (IHC). Additionally, expression levels between neoplasms of varying malignancy were compared (patient cohort n=52; n=204; n=24, respectively).

This study could show that patients with high protein expression of the mannosidase MAN1A1 had a significantly poorer overall survival and a shorter recurrence free interval compared with patients with low expression of this enzyme. Multivariate Cox regression analysis revealed that high MAN1A1 expression was an independent prognostic factor for overall survival of patients with ovarian cancer. In addition to that, significant clinico-pathological correlations were detected, linking high MAN1A1 expression measured on an mRNA or protein level to an advanced FIGO stage (WB), metastatic infiltration of lymph nodes (WB), distant metastasis at the time of diagnosis (qPCR, WB), and only suboptimal debulking surgery (WB). These are novel results, since the few prior analyses suggested a beneficial impact of high MAN1A1 expression levels in cancerous processes, e.g. breast cancer.

Furthermore, significant correlations of high mRNA and protein levels of the sialyltransferase ST6GAL1 were found with distant metastasis at diagnosis (qPCR, WB). Regarding the prognostic significance, WB analysis could show the association of high

ST6GAL1 expression with significantly shorter time to relapse compared to patients with low expression of ST6GAL1.

The sialidase NEU1 presented itself as a third promising candidate in this study. Significant correlations were found between lower mRNA levels of NEU1 and no metastatic lymph node infiltration, no distant metastasis at diagnosis, and optimal debulking rates. A reliable protein detection of NEU1 could not be established in our laboratory.

As for expression differences in tumour entities of different malignancies, mRNA levels of GCNT3 were significantly higher in patients diagnosed with borderline tumours compared to ovarian cancer and serous cystadenoma. Moreover, high GCNT3 mRNA levels correlated with M1 status at diagnosis.

The analysis of GALNT12, GALNT14, and GANAB did not yield reliable significant results on their aptitude as prognostic markers.

To sum up the most important findings, this study described MAN1A1 for the first time as an independent prognostic marker for shortened overall survival in ovarian cancer and provides incentives to further look into the aptitude of ST6GAL1 and NEU1 as prognostic or predictive markers and possible therapeutic targets.

6.2   Zusammenfassung

Trotz fallender Tendenz hinsichtlich seiner Inzidenz und Mortalitätsraten bleibt Eierstockskrebs eine der führenden Ursachen krebsassoziierter Todesfälle in den Industriestaaten. Ein Fortschritt in der Patientinnenversorgung durch frühere Diagnosestellung, Stratifizierung in Risikogruppen oder individualisierte Therapiekonzepte könnte durch molekulares Tumorprofiling gelingen. Die Suche nach verbesserten diagnostischen, prognostischen und prädiktiven Biomarkern ist daher unerlässlich. In diesem Forschungsgebiet nehmen Veränderungen der Glykosylierung in Neoplasien mit ihren entsprechenden Enzymexpressionen eine vielversprechende Rolle ein.

In der vorliegenden Arbeit wurde die prognostische Relevanz von 7 Glykosylierungsenzymen (GALNT12, GALNT14, GCNT3, GANAB, MAN1A1, NEU1 und ST6GAL1) für das Ovarialkarzinom mittels qPCR, Western Blot-Analysen (WB) und Immunhistochemie (IHC) untersucht. Weiterhin wurden Expressionsmuster der Enzyme in verschieden Tumorentitäten des Ovars verglichen (Patientinnenkollektiv: qPCR n=52; WB n=204; IHC n=24).

Patientinnen mit hoher Protein-Expression der Mannosidase MAN1A1 zeigten in Kaplan-Meier-Analysen ein ungünstiges Gesamtüberleben und ein verkürztes rezidivfreies Intervall im Vergleich zu Patientinnen mit einer niedrigen Expression dieses Enzyms. Eine Cox-Regressionsanalyse bestätigte hohe MAN1A1-Expression als einen unabhängigen prognostischen Faktor für das allgemeine Überleben der Patientinnen mit Ovarial-Ca. Darüber hinaus korrelierte eine hohe MAN1A1-Expression auf mRNA- und Proteinebene mit etablierten Prognosefaktoren, wie einem fortgeschrittenen FIGO-Stadium (WB), Fernmetastasierung zum Diagnosezeitpunkt (qPCR, WB), metastatischen Lymphknoteninfiltrationen (WB) und suboptimalem Debulking (WB). Diese Ergebnisse stehen im Gegensatz zu den bestehenden Veröffentlichungen bezüglich MAN1A1, die einen vorteilhaften Einfluss einer hohen Expression in Tumoren, wie zum Beispiel Brustkrebs, nahegelegt hatten.

Hohe Protein- und mRNA-Expressionen der Sialyltransferase ST6GAL1 korrelierten signifikant mit M1-Staging. Hinsichtlich der prognostischen Signifikanz zeigte sich auf

Proteinebene eine Assoziation zwischen hoher ST6GAL1-Expression und einem signifikant kürzeren rezidivfreien Intervall im Vergleich zu Patientinnen mit einer niedrigen Expression dieses Enzyms.

Für die Sialidase NEU1 konnten signifikante Korrelationen zwischen niedrigeren mRNA-Spiegeln und dem Fehlen von Lymphknoten- oder Fernmetastasen sowie optimalem Debulking gefunden werden. Eine verlässliche Protein-Detektion von NEU1 konnte in unserem Labor nicht etabliert werden.

Bezüglich der Expressionsunterschiede von Glykosylierungsenzymen in Tumorentitäten unterschiedlicher Malignität fanden sich signifikant höhere GCNT3 - mRNA-Spiegel bei Patientinnen mit Borderline-Tumoren verglichen mit Fällen von Ovarial-Ca oder serösem Zystadenom. Weiterhin korrelierten hohe GCNT3 - mRNA-Spiegel mit einem M1-Stadium bei Diagnosestellung.

Die Analyse von GALNT12, GALNT14 und GANAB ergab keine belastbaren, signifikanten Ergebnisse bezüglich einer möglichen prognostischen Relevanz im Ovarialkarzinom.

Zusammenfassend kann gesagt werden, dass die vorliegende Arbeit MAN1A1 als einen neuen unabhängigen prognostischen Marker für eine verkürzte Gesamtüberlebenszeit beim Ovarialkarzinom aufgezeigt hat und Anreize für weitere Untersuchungen von ST6GAL1 und NEU1 bezüglich ihrer Eignung als prognostische oder prädiktive Marker setzt.

7.   References

Abbott KL (2010) Glycomic analysis of ovarian cancer: Past, present, and future. *Cancer Biomarkers* 8(4): 273–280.

abcam (2014) IHC-PARAFFIN PROTOCOL (IHC-P). Available online at URL: http://www.abcam.com/ps/pdf/protocols/ihc_p.pdf (accessed 30/11/15 at 16:34).

Abdulkhalek S and Szewczuk MR (2013) Neu1 sialidase and matrix metalloprotein-ase-9 cross-talk regulates nucleic acid-induced endosomal TOLL-like receptor-7 and-9 activation, cellular signaling and pro-inflammatory responses. *Cellular signalling* 25(11): 2093–2105.

Alper J (2003) Glycobiology. Turning sweet on cancer. *Science* 301(1): 159–160.

Altevogt P, Doberstein K and Fogel M (2016) L1CAM in human cancer: L1CAM in human cancer. *International Journal of Cancer* 138(7): 1565–1576.

Amano M (2003) The ST6Gal I Sialyltransferase Selectively Modifies N-Glycans on CD45 to Negatively Regulate Galectin-1-induced CD45 Clustering, Phosphatase Modulation, and T Cell Death. *Journal of Biological Chemistry* 278(9): 7469–7475.

Anji A and Kumari M (2006) A novel RNA binding protein that interacts with NMDA R1 mRNA: regulation by ethanol. *European Journal of Neuroscience* 23(9): 2339–2350.

Antony P, Rose M, Heidenreich A, Knüchel R, Gaisa NT and Dahl E (2014) Epige-netic inactivation of ST6GAL1 in human bladder cancer. *BMC cancer* 14(1): 901.

Anugraham M, Jacob F, Nixdorf S, Everest-Dass AV, Heinzelmann-Schwarz V and Packer NH (2014) Specific Glycosylation of Membrane Proteins in Epithelial Ovarian Cancer Cell Lines: Glycan Structures Reflect Gene Expression and DNA Methylation Status. *Molecular & Cellular Proteomics* 13(9): 2213–2232.

Beaman E-M and Brooks SA (2014) The extended ppGalNAc-T family and their functional involvement in the metastatic cascade. *Histology and Histopathology* 29(3): 293-304.

Birt JA, Nabli H, Stilley JA, Windham EA, Frazier SR and Sharpe-Timms KL (2013) Elevated Peritoneal Fluid TNF-α Incites Ovarian Early Growth Response Factor 1 Expression and Downstream Protease Mediators. *Reproductive Sciences* 20(5): 514–523.

Bouralexis S, Findlay D and Evdokiou A (2005) Death to the bad guys: targeting cancer via Apo2L/TRAIL. *Apoptosis* (10): 35–51.

Brockhausen I (1999) Pathways of O-glycan biosynthesis in cancer cells. *Biochimica et Biophysica Acta* 1473(1): 67–95.

Brockhausen I (2006) Mucin-type O-glycans in human colon and breast cancer: glycodynamics and functions. *EMBO reports* 7(6): 599–604.

Brodsky AS, Fischer A, Miller DH, Vang S, MacLaughlan S, Wu H-T, Yu J, Steinhoff M, Collins C, Smith PJS, Raphael BJ and Brard L (2014) Expression Profiling of Primary and Metastatic Ovarian Tumors Reveals Differences Indicative of Aggressive Disease. *PLoS ONE* 9(4): e94476.

Büll C, Stoel MA, den Brok MH and Adema GJ (2014) Sialic Acids Sweeten a Tumor's Life. *Cancer Research* 74(12): 3199–3204.

Chauhan SC, Vannatta K, Ebeling MC, Vinayek N, Watanabe A, Pandey KK, Bell MC, Koch MD, Aburatani H, Lio Y and Jaggi M (2009) Expression and Functions of Transmembrane Mucin MUC13 in Ovarian Cancer. *Cancer Research* 69(3): 765–774.

Chen J-Y, Tang Y-A, Huang S-M, Juan H-F, Wu L-W, Sun Y-C, Wang S-C, Wu K-W, Balraj G, Chang T-T, Li W-S, Cheng H-C and Wang Y-C (2011) A Novel Sialyltransferase Inhibitor Suppresses FAK/Paxillin Signaling and Cancer Angiogenesis and Metastasis Pathways. *Cancer Research* 71(2): 473–483.

Chiu C-C, Lin C-Y, Lee L-Y, Chen Y-J, Lu Y-C, Wang H-M, Liao C-T, Chang JT-C and Cheng A-J (2011) Molecular Chaperones as a Common Set of Proteins That Regulate the Invasion Phenotype of Head and Neck Cancer. *Clinical Cancer Research* 17(14): 4629–4641.

Cho S-H, Sahin A, Hortobagyi GN, Hittelman WN and Dhingra K (1994) Sialyl-Tn antigen expression occurs early during human mammary carcinogenesis and is associated with high nuclear grade and aneuploidy. *Cancer research* 54(24): 6302–6305.

Christie DR, Shaikh FM, Lucas JA, Lucas JA and Bellis SL (2008) ST6Gal-I expression in ovarian cancer cells promotes an invasive phenotype by altering integrin glycosylation and function. *Journal of Ovarian Research* 1(1): 3.

Christofori G (2006) New signals from the invasive front. *Nature* 441(7092): 444–450.

Coleman RL, Monk BJ, Sood AK and Herzog TJ (2013) Latest research and treatment of advanced-stage epithelial ovarian cancer. *Nature Reviews Clinical Oncology* 10(4): 211–224.

Corney D.C., Flesken-Nikitin A., Choi J., Nikitin A.Y. (2008) Role of p53 and Rb in Ovarian Cancer. In: Coukos G., Berchuck A., Ozols R. (eds) *Ovarian Cancer. Advances in Experimental Medicine and Biology*, vol 622. Springer, New York, 99-117.

Cressey R (2013) Glucosidase II exhibits similarity to the p53 tumor suppressor in regards to structure and behavior in response to stress signals: A potential novel cancer biomarker. *Oncology Reports* 30(5): 2511-2519.

D'Alessio C, Caramelo JJ and Parodi AJ (2010) UDP-Glc:glycoprotein glucosyltransferase-glucosidase II, the ying-yang of the ER quality control. *Seminars in Cell & Developmental Biology* 21(5): 491–499.

De Mariano M, Gallesio R, Chierici M, Furlanello C, Conte M, Garaventa A, Croce M, Ferrini S, Tonini GP and Longo L (2015) Identification of GALNT14 as a novel neuroblastoma predisposition gene. *Oncotarget* 6(28): 26335–26346.

Ebell MH, Culp MB and Radke TJ (2015) A Systematic Review of Symptoms for the Diagnosis of Ovarian Cancer. *American Journal of Preventive Medicine* 50(3): 384-394.

Eskander RN and Tewari KS (2014) Incorporation of anti-angiogenesis therapy in the management of advanced ovarian carcinoma—Mechanistics, review of phase III randomized clinical trials, and regulatory implications. *Gynecologic Oncology* 132(2): 496–505.

Ferlay J, Soerjomataram I, Dikshit R, Eser S, Mathers C, Rebelo M, Parkin DM, Forman D and Bray F (2015) Cancer incidence and mortality worldwide: Sources, methods and major patterns in GLOBOCAN 2012: Globocan 2012. *International Journal of Cancer* 136(5): E359–E386.

Ferlay J, Steliarova-Foucher E, Lortet-Tieulent J, Rosso S, Coebergh JWW, Comber H, Forman D and Bray F (2013) Cancer incidence and mortality patterns in Europe: Estimates for 40 countries in 2012. *European Journal of Cancer* 49(6): 1374–1403.

Fleming JS, Beaugié CR, Haviv I, Chenevix-Trench G and Tan OL (2006) Incessant ovulation, inflammation and epithelial ovarian carcinogenesis: Revisiting old hypotheses. *Molecular and Cellular Endocrinology* 247(1–2): 4–21.

Fuster MM and Esko JD (2005) The sweet and sour of cancer: glycans as novel therapeutic targets. *Nature Reviews Cancer* 5(7): 526–542.

Garbar C, Mascaux C, Giustiniani J, Salesse S, Debelle L, Antonicelli F, Merrouche Y and Bensussan A (2015) Autophagy is decreased in triple-negative breast carcinoma involving likely the MUC1-EGFR-NEU1 signalling pathway. *International journal of clinical and experimental pathology* 8(5): 4344.

Garcia-Bunuel R and Monis B (1964) Histochemical Observations on Mucins in Human Ovarian Neoplasms. *Cancer* (17): 1108–1118.

Gebuhr I, Kathrin Keeren, Christine Appelt, Ulrike Schließer, Katrin Vogt, Christine Brandt, Conny Höflich, Christian Meisel, Hans-Dieter Volk and Birgit Sawitzki (2011) Differential Expression and Function of a -Mannosidase I in Stimulated Naive and Memory CD4 + T Cells. *Journal of Immunotherapy* 34(5): 428-437.

Geßner P, Riedl S, Quentmaier A and Kemmner W (1993) Enhanced activity of CMP-NeuAc:Galβ1-4GlcNAc:α2,6-sialyltransferase in metastasizing human colorectal tumor tissue and serum of tumor patients. *Cancer Letters* 75(3): 143–149.

Gilbert L, Basso O, Sampalis J, Karp I, Martins C, Feng J, Piedimonte S, Quintal L, Ramanakumar AV, Takefman J and others (2012) Assessment of symptomatic women for early diagnosis of ovarian cancer: results from the prospective DOvE pilot project. *The lancet oncology* 13(3): 285–291.

Gilmour AM, Abdulkhalek S, Cheng TS, Alghamdi F, Jayanth P, O'Shea LK, Geen O, Arvizu LA and Szewczuk MR (2013) A novel epidermal growth factor receptor-signaling platform and its targeted translation in pancreatic cancer. *Cellular signalling* 25(12): 2587–2603.

Glaysher S, Bolton LM, Johnson P, Atkey N, Dyson M, Torrance C and Cree IA (2013) Targeting EGFR and PI3K pathways in ovarian cancer. *British Journal of Cancer* 109(7): 1786–1794.

Gomes J, Gomes-Alves P, Carvalho S, Peixoto C, Alves P, Altevogt P and Costa J (2015) Extracellular Vesicles from Ovarian Carcinoma Cells Display Specific Glycosignatures. *Biomolecules* 5(3): 1741–1761.

González-Vallinas M, Vargas T, Moreno-Rubio J, Molina S, Herranz J, Cejas P, Burgos E, Aguayo C, Custodio A, Reglero G, Feliu J and Ramírez de Molina A (2015) Clinical relevance of the differential expression of the glycosyltransferase gene GCNT3 in colon cancer. *European Journal of Cancer* 51(1): 1–8.

Guda K, Moinova H, He J, Jamison O, Ravi L, Natale L, Lutterbaugh J, Lawrence E, Lewis S, Willson JK and others (2009) Inactivating germ-line and somatic mutations in polypeptide N-acetylgalactosaminyltransferase 12 in human colon cancers. *Proceedings of the National Academy of Sciences* 106(31): 12921–12925.

Guo J-M, Chen H-L, Wang G-M, Zhang Y-K and Narimatsu H (2004) Expression of UDP-GalNAc:Polypeptide N-Acetylgalactosaminyltransferase-12 in Gastric and Colonic Cancer Cell Lines and in Human Colorectal Cancer. *Oncology* 67(3–4): 271–276.

Guo J-M, Zhang Y, Cheng L, Iwasaki H, Wang H, Kubota T, Tachibana K and Narimatsu H (2002) Molecular cloning and characterization of a novel member of the UDP-GalNAc: polypeptide N-acetylgalactosaminyltransferase family, pp-GalNAc-T12. *FEBS letters* 524(1): 211–218.

Huang MC, Chen HY, Huang HC, Huang J, Liang JT, Shen TL, Lin NY, Ho CC, Cho IM and Hsu SM (2006) C2GnT-M is downregulated in colorectal cancer and its re-expression causes growth inhibition of colon cancer cells. *Oncogene* 25(23): 3267–3276.

Huanna T, Tao Z, Xiangfei W, Longfei A, Yuanyuan X, Jianhua W, Cuifang Z, Manjing J, Wenjing C, Shaochuan Q, Feifei X, Naikang L, Jinchao Z and Chen W (2014) GALNT14 mediates tumor invasion and migration in breast cancer cell MCF-7. *Molecular Carcinogenesis* 54(10): 1159-1171.

Jayanth P, Amith SR, Gee K and Szewczuk MR (2010) Neu1 sialidase and matrix metalloproteinase-9 cross-talk is essential for neurotrophin activation of Trk receptors and cellular signaling. *Cellular signalling* 22(8): 1193–1205.

Jayson GC, Kohn EC, Kitchener HC and Ledermann JA (2014) Ovarian cancer. *The Lancet* 384(9951): 1376-1388.

Kato T, Wang Y, Yamaguchi K, Milner CM, Shineha R, Satomi S and Miyagi T (2001) Overexpression of lysosomal-type sialidase leads to suppression of metastasis associated with reversion of malignant phenotype in murine B16 melanoma cells. *International journal of cancer* 92(6): 797–804.

Köbel M, Reuss A, Bois A du, Kommoss S, Kommoss F, Gao D, Kalloger SE, Huntsman DG and Gilks CB (2010) The biological and clinical value of p53 expression in pelvic high-grade serous carcinomas. *The Journal of Pathology* 222(2): 191–198.

Kurman RJ, Carcangiu ML, Young RH and Herrington CS (2014) 1. Tumours of the ovary. In: Kurman RJ, Carcangiu ML, Young RH and Herrington CS (eds) *WHO Classification of Tumours of Female Reproductive Organs - WHO/IARC Classification of Tumours*, 4th Edition, vol 6. IARC Press, Lyon, 11-40.

Kurman RJ and Shih I-M (2010) The Origin and pathogenesis of epithelial ovarian cancer-a proposed unifying theory. *The American journal of surgical pathology* 34(3): 433.

Kuzmanov U, Musrap N, Kosanam H, Smith CR, Batruch I, Dimitromanolakis A and Diamandis EP (2012) Glycoproteomic identification of potential glycoprotein biomarkers in ovarian cancer proximal fluids. *Clinical Chemistry and Laboratory Medicine* 51(7): 1467–1476.

Lee M, Park JJ and Lee YS (2010) Adhesion of ST6Gal I-mediated human colon cancer cells to fibronectin contributes to cell survival by integrin \s s1-mediated paxillin and AKT activation. *Oncology reports* 23(3): 757–761.

Leitlinienprogramm Onkologie (2013) Leitlinienprogramm   Onkologie   (Deutsche Krebsgesellschaft,   Deutsche Krebshilfe, AWMF): S3-Leitlinie Diagnostik, Therapie und Nachsorge maligner Ovarialtumoren, Langversion 1.0, AWMF Registrierungs-nummer: 032-035OL. Available online at URL: http://leitlinienprogramm-onkolo-gie.de/Leitlinien.7.0.html (accessed 06/04/16 at 20:29).

Levy-Ontman O, Fisher M, Shotland Y, Weinstein Y, Tekoah Y and Arad S (2014) Genes Involved in the Endoplasmic Reticulum N-Glycosylation Pathway of the Red Microalga Porphyridium sp.: A Bioinformatic Study. *International Journal of Molecular Sciences* 15(2): 2305–2326.

Lheureux S, Karakasis K, Kohn EC and Oza AM (2015) Ovarian cancer treatment: The end of empiricism?: Ovarian Cancer Strategy. *Cancer* 121(18): 3203–3211.

Liang F, Seyrantepe V, Landry K, Ahmad R, Ahmad A, Stamatos NM and Pshezhetsky AV (2006) Monocyte differentiation up-regulates the expression of the lysosomal sialidase, Neu1, and triggers its targeting to the plasma membrane via ma-jor histocompatibility complex class II-positive compartments. *Journal of Biological Chemistry* 281(37): 27526–27538.

Lillehoj EP, Hyun SW, Feng C, Zhang L, Liu A, Guang W, Nguyen C, Luzina IG, Ata-mas SP, Passaniti A, Twaddell WS, Puche AC, Wang L-X, Cross AS and Goldblum SE (2012) NEU1 Sialidase Expressed in Human Airway Epithelia Regulates Epider-mal Growth Factor Receptor (EGFR) and MUC1 Protein Signaling. *Journal of Biologi-cal Chemistry* 287(11): 8214–8231.

Lin S, Kemmner W, Grigull S and Schlag PM (2002) Cell surface α2, 6-sialylation af-fects adhesion of breast carcinoma cells. *Experimental cell research* 276(1): 101–110.

Lise M, Belluco C, Perera SP, Patel R, Thomas P and Ganguly A (2000) Clinical correlations of α2, 6-sialyltransferase expression in colorectal cancer patients. *Hybridoma* 19(4): 281–286.

Liu H-O, Wu Q, Liu W-S, Liu Y-D, Fu Q, Zhang W-J, Xu L and Xu J-J (2015) ST6Gal-I Predicts Postoperative Clinical Outcome for Patients with Localized Clear-cell Renal Cell Carcinoma. *Asian Pacific Journal of Cancer Prevention* 15(23): 10217–10223.

Liu T, Zhang S, Chen J, Jiang K, Zhang Q, Guo K and Liu Y (2014) The Transcriptional Profiling of Glycogenes Associated with Hepatocellular Carcinoma Metastasis. *PLoS ONE* 9(9): e107941.

Liu Z, Swindall AF, Kesterson RA, Schoeb TR, Bullard DC and Bellis SL (2011) ST6Gal-I Regulates Macrophage Apoptosis via 2-6 Sialylation of the TNFR1 Death Receptor. *Journal of Biological Chemistry* 286(45): 39654–39662.

Ma H, Cheng L, Hao K, Li Y, Song X, Zhou H and Jia L (2014) Reversal Effect of ST6GAL 1 on Multidrug Resistance in Human Leukemia by Regulating the PI3K/Akt Pathway and the Expression of P-gp and MRP1. *PLoS ONE* 9(1): e85113.

Mahner S, Baasch C, Schwarz J, Hein S, Wölber L, Jänicke F and Milde-Langosch K (2008) C-Fos expression is a molecular predictor of progression and survival in epithelial ovarian carcinoma. *British Journal of Cancer* 99(8): 1269–1275.

Mahner S, Woelber L, Mueller V, Witzel I, Prieske K, Grimm D, Keller-v Amsberg G and Trillsch F (2015) Beyond Bevacizumab: An Outlook to New Anti-Angiogenics for the Treatment of Ovarian Cancer. *Frontiers in Oncology* 5: 211.

Man Ip CK, Susan Yung, Tak-Mao Chan, Sai-Wah Tsao and Alice Sze Tsai Wong (2014) p70 S6 kinase drives ovarian cancer metastasis through multicellular spheroid-peritoneum interaction and P-cadherin/ β1 integrin signaling activation. *Oncotarget* 5(19): 9133–9149.

Martins FC, de Santiago I, Trinh A, Xian J, Guo A, Sayal K, Jimenez-Linan M, Deen S, Driver K, Mack M and others (2014) Combined image and genomic analysis of high-grade serous ovarian cancer reveals PTEN loss as a common driver event and prognostic classifier. *Genome biology* 15(12): 1.

Masic I, Hodzic A and Mulic S (2014) Ethics in medical research and publication. *International journal of preventive medicine* 5(9): 1073.

Mavaddat N, Peock S, Frost D, Ellis S, Platte R, Fineberg E, Evans DG, Izatt L, Eeles RA, Adlard J, Davidson R, Eccles D, Cole T, Cook J, Brewer C, Tischkowitz M, Douglas F, Hodgson S, Walker L, Porteous ME, Morrison PJ, Side LE, Kennedy MJ, Houghton C, Donaldson A, Rogers MT, Dorkins H, Miedzybrodzka Z, Gregory H, Eason J, Barwell J, McCann E, Murray A, Antoniou AC, Easton DF and on behalf of EMBRACE (2013) Cancer Risks for BRCA1 and BRCA2 Mutation Carriers: Results From Prospective Analysis of EMBRACE. *JNCI Journal of the National Cancer Institute* 105(11): 812–822.

Milde-Langosch K, Karn T, Schmidt M, zu Eulenburg C, Oliveira-Ferrer L, Wirtz RM, Schumacher U, Witzel I, Schütze D and Müller V (2014) Prognostic relevance of glycosylation-associated genes in breast cancer. *Breast Cancer Research and Treatment* 145(2): 295–305.

Milde-Langosch K, Schütze D, Oliveira-Ferrer L, Wikman H, Müller V, Lebok P, Pantel K, Schröder C, Witzel I and Schumacher U (2015) Relevance of βGal–βGalNAc-containing glycans and the enzymes involved in their synthesis for invasion and survival in breast cancer patients. *Breast Cancer Research and Treatment* 151(3): 515–528.

Millipore (2008) *Re-blot Plus Mild Antibody Stripping Solution*. Available online at URL: http://www.merckmillipore.com/INTERSHOP/web/WFS/Merck-DE-Site/de_DE/-/EUR/ShowDocument-File?ProductSKU=MM_NF-2502&DocumentId=201306.4632.ProNet&DocumentType=UG&Language=EN&Country=NF&Origin=PDP (accessed 27/11/15 at 01:23).

Miyagi T, Sato K, Hata K and Taniguchi S (1994) Metastatic potential of transformed rat 3Y1 cell lines is inversely correlated with lysosomal-type sialidase activity. *FEBS letters* 349(2): 255–259.

Miyagi T, Wada T, Yamaguchi K, Shiozaki K, Sato I, Kakugawa Y, Yamanami H and Fujiya T (2008) Human sialidase as a cancer marker. *PROTEOMICS* 8(16): 3303–3311.

Moremen KW and Nairn AV (2014) Mannosidase, Alpha, Class 1 (MAN1A1 (Golgi Alpha-Mannnosidase IA), Man1A2 (Golgi Alpha-Mannosidase IB), MAN1B1 (ER Alpha-Mannosidase I), MAN1C1 (Golgi Alpha-Mannosidase IC)). In: Tamiguchi et al (eds) *Handbook of Glycosyltransferases and Related Genes*. Springer Japan, 1297–1312*.

Mueller MM and Fusenig NE (2004) Friends or foes — bipolar effects of the tumour stroma in cancer. *Nature Reviews Cancer* 4(11): 839–849.

Nonaka M, Fukuda MN, Gao C, Li Z, Zhang H, Greene MI, Peehl DM, Feizi T and Fukuda M (2014) Determination of Carbohydrate Structure Recognized by Prostate-specific F77 Monoclonal Antibody through Expression Analysis of Glycosyltransfer-ase Genes. *Journal of Biological Chemistry* 289(23): 16478–16486.

Oliveira-Ferrer L, Legler K and Milde-Langosch K (2017) Role of protein glycosylation in cancer metastasis. *Seminars in Cancer Biology*. Available online at URL: http://www.sciencedirect.com/science/article/pii/S1044579X17300408 (accessed 23/06/2017 at 01:46) .

Oliveira-Ferrer L, Rößler K, Haustein V, Schröder C, Wicklein D, Maltseva D, Khaustova N, Samatov T, Tonevitsky A, Mahner S, Jänicke F, Schumacher U and Milde-Langosch K (2014) c-FOS suppresses ovarian cancer progression by changing adhesion. *British Journal of Cancer* 110(3): 753–763.

Park J-J and Lee M (2013) Increasing the α 2, 6 Sialylation of Glycoproteins May Contribute to Metastatic Spread and Therapeutic Resistance in Colorectal Cancer. *Gut and Liver* 7(6): 629–641.

Park J-J, Yi JY, Jin YB, Lee Y-J, Lee J-S, Lee Y-S, Ko Y-G and Lee M (2012) Sialyla-tion of epidermal growth factor receptor regulates receptor activity and chemosensi-tivity to gefitinib in colon cancer cells. *Biochemical Pharmacology* 83(7): 849–857.

Perets R and Drapkin R (2016) It's Totally Tubular...Riding The New Wave of Ovar-ian Cancer Research. *Cancer Research* 76(1): 10–17.

Potapenko IO, Haakensen VD, Lüders T, Helland Å, Bukholm I, Sørlie T, Kristensen VN, Lingjærde OC and Børresen-Dale A-L (2010) Glycan gene expression signatures in normal and malignant breast tissue; possible role in diagnosis and progression. *Molecular Oncology* 4(2): 98–118.

Prat for the FIGO Committee on Gynecologic Oncology J (2015) Abridged republication of FIGO's staging classification for cancer of the ovary, fallopian tube, and peritoneum: FIGO's Staging Classification. *Cancer* 121(19): 3452–3454.

Pshezhetsky AV and Hinek A (2011) Where catabolism meets signalling: neuraminidase 1 as a modulator of cell receptors. *Glycoconjugate Journal* 28(7): 441–452.

QIAGEN (2012) *RNeasy Mini Handbook.* Available online at URL: https://www.qiagen.com/de/resources/download.aspx?id=14e7cf6e-521a-4cf7-8cbc-bf9f6fa33e24&lang=en (accessed 23/11/15 at 23:54).

Ren L, Zhang L, Huang S, Zhu Y, Li W, Fang S, Shen L and Gao Y (2015) Effects of sialidase NEU1 siRNA on proliferation, apoptosis, and invasion in human ovarian cancer. *Molecular and Cellular Biochemistry* 411(1-2): 213-219.

RKI (2015) *Krebs in Deutschland - Eierstöcke - ICD-10 C56.* Available online at URL: http://www.krebsdaten.de/Krebs/DE/Content/Publikationen/Krebs_in_Deutschland/kid_2015/kid_2015_c56_eierstoecke.pdf?__blob=publicationFile (accessed 11/01/16 at 11:22).

Schultz MJ, Swindall AF, Wright JW, Sztul ES, Landen CN and Bellis SL (2013) ST6Gal-I sialyltransferase confers cisplatin resistance in ovarian tumor cells. *J Ovarian Res* 6(1): 25.

Seales EC, Jurado GA, Singhal A and Bellis SL (2003) Ras oncogene directs expression of a differentially sialylated, functionally altered β1 integrin. *Oncogene* 22(46): 7137–7145.

Sethi M and Fanayan S (2015) Mass Spectrometry-Based N-Glycomics of Colorectal Cancer. *International Journal of Molecular Sciences* 16(12): 29278–29304.

Stern HM, Padilla M, Wagner K, Amler L and Ashkenazi A (2010) Development of Immunohistochemistry Assays to Assess GALNT14 and FUT3/6 in Clinical Trials of Dulanermin and Drozitumab. *Clinical Cancer Research* 16(5): 1587–1596.

Sundar S, Neal RD and Kehoe S (2015) Diagnosis of ovarian cancer. *BMJ* 351: h4443.

Suzuki O, Abe M and Hashimoto Y (2015) Sialylation by β-galactoside α-2,6-sialyltransferase and N-glycans regulate cell adhesion and invasion in human anaplastic large cell lymphoma. *International Journal of Oncology* 46(3): 973-980.

Swindall AF and Bellis SL (2011) Sialylation of the Fas Death Receptor by ST6Gal-I Provides Protection against Fas-mediated Apoptosis in Colon Carcinoma Cells. *Journal of Biological Chemistry* 286(26): 22982–22990.

Swindall AF, Londoño-Joshi AI, Schultz MJ, Fineberg N, Buchsbaum DJ and Bellis SL (2013) ST6Gal-I Protein Expression Is Upregulated in Human Epithelial Tumors and Correlates with Stem Cell Markers in Normal Tissues and Colon Cancer Cell Lines. *Cancer Research* 73(7): 2368–2378.

Szewczuk M, Haxho F, Allison S, Alghamdi F, Brodhagen L, Kuta V, Abdulkhalek S and Neufeld R (2014) Oseltamivir phosphate monotherapy ablates tumor neovascularization, growth, and metastasis in mouse model of human triple-negative breast adenocarcinoma. *Breast Cancer: Targets and Therapy* 9(6): 191-203.

Szewczuk M, O'Shea L, Abdulkhalek S, Allison S and Neufeld R (2014) Therapeutic targeting of Neu1 sialidase with oseltamivir phosphate (Tamiflu) disables cancer cell survival in human pancreatic cancer with acquired chemoresistance. *Onco Targets and Therapy* 7(1): 117-134.

Takara Bio Inc. (2014) *Product Manual - SYBR® Premix Ex Taq^{TM} II (Tli RNaseH Plus)*. Available online at URL: http://www.takara.co.kr/file/manual/pdf/RR820L_ev1201Da-final.pdf (accessed 25/11/15 at 19:19).

Tavassoli FA, Lee KR, Prat J, Dietel M, Gersell DJ, Kaseladze AI, Hauptmann S, Rutgers J, Russel P, Buckley CH, Pisani P, Schwartz P, Goldgar DE, Silva E, Caduff R, Kubick-Huch RA (2003) Chapter 2: Tumours of the Ovary and Peritoneum. In: Tavassoli FA and Devilee P (eds) *World Health Organization Classification of Tumours. Pathology and Genetics of Tumours of the Breast and Female Genital Organs*. IARC Press, Lyon, 119-124.

Taylor SC, Berkelman T, Yadav G and Hammond M (2013) A Defined Methodology for Reliable Quantification of Western Blot Data. *Molecular Biotechnology* 55(3): 217–226.

Thermo Fisher Scientific Inc. (2008) *- nd-1000-v3.7-users-manual-8.5x11.pdf*. *NanoDrop 1000 Spectrophotometer V3.7 User's Manual*. Available online at URL: http://www.nanodrop.com/library/nd-1000-v3.7-users-manual-8.5x11.pdf (accessed 23/11/15 at 17:36).

Thermo Fisher Scientific Inc. (2012) *Product information: Maxima First Strand cDNA Synthesis Kit for RT-qPCR, #K1642 - MAN0012719_200rxns_Maxima_FirstStrand_cDNA_Syn_RTqPCR_UG.pdf*. Available online at URL: https://tools.thermofisher.com/content/sfs/manuals/MAN0012719_200rxns_Maxima_FirstStrand_cDNA_Syn_RTqPCR_UG.pdf (accessed 23/11/15 at 23:23).

Thermo Fisher Scientific Inc. (2015) *Pierce BCA Protein Assay Kit*. Available online at URL: https://tools.thermofisher.com/content/sfs/manuals/MAN0011430_Pierce_BCA_Protein_Asy_UG.pdf (accessed 23/11/15 at 00:44).

Tian Y, Yao Z, Roden RBS and Zhang H (2011) Identification of glycoproteins associated with different histological subtypes of ovarian tumors using quantitative glycoproteomics. *PROTEOMICS* 11(24): 4677–4687.

Uemura T, Shiozaki K, Yamaguchi K, Miyazaki S, Satomi S, Kato K, Sakuraba H and Miyagi T (2009) Contribution of sialidase NEU1 to suppression of metastasis of human colon cancer cells through desialylation of integrin β4. *Oncogene* 28(9): 1218–1229.

Vajaria BN, Patel KR, Begum R and Patel PS (2015) Sialylation: an Avenue to Target Cancer Cells. *Pathology & Oncology Research* 22(3): 443-447.

Valle L, Pineda M, Navarro M, Lázaro C, Brunet J, Infante M and Seguí N (2014) GALNT12 is Not a Major Contributor of Familial Colorectal Cancer Type X. *Human Mutation* 35(1): 50–52.

Varki A, Kannagi R, Toole BP (2009a) Chapter 44 Glycosylation Changes in Cancer. In: Varki A, Cummings R, Esko J, Freeze HH, Stanley P, Bertozzi CR, Hart GW, and Etzler EM (eds) *Essentials of Glycobiology – NCBI Bookshelf,* 2nd Edition. Cold Spring Harbor Laboratory Press, New York, Chapter 44. Available online at URL: http://www.ncbi.nlm.nih.gov/books/NBK1963/ (accessed 27/10/14 at 10:49).

Varki A, Brockhausen I, Schachter S, Stanley P (2009b) Chapter 9 O-GalNAc Glycans. In: Varki A, Cummings R, Esko J, Freeze HH, Stanley P, Bertozzi CR, Hart GW, and Etzler EM (eds) *Essentials of Glycobiology – NCBI Bookshelf,* 2nd Edition. Cold Spring Harbor Laboratory Press, New York, Chapter 9. Available online at URL: http://www.ncbi.nlm.nih.gov/books/NBK1896/ (accessed 14/01/16 at 14:00).

Varki A, Stanley P, Schachter H, Taniguchi N (2009c) Chapter 8 N-Glycans. In: Varki A, Cummings R, Esko J, Freeze HH, Stanley P, Bertozzi CR, Hart GW, and Etzler EM (eds) *Essentials of Glycobiology – NCBI Bookshelf,* 2nd Edition. Cold Spring Harbor Laboratory Press, New York, Chapter 8. Available online at URL: http://www.ncbi.nlm.nih.gov/books/NBK1917/ (accessed 25/01/16 at 14:14).

Vázquez-Martín C, Gil-Martín E and Fernández-Briera A (2005) Elevation of ST6Gal I activity in malignant and transitional tissue in human colorectal cancer. *Oncology* 69(5): 436–444.

Vogel C and Marcotte EM (2012) Insights into the regulation of protein abundance from proteomic and transcriptomic analyses. *Nature Reviews Genetics* 13(4): 227-232.

Wagner KW, Punnoose EA, Januario T, Lawrence DA, Pitti RM, Lancaster K, Lee D, von Goetz M, Yee SF, Totpal K, Huw L, Katta V, Cavet G, Hymowitz SG, Amler L and Ashkenazi A (2007) Death-receptor O-glycosylation controls tumor-cell sensitivity to the proapoptotic ligand Apo2L/TRAIL. *Nature Medicine* 13(9): 1070–1077.

Wandall HH, Blixt O, Tarp MA, Pedersen JW, Bennett EP, Mandel U, Ragupathi G, Livingston PO, Hollingsworth MA, Taylor-Papadimitriou J, Burchell J and Clausen H (2010) Cancer Biomarkers Defined by Autoantibody Signatures to Aberrant O-Glyco-peptide Epitopes. *Cancer Research* 70(4): 1306–1313.

Wang H, Tachibana K, Zhang Y, Iwasaki H, Kameyama A, Cheng L, Guo J-M, Hiruma T, Togayachi A, Kudo T, Kikuchi N and Narimatsu H (2003) Cloning and characterization of a novel UDP-GalNAc:polypeptide N-acetylgalactosaminyltransfer-ase, pp-GalNAc-T14. *Biochemical and Biophysical Research Communications* 300(3): 738–744.

Wang P, Lee W, Juang C, Yang Y, Lo W, Lai C, Hsieh S and Yuan C (2005) Altered mRNA expressions of sialyltransferases in ovarian cancers. *Gynecologic Oncology* 99(3): 631–639.

Wang Y-C, Stein JW, Lynch CL, Tran HT, Lee C-Y, Coleman R, Hatch A, Antontsev VG, Chy HS, O'Brien CM, Murthy SK, Laslett AL, Peterson SE and Loring JF (2015) Glycosyltransferase ST6GAL1 contributes to the regulation of pluripotency in human pluripotent stem cells. *Scientific Reports* 5: 13317.

Winter WE, Maxwell GL, Tian C, Carlson JW, Ozols RF, Rose PG, Markman M, Arm-strong DK, Muggia F and McGuire WP (2007) Prognostic Factors for Stage III Epithe-lial Ovarian Cancer: A Gynecologic Oncology Group Study. *Journal of Clinical Oncol-ogy* 25(24): 3621–3627.

Wu C, Guo X, Wang W, Wang Y, Shan Y, Zhang B, Song W, Ma S, Ge J, Deng H and others (2010) N-Acetylgalactosaminyltransferase-14 as a potential biomarker for breast cancer by immunohistochemistry. *BMC cancer* 10(1): 123.

Wu C, Ma S-S, Ge J-F, Wang Y-Y, Tian H-N, Liu X-B, Zhang B, Liu F-M, Zhang X-K and Li Q-J (2012) Colocalization and identification of interaction sites between IGFBP-3 and GalNAc-T14. *Gene* 499(2): 347–351.

Wu Y, Termine DJ, Swulius MT, Moremen KW and Sifers RN (2007) Human Endoplasmic Reticulum Mannosidase I Is Subject to Regulated Proteolysis. *Journal of Biological Chemistry* 282(7): 4841–4849.

Yang Z (2013) The mucin-type glycosylating enzyme polypeptide N-acetylgalactosaminyltransferase 14 promotes the migration of ovarian cancer by modifying mucin 13. *Oncology Reports* 30(2): 667-676.

Yeh C-T, Liang K-H, Lin C-C, Chang M-L, Hsu C-L and Hung C-F (2014) A single nucleotide polymorphism on the GALNT14 gene as an effective predictor of response to chemotherapy in advanced hepatocellular carcinoma. *International Journal of Cancer* 134(5): 1214–1224.

Yeh J-C, Ong E and Fukuda M (1999) Molecular cloning and expression of a novel β-1, 6-N-acetylglucosaminyltransferase that forms core 2, core 4, and I branches. *Journal of Biological Chemistry* 274(5): 3215–3221.

Zhao Y, Li Y, Ma H, Dong W, Zhou H, Song X, Zhang J and Jia L (2014) Modification of Sialylation Mediates the Invasive Properties and Chemosensitivity of Human Hepatocellular Carcinoma. *Molecular & Cellular Proteomics* 13(2): 520–536.

Zhou X, Zhang H and Han X (2014) Role of epithelial to mesenchymal transition proteins in gynecological cancers: pathological and therapeutic perspectives. *Tumor Biology* 35(10): 9523–9530.

Zhu Y, Srivatana U, Ullah A, Gagneja H, Berenson CS and Lance P (2001) Suppression of a sialyltransferase by antisense DNA reduces invasiveness of human colon cancer cells in vitro. *Biochimica et Biophysica Acta (BBA)-Molecular Basis of Disease* 1536(2): 148–160.

Zhuo Y and Bellis SL (2011) Emerging Role of 2,6-Sialic Acid as a Negative Regulator of Galectin Binding and Function. *Journal of Biological Chemistry* 286(8): 5935–5941.

8.   Danksagung

9.   Lebenslauf

Beatrice Wichert, geb. 03.02.1990, Osnabrück

Hochschulausbildung

Sep 2009 – Mai 2017	**Universitätsklinikum Hamburg-Eppendorf (UKE), Hamburg** **Gesamtnote –sehr gut (1.16) -**
Jul 2016 – Sep 2016	**Ninewells University Hospital, Dundee, Schottland**
Mai 2016 – Jul 2016	**CHU Pointe-à-Pitre, Guadeloupe, Frankreich**
Okt 2012 – Jul 2013	**CHU Bordeaux, Frankreich**

Praktisches Jahr

Dez 2016 – Apr 2017	**Wahlfach Neurologie**, Albertinenkrankenhaus, Hamburg
Sep 2016 – Dez 2016	**Innere Medizin**, Asklepios Klinik Altona, Hamburg
Jul 2016 – Sep 2016	**Orthopädie u. Unfallchirurgie**, Ninewells University Hospital, Dundee, Schottland
Mai 2016 – Jul 2016	**Allgemein- u. Viszeralchirurgie**, CHU Pointe-à-Pitre, Guadeloupe, Frankreich

Famulaturen

Apr 2015 – Mai 2015	**Akute Geriatrie u. Palliativstation**, Albertinenhaus, Hamburg
Jan 2014 – Feb 2014	**Allgemeinmedizin**, Osnabrück
Mai 2013 – Mai 2013	**ZNA**, Hôpital Pellegrin, CHU Bordeaux, Frankreich
Okt 2012 – Okt 2012	**Intensiv-Station**, Hôpital Pellegrin, CHU Bordeaux, Frankreich

Abitur

Aug 2002 – Jul 2009	Gymnasium Ursulaschule Osnabrück, Abschlussnote 1.2

Dissertation, Auszeichnungen

2014 – 2017	**Gynäkologisches Forschungslabor, UKE** Dissertation betreut durch **Dr. rer. nat. habil. Karin Milde-Langosch** Thema: **Expression of glycosylation-associated genes in ovarian neoplasms and prognostic relevance of MAN1A1 and ST6GAL1 in ovarian cancer.**
2012 – 2017	Stipendiatin der bischöflichen Studienförderung **Cusanuswerk**
2011 – 2017	**Mentoringprogramm für exzellente Studierende** des UKE, Schwerpunkt: Neurowissenschaften/Psychiatrie

Beatrice Wichert

Hamburg, 28. Juni 2017

10. Eidesstattliche Versicherung

Ich versichere ausdrücklich, dass ich die Arbeit selbständig und ohne fremde Hilfe verfasst, andere als die von mir angegebenen Quellen und Hilfsmittel nicht benutzt und die aus den benutzten Werken wörtlich oder inhaltlich entnommenen Stellen einzeln nach Ausgabe (Auflage und Jahr des Erscheinens), Band und Seite des benutzten Werkes kenntlich gemacht habe.

Ferner versichere ich, dass ich die Dissertation bisher nicht einem Fachvertreter an einer anderen Hochschule zur Überprüfung vorgelegt oder mich anderweitig um Zulassung zur Promotion beworben habe.

Ich erkläre mich einverstanden, dass meine Dissertation vom Dekanat der Medizinischen Fakultät mit einer gängigen Software zur Erkennung von Plagiaten überprüft werden kann.

Unterschrift: ....